ANALYSIS OF THE FM RECEIVER WITH FREQUENCY FEEDBACK

F. G. M. BAX

ANALYSIS OF THE FM RECEIVER WITH FREQUENCY FEEDBACK*)

PROMOTOR: PROF. DR. F. L. H. M. STUMPERS

ANALYSIS OF THE FM RECEIVER WITH FREQUENCY FEEDBACK

PROEFSCHRIFT

TER VERKRIJGING VAN DE GRAAD VAN DOCTOR IN DE WISKUNDE EN NATUURWETENSCHAPPEN AAN DE KATHOLIEKE UNIVERSITEIT TE NIJMEGEN, OP GEZAG VAN DE RECTOR MAGNIFICUS MR. W. C. L. VAN DER GRINTEN, HOOGLERAAR IN DE FACULTEIT DER RECHTSGELEERDHEID, VOLGENS BESLUIT VAN DE SENAAT IN HET OPENBAAR TE VERDEDIGEN OP 23 OCTOBER 1970, DES NAMIDDAGS TE 4 UUR

DOOR

FRANCISCUS GODEFRIDUS MARIA BAX

GEBOREN TE EINDHOVEN

Aan Miep, Frank en Monique

Aan mijn ouders

Acknowledgement

The investigations described in this thesis were carried out in the Research Laboratories of N.V. Philips' Gloeilampenfabrieken, Waalre, during the years 1965–1969.

I am greatly indebted to the management of these laboratories for affording me the opportunity of publishing the results of these investigations as a thesis.

The measurements were performed by Mr R. van Dam. His enthusiasm and perseverance contributed significantly to the realization of this work.

I would also like to thank Dr R. H. Bathgate for the care he took on the English text, and Mr B. M. A. Hijdra, Dr J. B. H. Peek and Mr M. Weeda for making helpful suggestions and reading the manuscript.

CONTENTS

INTRODUCTION

A telecommunication system is designed to transmit and to receive information. In the most common types, the information is first converted into an electrical signal, which we shall refer to as the "information signal". This conversion may be linear (in which case only the physical form of the information changes) or non-linear (coding). The transmission of the information signal should be as efficient as possible; to this end, the information signal must often be processed before transmission. Such processing is known as modulation. If a modulated signal is used, the receiver will have the task of extracting the information signal from the signal received; this process is known as detection or demodulation. Together with the desired signal, noise or other types of interference may also appear at the input of the receiver. There are many different modulation methods, each with its characteristic advantages and disadvantages. Some of the factors which determine the quality of a modulation system are the simplicity of the equipment involved, the bandwidth required and the quality of the detected information signal when noise and other types of interference are present at the input of the receiver. In many modulation systems, one or more parameters of a sinusoidal function (carrier wave) are varied in relation to the information signal to be transmitted. As a result of the modulation, the bandwidth of the signal to be transmitted may exceed that of the information signal alone. Two widely used modulation systems are those in which only the amplitude or only the frequency of the carrier wave is varied. These systems are known as amplitude modulation (AM) and frequency modulation (FM), respectively. The advantages of AM are the simplicity of the equipment required and the small bandwidth. The advantages of FM, apart from the relative simplicity of the equipment involved, are in particular the good noise and interference properties. However, in order to obtain these good noise properties, one must make the bandwidth extra large. The possibility of "trading in" bandwidth for improved protection against noise is a very important property, which FM shares with various other modulation systems.

This thesis deals with a number of aspects of FM, in particular its noise properties. The good noise properties of FM signals are due to the fact that the power of the detected signal is proportional to the bandwidth used, while the power of the detected noise depends on the bandwidth of the information signal. However, this relation only holds when the signal power at the input of the FM receiver is appreciably greater than the noise power within the signal bandwidth there. If the ratio of signal power to noise power falls below a certain level, the noise will drown the signal, and the noise properties of the modulation system will be exceptionally bad. The lowest ratio of signal power to noise power at which the noise properties are still good is known as the threshold of the FM receiver. As the bandwidth of the signal transmitted increases with

respect to that of the information signal, the quality of the detected signal will improve. However, it will be clear that the noise power at the input will also increase with this increase in bandwidth, so that the signal power at the input must also increase in order to stay above the threshold.

For most applications (e.g. in broadcasting), the transmitter power and the bandwidth used will be such that standard receivers will operate well above the threshold throughout the whole region which the transmitter is supposed to cover. In such cases, it is unnecessary to know the threshold value exactly, and rough approximations will serve the purpose quite well. For professional purposes (e.g. satellite communication), however, the situation may be quite different. In these cases, one generally tries to achieve the optimum compromise between transmitter power, the bandwidth to be used, the properties of the antennae and the sensitivity of the pre-amplifiers which will guarantee the desired quality of the detected information signal. The combination of transmitter and receiver is then designed so that the receiver works just above the threshold, even under unfavourable circumstances. It will be clear that the threshold will now have to be known exactly, and that the mechanism determining the threshold must be well understood. The most important work in this field has been done by Rice [1,2]) and Stumpers [3]). The threshold can be calculated for "unmodulated carrier waves", and in principle also for modulated carrier waves on the basis of their results. However, as yet few numerical results have been obtained for the calculated threshold with modulated carrier waves.

The development of satellite communication has been accompanied by many attempts to lower the threshold of FM receivers. One of the results of such investigations has been the development of the FM receiver with frequency feedback. In this receiver, the local oscillator is replaced by a voltage-controlled oscillator (VCO), so that the frequency is controlled by the detected signal. Two FM signals are now applied to the mixer stage, and (at least in the ideal case) the frequency variation of the VCO carrier wave follows that of the original signal. As a result, the bandwidth of the FM signal coming from the mixer stage is lower than that of the FM signal at the input of the receiver. For signals above the threshold, the good noise properties are retained, because the information signal and the noise are fed back to the same extent. Owing to the reduction in bandwidth, however, the mixer output signal can be filtered so that less noise reaches the input of the detector than in the case without feedback; in other words, the threshold is lowered. This method of feedback makes use of the a priori information implied in the FM signal, that the frequency of the carrier wave cannot vary in a faster rhythm than that corresponding to the highest frequency of the information signal.

The aim of this thesis is to gain further insight into the operation of the FM receiver with feedback, and to describe a method of calculating the threshold of this receiver. There are two possible ways of carrying out such a study.

The first is the purely mathematical approach. Many workers have tried this, without arriving at clearly defined results. In view of the complexity of the calculations required for the conventional receiver, this is hardly surprising. The other possibility is to make use of both measurements and calculations, in an attempt to gain an empirical physical insight into the mechanism on which the threshold effect is based. On the basis of this insight, one can then look for the causal relations which will allow calculation of the threshold for arbitrary system configurations. This approach has already borne fruit (Enloe [13]). Our investigations have also been carried out along these lines.

A large number of measurements will be discussed in the following chapters. It may strike the reader that a part of these measurements has been carried out on system configurations which would never be used for practical applications. However, this has been done on purpose, as it is precisely the comparison of theory and experiment which allows the limits of applicability of a given theoretical approach to be determined. Another reason is that study of the differences between measurement and calculations often leads to new insights which can be used for further extension of the theory.

In this thesis, most attention is paid to the study of the threshold mechanism. We shall see that the mechanism which determines the threshold of the FM receiver with feedback is basically the same as that determining the threshold of the receiver without feedback. This implies that there is no extra threshold mechanism in the FM receiver with feedback, in contradiction to what is claimed in many publications (Enloe [13]). As will be explained in detail in chapter 1, the threshold in "open-loop" FM receivers for unmodulated carrier waves occurs at the point where the instantaneous noise level after the IF filter exceeds the amplitude of the carrier wave during a certain percentage of the time. When the carrier wave is modulated, its frequency varies in accordance with the instantaneous frequency of the information signal; as a result, the carrier wave "moves up and down" in the IF filter. As a result of this shift, the carrier wave will be attenuated in a manner depending on the amplitude characteristic of the IF filter. The ratio of signal power to noise power will thus change, and will give rise to a change in the threshold. In the FM receiver with feedback, we find basically the same situation as in the open-loop FM receiver. However, the frequency of the carrier wave is now varied not only by the modulation from the baseband signal but also by the modulation present in the VCO carrier wave, due to the feedback of the noise. This effect causes some of the gain in threshold due to the feedback to be lost. As a first approximation we consider the frequency modulation as a quasi-stationary process. Comparison with the experiments will show that this approximation is sufficient as far as threshold calculations are concerned. Our theory about the threshold mechanism is developed in chapter 4.

On the basis of the above view, an attempt is made to relate the threshold of

the receivers with and without feedback to the modulation and feedback noise at the input of the VCO. A simple relation has been found on the basis of experiments, and the applicability of this relation has been tested with the aid of a very large number of further measurements. It will be shown that the threshold can be calculated for an arbitrary system configuration, with or without modulation of the carrier wave. The threshold calculations are described in chapter 4.

It will be shown that a very important design characteristic of FM receivers with frequency feedback is the distortion: the object is to obtain as low a threshold as possible at the maximum permissible distortion. This makes it necessary to calculate the distortion in the receiver with feedback. This calculation is given in chapter 3, while chapter 2 gives the calculation of the distortion in the receiver without feedback.

The low-frequency transfer functions of the FM receiver with feedback are used in many calculations. These may be needed e.g. for the calculation of the reduction in the bandwidth or for the determination of the amount of noise driving the VCO, or to investigate the influence of the feedback on the distortion. The low-frequency transfer functions of the FM receiver with feedback are dealt with in chapter 3, and those of the receiver without feedback in chapter 2.

Chapter 5 deals briefly with the synthesis of FM receivers with feedback and gives a specimen calculation of the threshold gain. This is an optimization process with a number of boundary conditions, which is dependent on many parameters. Since considerable interaction also exists between these parameters, it was not possible to arrive at a solution using one of the classical optimization methods. An optimization procedure which does lead to a solution is the trial-and-error approach. This approach can in principle be completely numerical, but in general it will prove more practical to optimize by a combination of measurement and calculation.

A great deal of literature has already appeared on the FM receiver with feedback [10–43]. Many different views on the threshold mechanism are represented in these publications. We do not share any of these views. One criticism which can be made in particular of the later publications is that they do not give a critical discussion of earlier papers. All the different views expressed thus lead a more or less independent existence, which does not make for great clarity. It seems to the author, therefore, that he should not give expression to a new point of view in this field without at the same time presenting a critical discussion of the earlier literature. It would not be possible to cover all the relevant literature in such a discussion; we have therefore restricted ourself to a thorough discussion of those works which seem to us to be the most important, namely those of Enloe [13,14], Frutiger [31] and Kühne [35,36]. A thorough consideration of these publications must deal not only with the papers in question as such, but also with their relation to the views expressed here. This

means that the discussion of the earlier literature cannot be given until our own views have been expounded. The discussion of the literature is therefore given in chapter 6.

The above-mentioned chapters are preceded by a general introduction, in which the principles of the conventional FM receiver and of the FM receiver with feedback are briefly described, and a number of definitions and conventions are given. This introduction is to be found in chapter 1.

1. PRINCIPLES OF THE OPEN-LOOP AND CLOSED-LOOP FM RECEIVER

1.1. The open-loop FM receiver

In this chapter we shall give a short survey of a number of aspects of frequency modulation (FM) which are of importance for our further considerations. First of all, we shall deal with the conventional FM receiver. The arguments for the use of frequency feedback under certain circumstances will follow from this discussion. This feedback is realized by frequency modulation of the local oscillator by the detected signal. The possibilities and problems of such feedback will be surveyed.

When frequency feedback is applied, we get a closed-loop system. From now on, therefore, we shall often refer to a conventional FM receiver as an open-loop receiver, and to one with frequency feedback as a closed-loop receiver. The closed-loop receiver is also sometimes called an FMFB receiver (Frequency Modulation with Feed-Back).

The block diagram of an open-loop FM receiver is shown in fig. 1.1. The

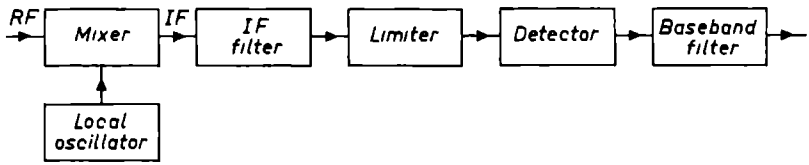

Fig. 1.1. Block diagram of an open-loop FM receiver.

radio-frequency (RF) signal is applied to the input of the mixer stage. This RF signal consists of the FM signal transmitted, together with any noise or other interference which may be present. Of the possible interfering signals, we shall only consider the noise here. The RF signal will be denoted from now on by $f_i(t)$. The frequency of the RF signal is shifted, by means of the mixer stage together with the local oscillator, to the intermediate-frequency (IF) range, where the signal is filtered and detected. The IF filter suppresses the interfering signals as well as possible, while the distortion of the desired signal which it produces must be kept within specified limits. The IF filter is followed by the limiter, which has the task of removing any amplitude modulation which may have been caused by the action of the filter and the interfering signals. In the detector, the frequency information from the FM signal is transformed into a baseband signal. The baseband filter which follows the detector ensures separation of the desired baseband signal from "out-of-band" interfering signals which may still be present.

The general expression for an FM signal without interference may be written:

$$f_i(t) = A \cos \{\omega_0 t + \psi_i(t)\}, \tag{1.1}$$

where ω_0 is the angular frequency of the carrier wave, and the derivative of $\psi_i(t)$ with respect to time is proportional to the baseband signal which modulates the carrier wave. The detector thus determines the derivative of the phase angle. For the sake of simplicity, we shall take the amplitude A as 1 from now on.

If the baseband signal is a cosine wave of angular frequency ω_m, then we find for $f_i(t)$:

$$f_i(t) = \cos \{\omega_0 t + m \sin (\omega_m t)\}, \tag{1.2}$$

where $m = \Delta\omega/\omega_m$ is the modulation index and $\Delta\omega$ is the maximum deviation of the angular frequency.

The derivative of the phase angle is $\omega_0 + \Delta\omega \cos (\omega_m t)$, and the detected baseband signal (with a detector constant of 1 V/Hz) is $\Delta\omega \cos (\omega_m t)$.

The total RF signal is the sum of the desired FM signal and the noise $n(t)$:

$$f_i(t) = \cos \{\omega_0 t + \psi_i(t)\} + n(t). \tag{1.3}$$

From now on, we shall assume that the noise at the input of the receiver has a normal distribution (Gaussian noise), a relatively small bandwidth, symmetrically disposed around the carrier-wave frequency and a flat power spectrum. We can then write (Panter [4])) for $f_i(t)$:

$$f_i(t) = \cos \{\omega_0 t + \psi_i(t)\} + n_c(t) \cos (\omega_0 t) - n_s(t) \sin (\omega_0 t), \tag{1.4}$$

where $n_c(t)$ and $n_s(t)$, respectively called the in-phase and quadrature component of the noise, are statistically independent, i.e. $E\,[n_c(t)\, n_s(t)] = 0$.

For the effective values, we may write:

$$E[n^2(t)] = E[n_c^2(t)] = E[n_s^2(t)]. \tag{1.5}$$

The operator E indicates the expected value.

If the total noise bandwidth about the carrier-wave frequency is B Hz, then $n_c(t)$ and $n_s(t)$ both occupy a bandwidth from 0 to $\frac{1}{2}B$ Hz, and both have a normal distribution and a flat power spectrum.

When the RF carrier wave is unmodulated, we can write for $f_i(t)$:

$$f_i(t) = [\{1 + n_c(t)\}^2 + n_s^2(t)]^{1/2} \cos \{\omega_0 t + \theta(t)\}, \tag{1.6}$$

where

$$\tan \{\theta(t)\} = \frac{n_s(t)}{1 + n_c(t)}. \tag{1.7}$$

The amplitude modulation is suppressed in the limiter. If moreover the

amplitude of the carrier wave is large compared with the effective noise level, we have:

$$\theta(t) \approx n_s(t). \tag{1.8}$$

The detected baseband noise is equal to $\theta'(t) \approx n_s'(t)$. If the carrier wave is modulated and no noise is present, then the detected baseband signal is equal to $\psi_i'(t)$. If both baseband signal and noise are present, the interaction between them must be taken into consideration.

Frequency modulation has better noise properties than amplitude modulation. If the noise power per unit bandwidth at the input of the receiver is the same for the two modulation systems, and the signal powers are also equal, then the signal-to-noise ratio after detection can be appreciably better with FM than with AM. The noise properties can be expressed by the characteristics giving the relationship between the signal-to-noise ratios (S/N) at the input and the output of the receiver. The best-known publications on these characteristics for open-loop FM receivers (the "open-loop S/N curves") are those of Rice [1,2]) and Stumpers [3]). We shall consider Stumpers' results by way of illustration. Some of his curves for a Gaussian IF filter are plotted in fig. 1.2. The signal-to-noise ratio at the input of the detector, $(S/N)_i$, is plotted as abscissa, and the signal-to-noise ratio after detection, $(S/N)_o$, as ordinate; both of these ratios are expressed in dB. The significance of the symbols used is as follows: S_i is the carrier-wave power after the IF filter, and N_i the noise power after the IF filter with flat noise at the input of the IF filter. S_o is the signal power after detection; this signal power depends on the frequency deviation. The curves given refer to a carrier wave modulated by a sine function such that the maximum frequency deviation is equal to half the bandwidth of the IF filter. N_o is the detected noise power in a baseband filter with rectangular amplitude characteristic and bandwidth B_{LF}. As parameter we use the quantity k, defined as the noise bandwidth of the IF filter divided by $2B_{LF}$.

With the given IF filter and the given normalizations, the S/N curves are completely determined by the value of k. However, if the amplitude characteristic of the IF filter changes, we get another family of curves.

For the S/N curves given in fig. 1.2, N_o has been calculated for an unmodulated carrier wave, and S_o for a modulated carrier wave without noise. The interaction between the noise and the modulation signal has not been taken into consideration here. These S/N curves are often called S/N curves for an unmodulated carrier wave. The S/N curves for modulated carrier waves do take this interaction into account; however, the calculations and measurements involved are very complex. For this reason, the S/N curves for unmodulated carrier wave are generally used in practice; they are quite accurate enough for most purposes, but there are some applications (e.g. for the closed-loop FM

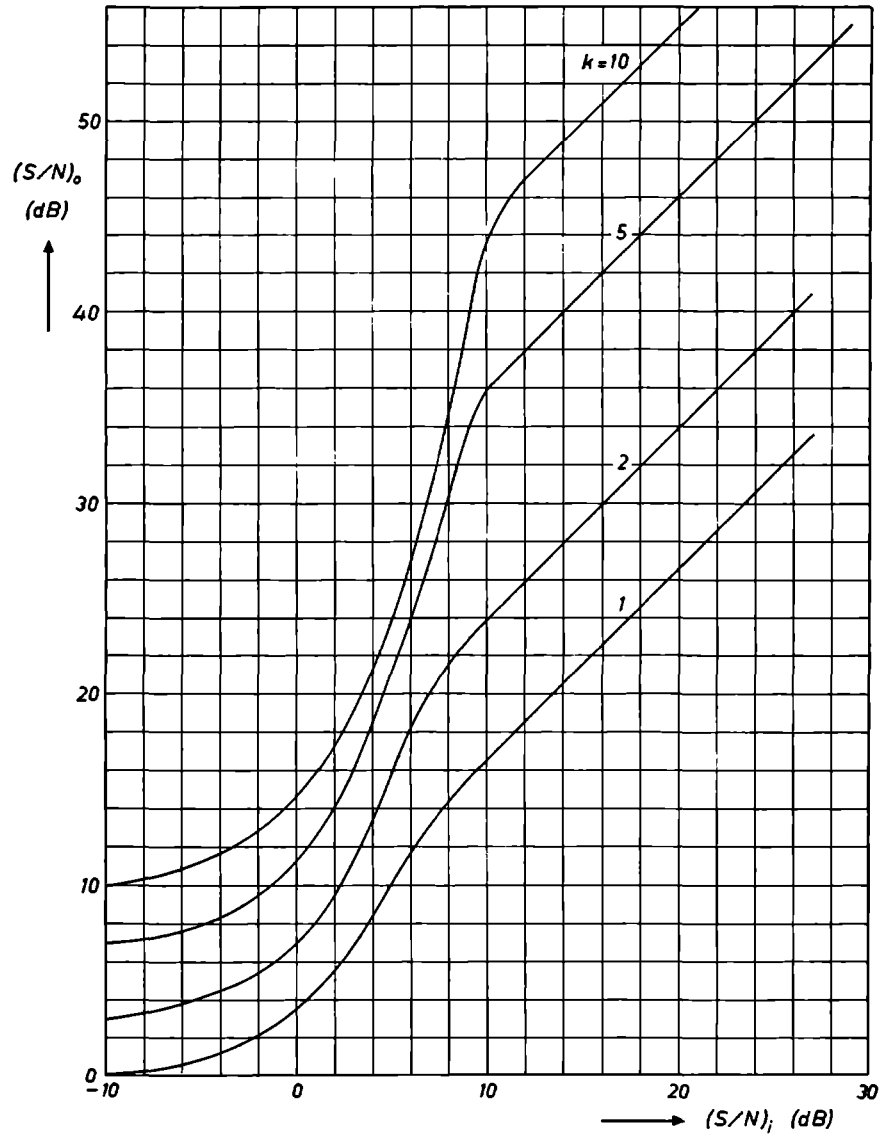

Fig. 1.2. $(S/N)_o$ as a function of $(S/N)_i$, with $k = B_{IF}/2B_{LF}$ as parameter. The IF filter has a Gaussian amplitude characteristic. N_i is normalized with respect to B_{IF}.

receiver) where an accurate knowledge of the S/N curves is required. We shall be returning to this point in chapter 4.

When two different FM receivers have to be compared, or an FM receiver has to be compared with receivers for signals modulated in other ways (e.g. AM), it may be more meaningful to refer the input noise N_i not to the band-

he IF filter but to a fixed bandwidth, e.g. twice B_{LF}. The S/N curv
ter case are obtained by shifting the curves of fig. 1.2 by 10 log k d
t; the result is plotted in fig. 1.3. By way of illustration, the S/N curv
-sideband amplitude modulation (DSBAM) is included in this figur
the carrier-wave power in the absence of modulation, and S_o is th
ignal power when the carrier wave is 100% modulated by a sir

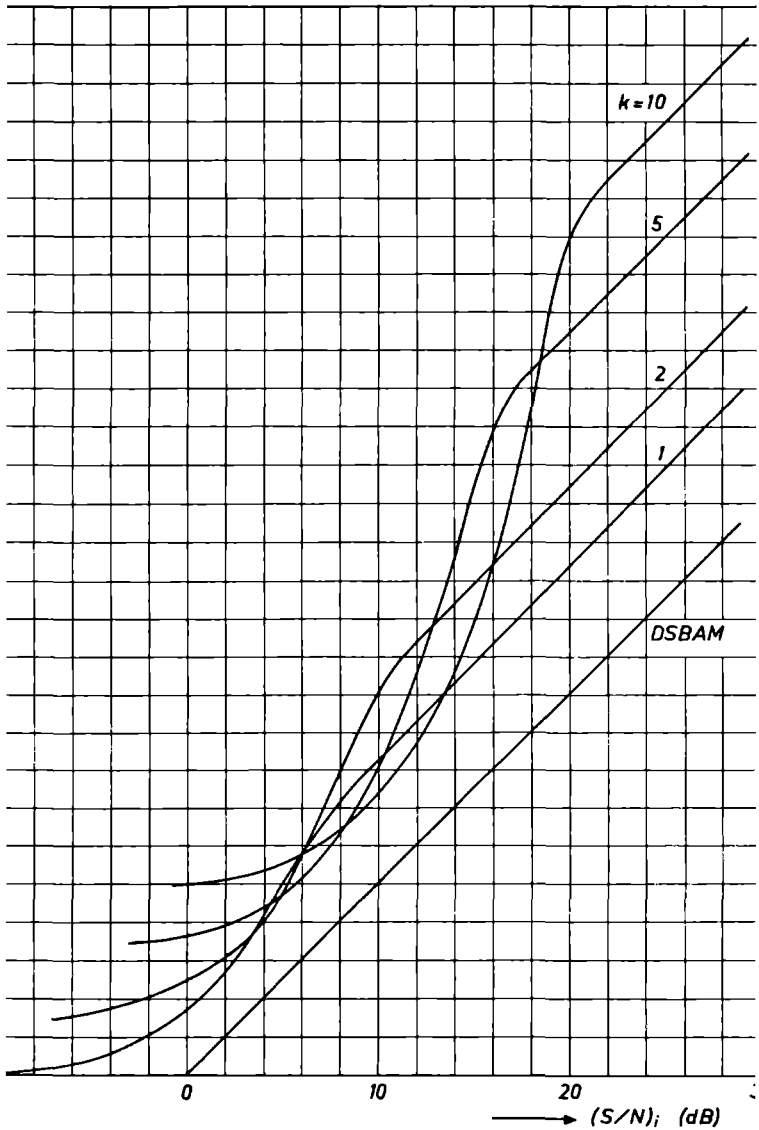

$N)_o$ as a function of $(S/N)_i$, with $k = B_{IF}/2B_{LF}$ as parameter. The IF filter h
amplitude characteristic. N_i is normalized with respect to $2B_{LF}$.

wave For AM we assume the detection to be coherent and the IF filter to have a rectangular amplitude characteristic.

In the literature, the modulation index m is often used instead of k Although k and m are related, it is incorrect to use m here, as there is no unambiguous relation between the modulation index m on the one hand and the bandwidths of the IF filter and the baseband filter on the other (this relation depends on the distortion requirement among other things)

The S/N curves can be split into two quite distinct parts. For high values of $(S/N)_i$, we find that $(S/N)_i$ and $(S/N)_o$ are proportional to one another, with a proportionality constant of unity Below a certain value of $(S/N)_i$, a threshold effect is produced as a result of which the slope of the curves increases Under these conditions, the signal is no longer satisfactorily detected; one reason for this is that nuisance from the noise at the output increases excessively (pulse noise) In order to give a well-defined reference point for measurements and calculations, we now state by way of definition that the threshold occurs at that value of $(S/N)_i$ at which $(S/N)_o$ differs by 1 dB from the extrapolated (S/N) curve for high values of $(S/N)_i$ It may be seen from fig. 1 2 that $(S/N)_i = 9$ dB is a fair approximation to the threshold

The S/N curve above the threshold can easily be calculated. For an IF filter with a rectangular transmission characteristic, we may write the well-known expression (Panter [4]):

$$(S/N)_o = 3\,\frac{\Delta f^2}{B_{\mathrm{LF}}{}^2}\,(S/N)_i, \tag{1 9}$$

where Δf is the maximum frequency deviation for modulation by a sine wave and N_i is the noise power in a bandwidth of $2B_{\mathrm{LF}}$ If Δf is equal to $B_{\mathrm{LF}}/2$, eq (1.9) becomes.

$$(S/N)_o = 3\,k^2\,(S/N)_i. \tag{1 10}$$

This equation represents the portions of the S/N curves for high values of $(S/N)_i$, as plotted in fig 1 3.

Since the improvement in the threshold is one of the main properties of the closed-loop FM receiver, we shall now devote some more attention to the mechanism which determines the threshold in the open-loop FM receiver When questions of distortion have to be considered, Carson's formula for the bandwidth of the IF filter is often used:

$$B_{\mathrm{IF}} = 2\,(\Delta f + f_m), \tag{1.11}$$

where $f_m = \omega_m/2\pi$ is the highest modulation frequency. However, this is a rough approximation which certainly cannot be used for optimum filter design,

though it is useful for showing the main lines of the relationship between B_{IF} and the frequency deviation.

If the instantaneous noise amplitude after the IF filter is less than the carrier-wave amplitude of the FM signal, then the detection is primarily with respect to the FM signal. In this case, the output noise power N_o is determined by the noise situated on both sides of the carrier wave, with a bandwidth of $2B_{LF}$. If however the instantaneous in-phase noise component becomes larger than the carrier while they are in anti-phase with each other and when at the same time the quadrature noise component passes through zero, then there will arise an extra phase jump of 2π radians, which after detection results in a noise pulse (Rice [3])). Now when noise pulses are produced too often (about one a second), the value of $(S/N)_o$ is influenced so much that we get a shift relative to the characteristic for high $(S/N)_i$. The chance that the instantaneous noise level will exceed the amplitude of the carrier wave depends on the effective noise level compared with the carrier-wave amplitude. It will be clear that, as far as the receiver is concerned, this ratio is determined by the bandwidth of the IF filter.

We thus see that the threshold is determined by the bandwidth of the IF filter, which in its turn is determined by the frequency deviation and the highest modulation frequency; this means that the threshold is fixed if the signal properties are given.

1.2. The closed-loop FM receiver

It will be clear from the above exposition that if we want to improve the S/N curves we will have to reduce the bandwidth of the IF filter, without increasing the distortion. One way of doing this is to make use of frequency feedback, as indicated in fig. 1.4. The output signal from the detector is now

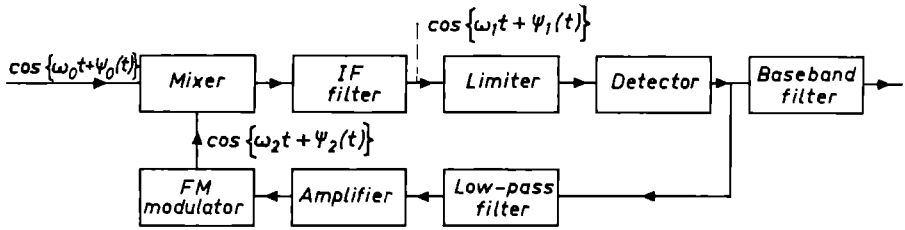

Fig. 1.4. Block diagram of an FM receiver with frequency feedback.

fed via a filter and an amplifier to the FM modulator which replaces the local oscillator in this set-up. This FM modulator is usually called a VCO (voltage-controlled oscillator). The mixer stage now receives two FM signals, namely the input signal cos $\{\omega_0 t + \psi_0(t)\}$ and the signal from the VCO, cos $\{\omega_2 t + + \psi_2(t)\}$, where ω_0 and ω_2 are the angular frequencies and $\dot{\psi}_0(t)$ and $\dot{\psi}_2(t)$

are proportional to the baseband signals by which the RF and VCO carrier waves respectively are modulated.

Since the IF filter only passes difference frequencies produced by the mixing, the FM signal appearing after the IF filter may be written:

$$\cos\{\omega_1 t + \psi_1(t)\} = \cos\{(\omega_0 - \omega_2)t + \psi_0(t) - \psi_2(t)\}. \tag{1.12}$$

If we ensure that the frequency deviation of the VCO is a linear function of the signal voltage after the linear detector, and if we can neglect other distortions and delays, then we may write:

$$\psi_2(t) = y\,\psi_1(t) = y\,\{\psi_0(t) - \psi_2(t)\}, \tag{1.13}$$

whence

$$\psi_1(t) = \frac{\psi_0(t)}{1+y}, \tag{1.14}$$

where y is the feedback factor of the FM receiver. Of course, the following relation now holds for the frequency deviations:

$$\dot{\psi}_1(t) = \frac{\dot{\psi}_0(t)}{1+y}. \tag{1.15}$$

If we further assume that the IF filter bandwidth is proportional to the frequency deviation, then we find that this bandwidth can be reduced by a factor of $(1 + y)$; and this lower bandwidth will correspond to an improved threshold.

The effect of feedback on the S/N curves may be seen from fig. 1.5. The

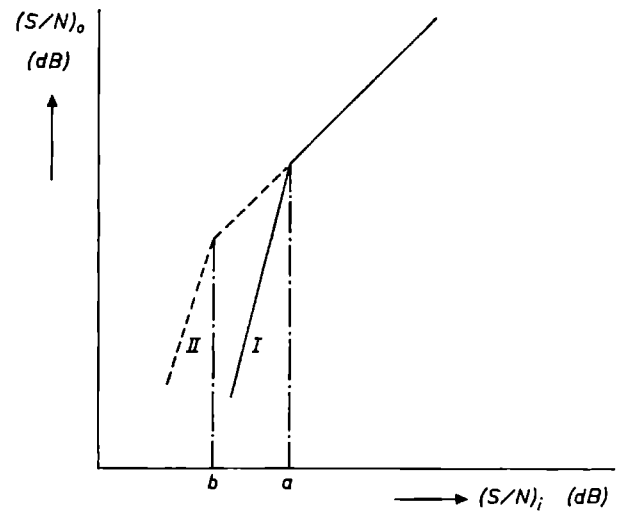

Fig. 1.5. $(S/N)_o$ as a function of $(S/N)_i$. Curve I is for the open-loop FM receiver, and curve II for the closed-loop FM receiver. The threshold gain is $(a - b)$ dB.

curve I is the S/N curve without feedback (with wide-band IF filter), and curve II with feedback (with narrow-band IF filter). The value of N_i is normalized with respect to the same bandwidth for both curves. At high values of $(S/N)_i$, the S/N curves coincide. The explanation for this is as follows. As a result of the feedback, the frequency deviation produced by the baseband signal is reduced by a factor $(1 + y)$. At high values of $(S/N)_i$ the frequency deviation due to the RF noise is of course also reduced by a factor $(1 + y)$. The ratio of the detected power of the baseband signal to the detected signal power is thus independent of the feedback. The only difference between the curves is that the thresholds occur at different values of $(S/N)_i$. The threshold improvement is defined as $(a - b)$ dB, where a and b are given in fig. 1.5.

It would thus appear as if the threshold could be improved without limit by increasing the feedback factor y and simultaneously reducing the bandwidth of the IF filter. However, there are a number of factors which limit the extent to which the threshold can be lowered.

In the first place, as the filtering in the loop is made sharper, or the feedback is stepped up, it becomes more difficult to keep the feedback constant throughout the given frequency band (baseband), or to keep the control loop stable. This places definite limitations on the permissible combinations of feedback factors and filters.

Secondly, the bandwidth of the IF filter cannot be reduced indefinitely: it should be at least twice the highest modulation frequency. The limit on the reduction of this bandwidth is determined by the associated increase in the distortion. We therefore need to gain a good insight into the relation between frequency deviation, modulation frequency, IF bandwidth and distortion. This relation is further complicated by the feedback, since on the one hand the frequency deviation within the loop now depends strongly on the system parameters, while on the other hand the distortion itself is influenced by the feedback. We shall see below that the frequency deviation and the distortion can be calculated from the closed-loop characteristics with the aid of the open-loop data. We shall therefore also need to consider how the open-loop distortion depends on the various system parameters. This is also of importance for the comparison of the noise properties of open-loop and closed-loop systems, which must be made on the basis of equal distortion. Another reason for studying the distortion is that the FMFB receiver can also be used to reduce distortion (here we have to take into account the noise properties).

Thirdly, the threshold found in practice is worse than would be expected from the considerations given above. A number of different explanations have been given for this. In agreement with Enloe [13]), we shall ascribe this effect to the noise which modulates the VCO; however, we shall differ from him in our explanation of the effects of the presence of noise.

A fourth factor is the influence of the modulation on the threshold. While

this effect is nearly always neglected in the literature, it is certainly not negligible. The modulation will thus also have to be considered in the course of our determination of the threshold.

Apart from the frequency feedback described above, a number of other ways of reducing the bandwidth of the IF filter have been proposed in the literature. The best-known of these are the variable filter which is supposed to follow the movement of the carrier wave [44–46]), supplying extra carrier wave to the FM signal [47,48]), and frequency division [49,50]). None of these methods has proved particularly successful. A much more promising method is to use the phase-locked loop as detector. Many publications have appeared about this subject (e.g. Viterbi [51]), Gardner [52])). We shall not consider these systems any further here.

1.3. Definitions and conventions

In the following chapters, we shall be developing theories to enable the calculation of the threshold and distortion of FMFB receivers, and testing these theories on a large number of system configurations with different parameters. It will be useful in this connection to work out a simple way of defining a system configuration clearly and unambiguously. We shall now lay down a number of conventions which will help in this respect. The following means can be used to vary the configuration of the FMFB receiver: the IF filter, the feedback filter, the baseband filter outside the loop and the feedback factor.

Three filters were tested as IF filter. We denote the bandwidth between the 3-dB points as B_{IF}. IF filter I is a simple LCR filter, while IF filters II and III consist of two simple LCR filters in cascade. In II, the quotient of the different bandwidths is 5, and in III it is 1. The separate filters are tuned at the same centre frequency. If we refer to the IF filter without any further qualification from now on, we shall mean IF filter I. All bandwidths and frequencies are normalized with respect to $B_{IF}/2$. One disadvantage of this is that the nice round values chosen for the measurements now get a rather arbitrary character.

A simple low-pass RC filter (one pole, no zero) is used in all cases for the feedback filter; only the 3-dB point of this filter is variable. This filter is characterized by x, which is defined as the 3-dB bandwidth divided by $B_{IF}/2$. The values of x used were 0·12, 0·29, 0·70, 1·05, 2·57 and ∞ (no feedback filter).

Apart from the above-mentioned filters, the presence of the amplifiers, the detector and the VCO also gives a filter effect in the loop. The over-all effect of these circuit elements more or less corresponds to a simple RC filter with its 3-dB point at $7B_{IF}/2$.

The feedback factor is characterized by the value of y, defined as the open-loop amplification for those frequencies at which the feedback is ideal. A system without feedback can be assigned the value $y = 0$.

The baseband filter outside the control loop is a filter with a rectangular transmission characteristic. Four baseband filters have been used for the measurements. Baseband filter I has a bandwidth of 0·57, II of 0·43, III of 0·86 and IV of 1·0 times $B_{IF}/2$. From now on, mention of a baseband filter without further qualification will be taken to refer to baseband filter I.

Apart from the above-mentioned system parameters, the threshold also depends on the signal modulating the RF carrier wave. We have dealt with three possibilities, namely, no modulation, modulation by a sine wave and modulation by low-frequency noise. Unless mention is made to the contrary, reference to modulation from now on will be taken to mean modulation by a sine wave. Such modulation is characterized by the modulation frequency and the maximum frequency deviation. We shall denote the maximum frequency deviation for modulation by a sine wave by Δf, and the corresponding angular-frequency deviation by $\Delta\omega$. The maximum frequency deviation at the RF input of the mixer stage, the output of the mixer stage and the output of the VCO is denoted by Δf_{IF}, Δf_{RF} and Δf_{VCO}, respectively. The maximum IF frequency deviation normalized with respect to $B_{IF}/2$ is made much use of in the measurements; this is denoted by z. When $z = 0$, there is no modulation. The modulation frequency f_m is also normalized with respect to $B_{IF}/2$, and is then written $f_{mn} = \omega_{mn}/2\pi$.

A system configuration can now be denoted by (x,y,z), where x denotes the value of the feedback filter, y that of the feedback factor and z the normalized maximum IF frequency deviation, as defined above. In all cases, use of IF filter I and baseband filter I is implied here.

We have mentioned in sec. 1.1 that a basis for the comparison of different S/N curves is given by normalizing the RF noise (N_i) for all curves to the same bandwidth. We have done this in our calculations. Since baseband filter I was used for most measurements, the RF noise has been normalized with respect to a bandwidth of $2\times0{\cdot}57\times B_{IF}/2 = 1{\cdot}14\ B_{IF}/2$, even when other baseband filters were used.

The detected signal power S_o depends on the frequency deviation. This is inconvenient for comparison of the thresholds of the S/N curves. In all figures, therefore, the S/N curves have been shifted vertically so that they coincide above the thresholds. The phrases "above the thresholds" and "to the right of the thresholds" will be taken to refer to values of $(S/N)_i$ higher than the value at which the threshold occurs. The horizontal and vertical scales are always chosen so that the slope of the curves above the threshold is 45°.

2. CALCULATION OF THE LF TRANSFER FUNCTIONS AND THE DISTORTION FOR THE OPEN-LOOP FM RECEIVER

2.1. Introduction

In this chapter we shall study the transmission properties of a filter followed by an ideal limiter, for frequency-modulated signals. We shall always consider the combination of filter and limiter together, though we shall often only mention the filter. As far as the transmission properties are concerned, we are only interested here in the influence of the filter with limiter on the baseband signal by which the carrier wave is modulated. This influence will be described with the aid of the low-frequency transfer function of the filter with limiter. This transfer function is given in the form of amplitude and phase characteristics, in which are plotted as functions of the frequency the amplitude ratio and the phase difference between a sinusoidal baseband signal with which the carrier wave is modulated and the first harmonic of the signal after detection. The filter and limiter are here assumed to be placed between an ideal modulator and an ideal detector. With the aid of this transfer function, we shall define the low-frequency model (LF) model of the filter plus limiter, such that with a given input signal, the LF model (or LF equivalent) gives the same output signal as the combination of modulator, filter, limiter and detector (apart from distortion).

The LF transfer function of a filter with transfer function $G(j\omega)$ can be written $G_L(j\omega_m;\Delta\omega)$, where ω_m is the angular frequency of the baseband signal and $\Delta\omega$ indicates that the LF transfer function can depend on the maximum frequency deviation (in which case it is non-linear). The situation is illustrated graphically in figs. 2.1 and 2.2. Figure 2.1 shows the real situation, and fig. 2.2 the LF model of this situation. The quantities a_1 and α_1 correspond to the amplitude and phase characteristics of the LF model, which are to be determined. In fig. 2.2 the distortion in the form of higher harmonics is not taken into consideration.

Wide use is made of the LF model in the literature on FMFB receiv-

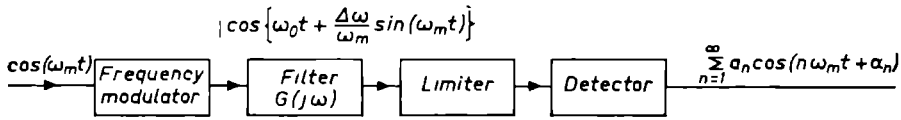

Fig. 2.1. Determination of the transmission properties of a filter plus limiter for an FM signal.

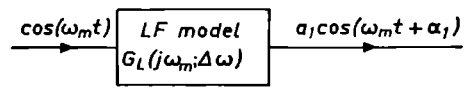

Fig. 2.2. LF model of a filter plus limiter for an FM signal.

ers [13,17,21,36]). The object of interest there is the LF model of the IF filter with limiter. In the publications in question, it is assumed that the frequency characteristics of this LF model are identical with the characteristics of the IF filter displaced until they pass through the origin of the frequency axis. However, a good insight into the relation between the transfer functions of the LF model and of the IF filter is not given. It has appeared from our measurements that for values of $\Delta\omega$ that are small compared with the bandwidth of the IF filter, the above identity is indeed found to a good approximation, but that at larger frequency deviations the discrepancy steadily increases. Further study thus proved necessary if we wanted to have a good insight into these LF transfer functions and to calculate them for all kinds of filters and all values of $\Delta\omega$.

It is also desirable to have a good insight into the distortion caused by the IF filter of an FM receiver (by distortion we understand non-linear distortion throughout). Since there is no difference in principle between the calculations for the first harmonic and those for higher harmonics, we shall discuss the calculation of the distortion together with that of the LF transfer functions.

Two methods are available for the calculation of the LF transfer functions and the distortion. In the first we work mainly in terms of time (differential equations, pulse responses), while in the second method we work mainly in terms of frequency (resolving the FM signal into a Fourier series). The first method (Carson and Fry [5]), Van der Pol [6]), Stumpers [7,8])) has led to analytic expressions which represent an approximate solution. This does give physical insight into the system involved, but the method does not lend itself well to numerical computation. Another drawback is that use is made of series which can give convergence problems. Further, it must be possible to describe all filters in terms of an analytic expression (either a transfer function or a differential equation). Further, this method is in principle not usable for filters whose transfer characteristics have only been determined by measurement.

The second method, in which we work in terms of frequencies, does not give any physical insight into the problem but it does allow exact numerical solutions to be obtained (albeit with a great deal of computation). Since computation is no problem in this case, we shall develop this method further here.

2.2. Calculation of the LF transfer functions and the distortion by a frequency method

In this method, the carrier wave modulated by a sine wave is resolved into its frequency components. We now calculate how the phase and amplitude of each component change on passage through the filter. After the filter, the components are combined again and detected in the normal way. The amplitude and phase of the detected signal are then compared with those of the signal

with which the carrier wave was modulated. When this has been done for a number of different frequencies, we get the LF transfer functions.

The determination of the transfer function of the LF model comes down in principle to determining the first harmonic of the detected signal. The higher harmonics can be determined in amplitude and phase in the same basic way as the fundamental.

The calculation proceeds as follows. The general form of a frequency-modulated signal is

$$\overline{f_i(t)} = \exp\,[j\,\{\omega_0 t + \psi_i(t)\}], \tag{2.1}$$

where the derivative of $\psi_i(t)$ is proportional to the baseband signal with which the carrier wave is modulated; $\psi_i(t)$ is thus the function carrying the information, and it is determined by the difference between the total phase angle and that of the carrier wave (by carrier wave we understand here the component with the central frequency ω_0).

Now let us suppose that the baseband signal by which the carrier wave is modulated is a cosine function with angular frequency ω_m. We may then write:

$$\overline{f_i(t)} = \exp\,[j\,\{\omega_0 t + m \sin(\omega_m t)\}]. \tag{2.2}$$

This expression can be expanded in the series

$$\overline{f_i(t)} = \exp(j\omega_0 t) \sum_{n=-\infty}^{\infty} J_n(m) \exp(jn\omega_m t) \tag{2.3}$$

$$= \sum_{n=-\infty}^{\infty} J_n(m) \exp\{j(\omega_0 + n\omega_m)\, t\}, \tag{2.4}$$

where $J_n(m)$ is the Bessel function of the first kind with index n and argument m.

This signal passes the filter for which we have to determine the transmission properties for the FM signal. Let us suppose that the transfer function $G(j\omega)$ of this filter can be written:

$$G(j\omega) = |G(j\omega)|\, \exp\{j\,\varphi(\omega)\}. \tag{2.5}$$

The general form of the signal behind this filter is

$$\overline{f_o(t)} = a(t) \exp\,[j\,\{\omega_0 t + \varphi(\omega_0) + \psi_o(t)\}], \tag{2.6}$$

where $a(t)$ is the amplitude modulation, resulting from the frequency modulation in the filter; $\psi_o(t)$ is again the part of the phase angle containing the information, and is again taken with respect to the phase of the carrier wave.

For a signal modulated by a sine function we find:

$$\overline{f_o(t)} = \sum_{n=-\infty}^{\infty} J_n(m)\,|G\{j(\omega_0 + n\omega_m)\}| \exp\,[j\,\{(\omega_0 + n\omega_m)\,t + \varphi(\omega_0 + n\omega_m)\}] \tag{2.7}$$

$$= \exp\,[j\,\{\omega_0 t + \varphi(\omega_0)\}] \sum_{n=-\infty}^{\infty} J_n(m)\,|G\{j(\omega_0 + n\omega_m)\}| \times$$

$$\times \exp\,[j\,\{n\omega_m t + \varphi(\omega_0 + n\omega_m) - \varphi(\omega_0)\}]. \tag{2.8}$$

This gives:

$$\psi_o(t) = \tan^{-1}\,\{x(t)\}, \tag{2.9}$$

where

$$x(t) = \frac{\sum_{n=-\infty}^{\infty} J_n(m)\,|G\{j(\omega_0 + n\omega_m)\}| \sin\,\{n\omega_m t + \varphi(\omega_0 + n\omega_m) - \varphi(\omega_0)\}}{\sum_{n=-\infty}^{\infty} J_n(m)\,|G\{j(\omega_0 + n\omega_m)\}| \cos\,\{n\omega_m t + \varphi(\omega_0 + n\omega_m) - \varphi(\omega_0)\}}. \tag{2.10}$$

$\psi_o(t)$ must now be differentiated with respect to time. $\psi_o(t)$ is periodic, with a frequency which corresponds to the modulation frequency ω_m. The same will then also be true of its derivative $\dot{\psi}_o(t)$. All the information we need can be obtained by expansion in a Fourier series. The first harmonic then gives the information about the transfer function, and the higher harmonics determine the distortion. All that remains to be done is to ensure that the values are normalized with respect to the right level. It is not difficult to combine the results of all these operations in one single equation. Since, however, this does not give any insight into the nature of the process involved, we shall not do that here.

We mentioned above that $\psi_o(t)$ must be differentiated and then expanded in a Fourier series. However, the calculations involved are simpler if $\psi_o(t)$ is expanded in a Fourier series first, after which each term of the Fourier series is differentiated separately. The Fourier series may be written:

$$\psi_o(t) = \sum_{r=1}^{\infty} A_r \cos\,(r\omega_m t) + \sum_{r=1}^{\infty} B_r \sin\,(r\omega_m t), \tag{2.11}$$

where

$$A_r = \frac{\omega_m}{\pi} \int_0^{2\pi/\omega_m} \psi_o(t) \cos\,(r\omega_m t)\,\mathrm{d}t, \tag{2.12}$$

$$B_r = \frac{\omega_m}{\pi} \int_0^{2\pi/\omega_m} \psi_o(t) \sin(r\omega_m t)\, \mathrm{d}t, \tag{2.13}$$

or

$$\psi_o(t) = \sum_{r=0}^{\infty} C_r \sin(r\omega_m t + \alpha_r), \tag{2.14}$$

where

$$C_r = (A_r^2 + B_r^2)^{1/2}, \tag{2.15}$$

$$\alpha_r = \tan^{-1}\left(\frac{A_r}{B_r}\right). \tag{2.16}$$

We now have to differentiate the Fourier series:

$$\dot{\psi}_o(t) = \sum_{r=1}^{\infty} D_r \cos(r\omega_m t + \alpha_r), \tag{2.17}$$

where

$$D_r = C_r\, r\, \omega_m. \tag{2.18}$$

In our calculation of $\dot{\psi}_o(t)$ we assumed, without explicit mention of the fact, that the detector constant is 1. If we now make the same assumption about the modulator constant, this means that the baseband signal at the input of the modulator will be

$$\Delta\omega \cos(\omega_m t). \tag{2.19}$$

The first harmonic of the resulting baseband signal after detection is then:

$$D_1 \cos(\omega_m t + \alpha_1). \tag{2.20}$$

We therefore write for the transfer function $G_L(j\omega_m;\Delta\omega)$ of the LF model:

$$|G_L(j\omega_m;\Delta\omega)| = \frac{D_1}{\Delta\omega} = \frac{C_1\,\omega_m}{\Delta\omega}, \tag{2.21}$$

$$\arg\{G_L(j\omega_m;\Delta\omega)\} = \alpha_1. \tag{2.22}$$

For low values of the modulation index m, eq. (2.10) can give a direct insight into the LF transfer functions of some filters. When $m \ll 1$, we have $J_0(m) \approx 1$ and $J_1(m) \ll 1$, while the other Bessel functions can be taken as zero. If we further assume that $|G(j\omega_0)| = 1$ and $\varphi(\omega_0) = 0$, we may write (2.10):

$$\begin{aligned} x(t) \approx\ & -J_1(m)\, |G\{j(\omega_0 - \omega_m)\}| \sin\{-\omega_m t + \varphi(\omega_0 - \omega_m)\} + \\ & + J_1(m)\, |G\{j(\omega_0 + \omega_m)\}| \sin\{\omega_m t + \varphi(\omega_0 + \omega_m)\}. \end{aligned} \tag{2.23}$$

Assuming also that the filter is symmetrical about the frequency ω_0, we may write (2.23):

$$x(t) \approx 2\, J_1(m)\, |G\{j(\omega_0 + \omega_m)\}| \sin \{\omega_m t + \varphi(\omega_0 + \omega_m)\}. \qquad (2.24)$$

Since $J_1(m) \ll 1$, we have further $\psi_o(t) \approx x(t)$. Without the filter, we would have found:

$$\psi_o(t) \approx x(t) \approx 2\, J_1(m) \sin (\omega_m t). \qquad (2.25)$$

Comparison of (2.24) with (2.25) shows that in this case the amplitude and phase characteristics of the LF model agree very well with those of the IF filter, shifted along the frequency axis until they pass through the origin.

For the case that the modulation frequency and the maximum frequency deviation are small relative to the bandwidth of the filter, the same result can be obtained by using the first two terms of the series as given by Van der Pol and Stumpers.

When calculating the LF transfer functions, we determine the relation between the baseband signals before modulation and after detection. However, we may also be interested in the LF transfer function in relation to the frequency deviation. Since there is a single-valued relationship between the baseband signal and the frequency deviation (via the modulator constant and the detector constant), we still get the same LF transfer functions in this case. However, the input signal of fig. 2.2 now becomes $\Delta\omega \cos (\omega_m t)$, and the output signal becomes $a_1\, \Delta\omega \cos (\omega_m t + \alpha_1)$.

2.3. Results of the calculations

The aim of this part of the investigation was to develop a computer programme which could be used for the calculation of the LF transfer functions and the distortion for all possible combinations of filters, maximum frequency deviations and modulation frequencies. The first application of this programme was the calculation of the LF transfer functions of the IF filters occurring in FMFB receivers. From the point of view of stability these filters may only give a slight phase shift and, consequently, they may only have a slight amplitude drop. However, from the point of view of noise, the cut-off of the IF filter at the edges of its frequency band must be as sharp as possible. As we shall see below, the simple LCR filter offers a reasonable compromise between these two demands. The first measurements and calculations were therefore carried out on the simple LCR circuit (IF filter I).

The LF transfer functions were calculated and measured for a large number of values of the normalized frequency deviation z. The agreement between theory and experiment is good. The calculated amplitude characteristics are plotted in fig. 2.3. In this figure we have also plotted (curve I), by way of comparison, the amplitude characteristic of the IF filter (shifted along the frequency axis

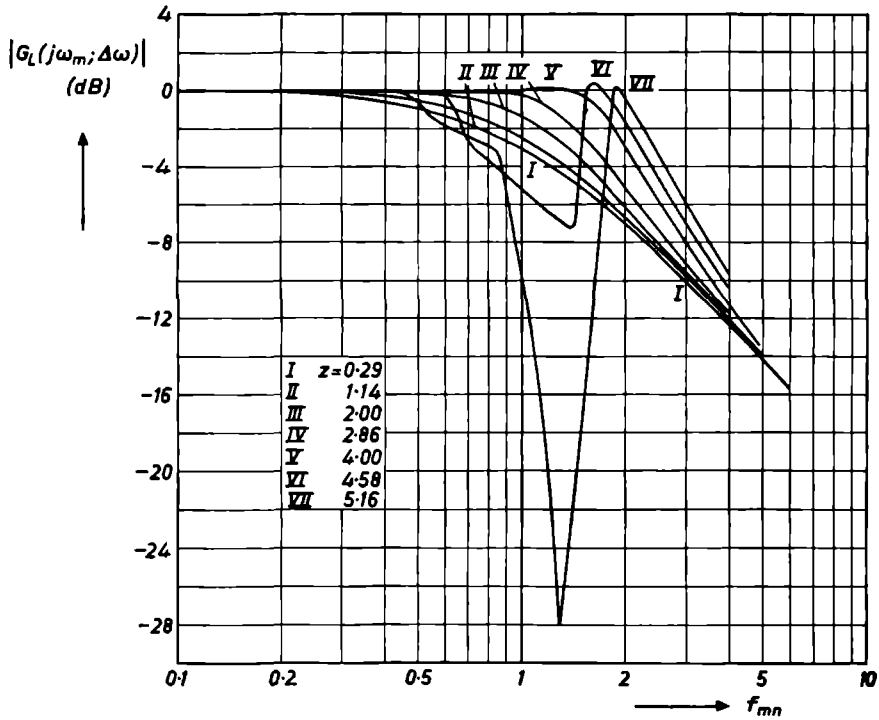

Fig. 2.3. LF amplitude characteristics for a simple LCR filter (IF filter I) plus limiter for a sinusoidally modulated FM signal, with the maximum frequency deviation as parameter. Curve I coincides with the amplitude characteristic of IF filter I, shifted along the frequency axis until its centre coincides with the origin.

so that the central frequency of the filter coincides with the origin). For $z < 1$, the agreement between the shifted amplitude characteristic of the IF filter and the amplitude characteristic of the LF model is good. However, for larger frequency deviations the difference gradually becomes greater and greater, until at very high values of z the two curves get entirely different forms. A minimum is then found in the LF transfer characteristics. The presence of this minimum can be explained as follows. If the modulation index remains high at high modulation frequencies, the frequency spectrum will consist of a number of components of interest. However, the higher sidebands will be strongly suppressed by the filter. Depending on the value of the modulation index m, $J_1(m)$ (which determines the amplitude of the first pair of sidebands) can become small. Without filter, this would be compensated for by the other odd sideband pairs, but with the filter this compensation is only slight. It will be clear that under these circumstances the signal after the IF filter will be distorted, with a high content of higher harmonics and not much fundamental. By way

of example we may mention (see fig. 2 3) that for $z = 5{\cdot}16$ we get a minimum at the normalized modulation frequency $f_{mn} = 1{\cdot}34$; m is then equal to 3·8. We find $J_1(3{\cdot}8) = 0$, while $J_3(3{\cdot}8)$ is 0·41, nearly its maximum value.

The LF transfer function $G_L(j\omega_m;\Delta\omega)$ will be called linear as long as its amplitude characteristics differ by less than 0·5 dB from those for $\Delta\omega \to 0$. For IF filter I (simple LCR filter), $G_L(j\omega_m;\Delta\omega)$ can still be called linear as long as $z < 1$.

The measured and calculated values of the distortion were also compared. The results for the third harmonic of IF filter I are plotted in fig. 2.4; the full

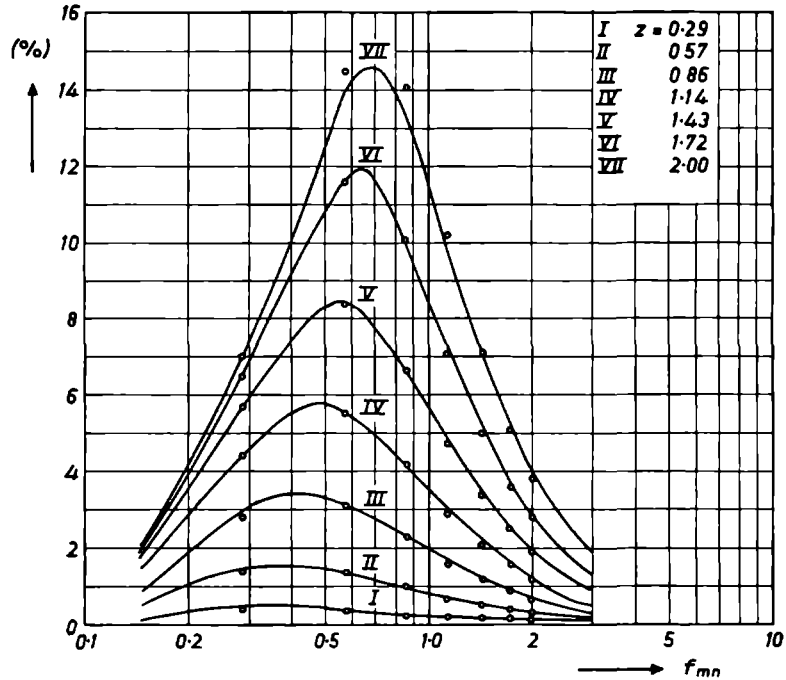

Fig 2 4 Percentage 3rd-harmonic distortion as a function of the modulation frequency of the FM signal The normalized maximum frequency deviation z is taken as parameter, and the filter is a simple LCR filter The full curves represent the results of the measurements, and the circles the results of the calculations

curve represents the measured distortion, while the circles indicate the calculated values It will be seen that the agreement is excellent.

The LF transfer function $G_L(j\omega_m;\Delta\omega)$ is found by modulating the carrier wave with a single sine wave. In practice, the baseband signal does not consist of a sine wave, but of a signal $r(t)$ (proportional to $\dot{\psi}_i(t)$) with a certain bandwidth. By analogy with the results obtained for linear electrical networks, we

could write for the signal $c(t)$ (proportional to $\dot{\psi}_o(t)$) obtained by passing the carrier wave modulated by $r(t)$ through the IF filter and the detector:

$$C(j\omega_m) = R(j\omega_m)\, G_L(j\omega_m;\Delta\omega), \tag{2.26}$$

where we take the linear transfer characteristic for $G_L(j\omega_m;\Delta\omega)$, and $R(j\omega_m)$ and $C(j\omega_m)$ are the Fourier transforms of $r(t)$ and $c(t)$, respectively.

Equation (2.26) was experimentally tested for IF filter I by modulating the carrier wave with a number of sine waves at the same time, which gives a noise-like signal (a mathematical description of an FM signal modulated with noise has been given by Middleton [9]). It was found that, as long as the effective deviation corresponding to the composite baseband signal did not exceed a certain value, the amplitudes of the individual sine waves after detection corresponded to the attenuation calculated with the linear transfer function $G_L(j\omega_m;\Delta\omega)$ for all the separate components. The maximum value of the effective frequency deviation for which eq. (2.26) is still valid was found to be at least equal to half the bandwidth of the IF filter. It was also found that this value depends strongly on the bandwidth of the baseband signal used. The permissible frequency deviation was found to be lowest for bandwidths up to a bit more than half the bandwidth of the IF filter. As the bandwidth increased further, the permissible frequency deviation also increased. This is not surprising, in view of the form of the distortion characteristics of fig. 2.4.

2.4. LF model of the FM receiver

So far, we have only been talking about the LF model of a filter with limiter. In principle, we should give the LF model of the detector too. However, the influence of the detector can always be made negligible with respect to that of the IF filter, the bandwidth and form of whose frequency characteristics are primarily determined by external factors (characteristics of the signal to be received, interference, threshold properties). We shall therefore not pay any further attention here to the calculation of the LF transfer functions of the detector.

2.5. Conclusion

The determination of the LF model and the distortion of an FM receiver is a simple matter. The filter used in such a receiver can be described in terms of an analytic expression, or by means of measured values. The complexity of the filter is not important in this connection; it only influences the computing time. The Fourier method of calculation used does not in itself give any physical insight into the mechanism involved, as is done to a certain extent by the calculations of Carson and Fry, Van der Pol and Stumpers. On the other hand, it is such an easy matter to repeat the calculations for various values of the parameters that an insight can easily be gained in this way.

3. CALCULATION OF THE LF TRANSFER FUNCTIONS AND THE DISTORTION FOR THE CLOSED-LOOP FM RECEIVER

3.1. Introduction

As we saw in chapter 1, when dealing with the FMFB receiver it is very important to know the influence of the feedback on the frequency deviation, the distortion and the noise driving the VCO. We shall see below that in order to calculate this influence, we need to know the closed-loop characteristics. Just as with the open-loop FM receiver, we shall develop an LF model which reproduces the basic features of the system. The LF transfer functions can then be determined from this model. In this connection, we can again e.g. look for the relation between a sine wave used to modulate a perfect modulator and the first harmonic of the signal after detection by the receiver in question.

The feedback in the FMFB receiver is applied in order to obtain a reduction in the frequency deviation. It would thus seem to be an obvious idea to calculate the LF transfer function in relationship to the frequency deviation. The maximum frequency deviation and the amplitude of the baseband sine wave are unambiguously related to one another via a transformation from frequency to voltage. The closed-loop LF transfer functions determined with respect to the frequency deviation are thus equal (save for a constant factor) to those determined with respect to the baseband sine function. The phase deviation may also be of importance in certain cases; this can be obtained from the frequency deviation by integration.

We shall first describe in detail how the transfer function with respect to the frequency deviation can be calculated. A number of calculations and measurements of closed-loop characteristics will then be given. The second part of this chapter is concerned with distortion. It will be shown that the closed-loop distortion can be calculated from the open-loop distortion with the aid of the above-mentioned closed-loop characteristics.

3.2. LF transfer functions related to the frequency deviation

The block diagram of the FMFB receiver has already been given in fig. 1.4. The corresponding LF model is shown in fig. 3.1. The significance of the sym-

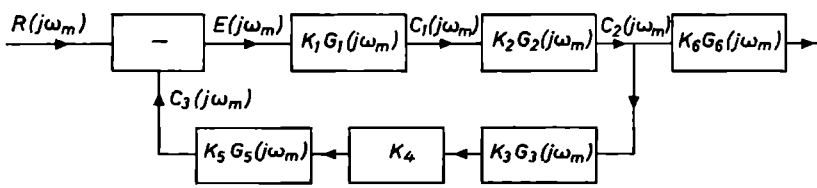

Fig. 3.1. Block diagram of the LF model of the FMFB receiver in relation to the frequency deviation.

bols and the various blocks will become clear from the following argument.

The general form of an FM signal is

$$f_i(t) = \cos \{\omega_0 t + \psi_i(t)\}. \tag{3.1}$$

The frequency deviation is proportional to $\dot{\psi}_i(t)$, and the Fourier transform of $\dot{\psi}_i(t)$ is equal to the input variable $R(j\omega_m)$ of the LF model.

Two FM signals are mixed in the mixer stage. With the aid of this stage, together with the IF filter, the frequency deviations of the two signals are subtracted. The mixer stage thus becomes a subtractor in the LF model.

$K_1\, G_1(j\omega_m) \equiv G_L(j\omega_m;\Delta\omega)$ is the transfer function of the LF model of the IF filter with limiter. This transfer function has already been discussed in chapter 2. For values of $\Delta\omega$ less than $B_{IF}/2$, the characteristics for $K_1\, G_1(j\omega_m)$ correspond to the IF filter characteristics, shifted towards the origin. For larger values of $\Delta\omega$, the transfer function must be calculated separately for each value of $\Delta\omega$.

In the detector, the frequency deviation is transformed into a voltage variation. The transfer function $G_L(j\omega_m;\Delta\omega)$ of the IF filter with limiter is determined with an ideal detector. However, the effect of a non-ideal detector can be taken into consideration without changing the method basically. In this case, we have to determine the transfer function of the IF filter, limiter and detector together. Alternatively, the transfer function of the detector can be determined separately, and multiplied by $G_L(j\omega_m;\Delta\omega)$. Of course, this last step is only possible if the detector itself is free of distortion; if this is not the case, second-order effects will be neglected in this way. The detector used in an FMFB receiver always has a very wide frequency band and is practically distortion-free. The separation of the blocks will then not give rise to difficulties. The LF transfer function of the detector will be written $K_2\, G_2(j\omega_m)$. The frequency dependence of this function can be made very small, and will therefore be neglected from now on. K_2 is the detector constant, of dimensions V/Hz.

$K_3\, G_3(j\omega_m)$ and $K_6\, G_6(j\omega_m)$ are the transfer functions of the low-pass filters. The filter with transfer function $K_3\, G_3(j\omega_m)$ serves to give the control loop the desired properties, while that with $K_6\, G_6(j\omega_m)$ is used to give the desired frequency characteristic after the control loop.

K_4 is an extra amplification or attenuation, and is used for adjustment of the feedback factor.

$K_5\, G_5(j\omega_m)$ is the transfer function of the VCO. This can also be replaced by a factor K_5, of dimensions Hz/V.

$G_1(0)$, $G_2(0)$, $G_3(0)$, $G_4(0)$, $G_5(0)$ and $G_6(0)$ are always taken as equal to 1, and K_1, K_3 and K_6 will generally be equal to 1 too.

In fig. 3.1 the closed-loop FM system is reduced to a conventional feedback system in which the various quantities characterizing the different parts of the

system can easily be expressed in terms of one another. For example, it is evident that as long as $G_L(j\omega_m;\Delta\omega)$ is linear, the following equations will hold:

$$C_2(j\omega_m) = R(j\omega_m)\frac{K_1\,G_1(j\omega_m)\,K_2\,G_2(j\omega_m)}{1 + H(j\omega_m)}, \tag{3.2}$$

$$C_3(j\omega_m) = R(j\omega_m)\frac{H(j\omega_m)}{1 + H(j\omega_m)} = R(j\omega_m)\,F(j\omega_m), \tag{3.3}$$

$$E(j\omega_m) = R(j\omega_m)\,\{1 - F(j\omega_m)\} = R(j\omega_m)\frac{1}{1 + H(j\omega_m)}, \tag{3.4}$$

where

$$H(j\omega_m) = y\,G_1(j\omega_m)\,G_2(j\omega_m)\,G_3(j\omega_m)\,G_5(j\omega_m) \tag{3.5}$$

and where

$$y = K_1\,K_2\,K_3\,K_4\,K_5 \tag{3.6}$$

is the feedback factor.

3.3. Calculated and measured closed-loop amplitude characteristics

If we want to calculate the distortion (sec. 3.4) and the noise power at the input of the VCO (sec. 4.4), we need to know the closed-loop amplitude characteristic. The presence of the filters in the loop is certainly likely to give rise to increased response at certain modulation frequencies, even if it does not lead to actual instability. As a result, the maximum frequency deviation $\Delta\omega_{IF}$ may become so great that $G_L(j\omega_m;\Delta\omega)$ becomes non-linear. The closed-loop characteristics are thus dependent on the maximum frequency deviation $\Delta\omega_{RF}$. This is illustrated in fig. 3.2, in which are plotted a number of measured and calculated closed-loop amplitude characteristics for a system with IF filter I, feedback factor $y = 5$ and a feedback filter with $x = 0{\cdot}5$. The value of $\Delta\omega_{RF}$ is adjusted for each amplitude characteristic so that, for the modulation frequencies for which the feedback is ideal (i.e. where there is no amplitude drop and phase shift in the open-loop system), z is equal to a fixed value which we shall call z_i from now on ($z_i = \{\Delta f_{RF}/(y + 1)\}/\frac{1}{2}B_{IF}$). The value of $\Delta\omega_{RF}$ chosen in this way is maintained for all modulation frequencies. Since the feedback is only ideal within a limited range of modulation frequencies, outside this range z will be greater than z_i. The modulation frequency is plotted along the horizontal axis of fig. 3.2. The vertical scale is in dB, and the values are expressed in terms of the value with ideal feedback. Curve I gives the (coincident) amplitude characteristics for $z_i = 0{\cdot}05$ and $z_i = 0{\cdot}1$. Curves II and III give the amplitude characteristics for $z_i = 0{\cdot}2$ and $z_i = 0{\cdot}5$, respectively. These curves were measured directly after the detector. Curve IV gives the amplitude characteristic measured after the mixer,

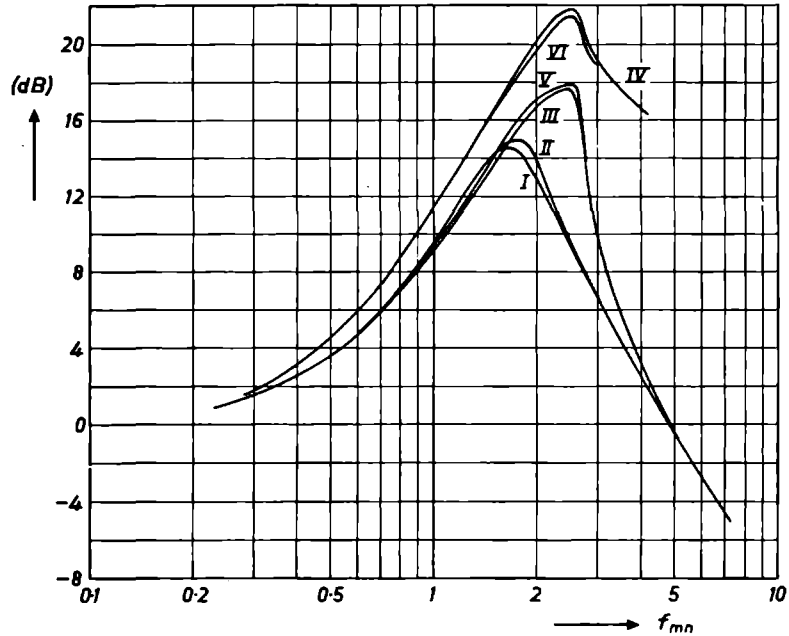

Fig. 3.2. Measured and calculated closed-loop amplitude characteristics for the FMFB receiver with IF filter I, $x = 0{\cdot}5$, $y = 5$ and various values of z_i.
I : measured characteristic after the detector for $z_i = 0{\cdot}1$,
II : measured characteristic after the detector for $z_i = 0{\cdot}2$,
III: measured characteristic after the detector for $z_i = 0{\cdot}5$,
IV: calculated characteristic after the detector for $z_i = 0{\cdot}5$,
V : measured characteristic after the mixer for $z_i = 0{\cdot}5$,
VI: calculated characteristic after the mixer for $z_i = 0{\cdot}5$,

for $z_i = 0{\cdot}5$. This measurement has been carried out with a separate limiter and detector. It may be seen that the magnitude and position of the maximum response are highly dependent on the value of z_i, but that at low values of z_i the characteristics coincide. The reason for this is that the maximum frequency deviation for the characteristic with $z_i = 0{\cdot}1$ is less than $\frac{1}{2}B_{IF}$, so that in this case the LF transfer function $G_L(j\omega_m;\Delta\omega)$ of the IF filter is still linear (see fig. 2.5). At the setting with $z_i = 0{\cdot}5$, on the other hand, the maximum frequency deviation can become so large that $G_L(j\omega_m;\Delta\omega)$ becomes highly nonlinear.

When calculating the closed-loop characteristics, we must make a distinction between large and small signals, as the linearity of $G_L(j\omega_m;\Delta\omega)$ depends on this.

The calculation of the amplitude characteristics for the linear system is a very simple matter. The calculation of $G_L(j\omega_m;\Delta\omega)$ has already been dealt with. The rest of the loop consists of low-frequency components, which are normally known. The amplitude and phase characteristics of the open loop

are thus known, and can be used directly for calculation of the closed-loop characteristics.

The calculation of the closed-loop amplitude characteristics for the non-linear system is somewhat more complicated, since in principle we need to know $\Delta\omega_{IF}$ before we can calculate $G_L(j\omega_m;\Delta\omega)$, while a knowledge of $G_L(j\omega_m;\Delta\omega)$ is required for the determination of $\Delta\omega_{IF}$. This problem can be solved by an iterative method, since we can always write for the LF frequency spectra at the mixer stage (see fig. 3.1):

$$E(j\omega_m) = R(j\omega_m) - C_3(j\omega_m). \tag{3.7}$$

For the calculation of the amplitude characteristic, the RF carrier wave is considered to be modulated by a cosine wave. $\Delta\omega_{RF}$ is kept constant for all modulation frequencies, but $\Delta\omega_{IF}$ and $\Delta\omega_{VCO}$ vary with the modulation frequency. If $\Delta\omega_{IF}$ is known, $\Delta\omega_{VCO}$ can be calculated with the aid of the open-loop amplitude characteristic (the form of the amplitude and phase characteristics of $G_L(j\omega_m;\Delta\omega)$ depends on the value of $\Delta\omega_{IF}$). The calculation proceeds as follows. For a given modulation frequency and a given $\Delta\omega_{RF}$, we estimate the corresponding value of $\Delta\omega_{IF}$. The value of $\Delta\omega_{VCO}$ is now calculated from this value of $\Delta\omega_{IF}$, and then the value of $\Delta\omega_{RF}$ is calculated with the aid of eq. (3.7). The value of $\Delta\omega_{RF}$ obtained in this way must agree with the value chosen initially, if the choice of $\Delta\omega_{IF}$ was correct. If this is not the case, the value chosen for $\Delta\omega_{IF}$ must have been wrong, and we choose a new value in the light of the difference found. This iterative process is continued until the values of $\Delta\omega_{RF}$ agree. It is of course possible to start with a completely arbitrary value of $\Delta\omega_{IF}$, but in general it will not be too difficult to make a reasonable estimate of this quantity. This process must be repeated for each new modulation frequency.

Once the closed-loop amplitude characteristic of $\Delta\omega_{IF}$ is known, it is a simple matter to calculate the closed-loop amplitude characteristic behind the IF filter. This is done by multiplying the characteristic for $\Delta\omega_{IF}$ at each modulation frequency by the value of $G_L(j\omega_m;\Delta\omega)$ for that modulation frequency and the value of $\Delta\omega_{IF}$ in question.

The results of a number of calculations are plotted in fig. 3.2. Curves IV and VI represent the closed-loop amplitude characteristics for $z_l = 0{\cdot}5$, after the detector and after the mixer respectively. The corresponding measured values are found in curves III and IV. As will be seen, the agreement is good.

3.4. Calculated and measured values of the closed-loop distortion

When a frequency-modulated carrier wave passes the IF filter, distortion can be produced; this manifests itself as higher harmonics and intermodulation products. It goes without saying that in the FMFB receiver, the distortion is fed back too. This makes it necessary to calculate the closed-loop distortion.

The distortion caused by the IF filter can be described as follows. If a carrier wave modulated by an information signal with a frequency spectrum $E(j\omega_m)$ is present at the input of the IF filter, then at the output of the IF filter the carrier wave is modulated by the sum of two frequency spectra, $C_1(j\omega_m)$ and $A(j\omega_m)$, where $C_1(j\omega_m)$ is the spectrum of the information signal ($C_1(j\omega_m) = E(j\omega_m)\, G_L(j\omega_m;\Delta\omega)$ as long as $G_L(j\omega_m;\Delta\omega)$ is linear), while $A(j\omega_m)$ is the spectrum of the non-linear distortion caused by the IF filter. This approach thus treats the distortion for the closed-loop system as an independent interference function. While $A(j\omega_m)$ is dependent on $E(j\omega_m)$, the way this function is affected by the feedback system is independent of $E(j\omega_m)$. The diagram of fig. 3.1 thus becomes that of fig. 3.3 for the present case. It is further assumed

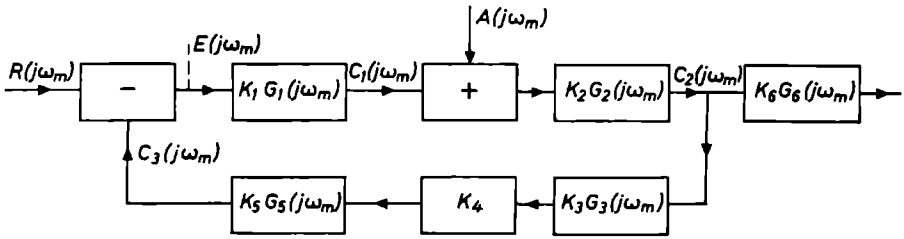

Fig. 3.3. Block diagram of the LF model of the FMFB receiver with the distortion $A(j\omega_m)$ shown as a separate interference function.

that the IF filter does not give rise to any distortion in the form of higher harmonics and intermodulation products.

As long as $G_L(j\omega_m;\Delta\omega)$ is linear, the following equations hold:

$$C_2(j\omega_m) = \frac{K_1\, G_1(j\omega_m)\, K_2\, G_2(j\omega_m)}{1 + H(j\omega_m)}\, R(j\omega_m) + \frac{K_2\, G_2(j\omega_m)}{1 + H(j\omega_m)}\, A(j\omega_m), \tag{3.8}$$

$$E(j\omega_m) = \frac{1}{1 + H(j\omega_m)}\, R(j\omega_m) - \frac{K_2\, G_2(j\omega_m)\, K_3\, G_3(j\omega_m)\, K_4\, K_5\, G_5(j\omega_m)}{1 + H(j\omega_m)}\, A(j\omega_m), \tag{3.9}$$

while for modulation frequencies at which the feedback is ideal we may write:

$$C_2(j\omega_m) = \frac{K_2}{1 + y}\, R(j\omega_m) + \frac{K_2}{1 + y}\, A(j\omega_m), \tag{3.10}$$

$$E(j\omega_m) = \frac{1}{1 + y}\, R(j\omega_m) - \frac{y}{1 + y}\, A(j\omega_m). \tag{3.11}$$

We may thus state that the influence of the feedback on the distortion (at least for ideal feedback) may be considered in the first place by division of the RF frequency deviation by $(1 + y)$; the reduced IF frequency deviation now

leads to the distortion, and as a result of the feedback this distortion is again divided by $(1 + y)$. With non-ideal feedback, the factor $1 + y$ is replaced by a frequency-dependent term.

In order to verify the above line of reasoning, a number of measurements and calculations were carried out for an RF carrier wave modulated by a sine wave; the 3rd-harmonic distortion was considered. The results of a number of measurements and calculations are plotted in fig. 3.4. The system involved

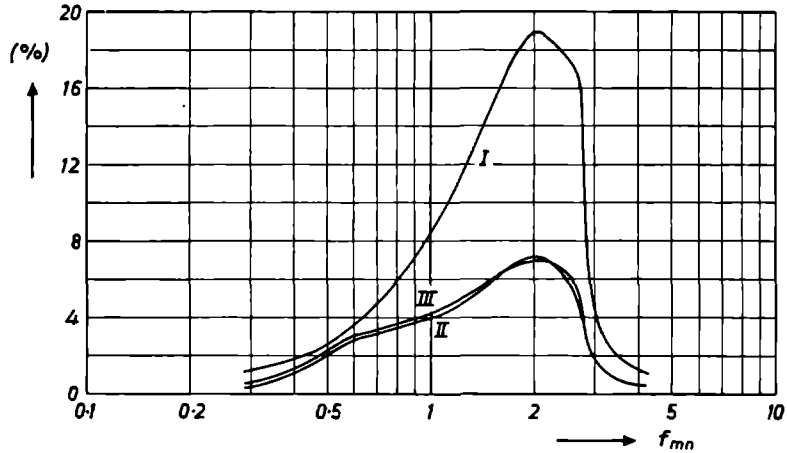

Fig. 3.4. 3rd-harmonic distortion in the FMFB receiver for $x = 0{\cdot}5$, $y = 5$ and $z_i = 0{\cdot}5$.
I : Calculated open-loop distortion after the detector, corresponding to the calculated value of $\Delta\omega_{IF}$ in the closed-loop system;
II : closed-loop distortion after the feedback filter, calculated from I;
III: measured closed-loop distortion after the feedback filter.

has IF filter I as the IF filter, a feedback filter with $x = 0{\cdot}5$, a feedback factor of $y = 5$ and $z_i = 0{\cdot}5$. The amplitude characteristics for this configuration have been given in fig. 3.2. The significance of the curves plotted is as follows. Curve I represents the calculated open-loop distortion corresponding to the calculated value of $\Delta\omega_{IF}$ for the closed-loop system (after the detector). Curve II gives the calculated closed-loop distortion (after the feedback filter), while curve III gives the measured closed-loop distortion (after the feedback filter).

Comparison of curves II and III shows that there is excellent agreement between the measured and calculated values, which implies that the model described can be regarded as correct.

4. CALCULATION OF THE THRESHOLD OF THE CLOSED-LOOP FM RECEIVER

4.1. Introduction

In this chapter we shall develop a theory which makes it possible to calculate the threshold of the closed-loop FM receiver. For this purpose, we will show that FM can be regarded as quasi-stationary. The mechanism determining the threshold in the FMFB receiver will be shown to be the same as that determining the threshold in the FM receiver without feedback. We shall see that the closed-loop thresholds for modulated RF carrier waves as well as for unmodulated ones can be calculated with the aid of a single experimentally determined figure. This theory is tested on a large number of system configurations obtained by varying the IF filter, the feedback filter, the feedback factor and the baseband filter outside the loop. We shall also indicate the range within which this theory is valid, and the reasons for the differences between theory and measurement outside this range. Before getting down to the calculation of the threshold, we shall give a general discussion of the S/N curves of the FMFB receiver and shall consider how they can in principle be compared with those of the corresponding open-loop FM receivers.

4.2. Discussion of the S/N curves of the closed-loop FM receiver

The open-loop S/N curves have already been discussed in chapter 1. We shall now discuss the S/N curves of the closed-loop FM receiver. We shall further look for a criterion with the aid of which the open-loop and closed-loop S/N curves can be compared with one another, thus allowing definition of the threshold gain. We shall only discuss the S/N curves for unmodulated carrier waves for the moment. The detected signal power S_o is thus measured or calculated in the absence of noise. A sine wave is used as baseband signal.

We shall determine the closed-loop S/N curves with reference to fig. 4.1. The frequency characteristics of the IF filter are given. The transmission characteristic of the baseband filter will again be taken to be rectangular; the bandwidth of this filter is also given. The input noise is normalized with respect

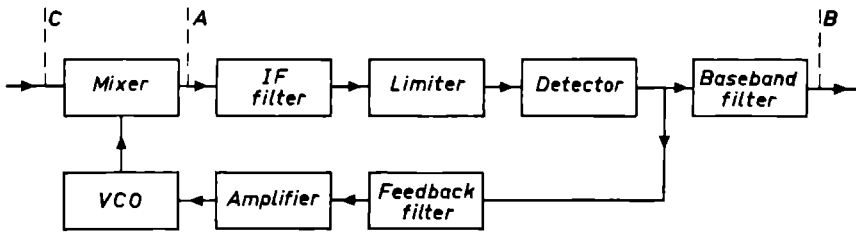

Fig. 4.1. Block diagram of the FMFB receiver.

to the bandwidth of the baseband filter. To begin with, we assume ideal feedback. The feedback factor is y.

First of all, we investigate the open-loop system between A and B. The S/N curves for this portion depend on the form of the amplitude characteristic of the IF filter, and are further determined by the parameter k. S_o is calculated for a given value of the frequency deviation Δf_{IF}. Now we close the loop. If Δf_{IF} remains constant, then Δf_{RF} must be equal to $(1 + y)\,\Delta f_{IF}$. Above the threshold we only have to consider the quadrature noise. As a result of the feedback, the quadrature noise will also be reduced. The S/N curve of the system between C and B must in any case have the same form as that for the open-loop system between A and B, since the filters have not changed. However, the quadrature noise is reduced by a factor $(1 + y)$ between C and A; the closed-loop S/N curve is thus obtained by shifting the open-loop S/N curve a distance $20 \log (1 + y)$ dB to the left. Δf_{IF} remains constant, so that no vertical shift is necessary.

In fig. 4.2, curve I is the open-loop S/N curve between the points A and B, and curve II that for an idealized feedback system. However, there is no reason why the threshold of the closed-loop receiver between the points C and B should appear at a lower value of $(S/N)_i$ than that of the open-loop system between the points A and B, because the threshold is mainly caused by the in-phase noise. The closed-loop threshold can thus never lie to the left of the open-loop threshold; in the most favourable case, the thresholds will coincide. This line of reasoning leads to curve III as a theoretical bound (for the IF and baseband filters used). The threshold is at the same value of $(S/N)_i$ as that of curve I, while above the threshold the curve is obtained by shifting curve I by $20 \log (1 + y)$ to the left. In reality, the closed-loop threshold lies more to the right, as indicated by curve IV. The reason for this (the feedback of the noise) and the calculation of the shift will be dealt with in this chapter.

This curve for the system with feedback must now be compared with the S/N curve of an open-loop system which detects the input RF signal in an equivalent way. The distortion gives a good criterion for comparison here. Both the closed-loop system (with narrow-band IF filter) and the open-loop system (with wide-band IF filter) should detect the RF signal with equal distortion. At present, the CCIR makes requirements for the sum of the intermodulation noise and the detected RF noise in the worst channel. This means that we must look for IF filters with frequency characteristics which offer an optimum compromise between the distortion and the position of the threshold. This compromise will depend on the amount of distortion which is considered permissible. The bandwidths of the IF filters, and hence the values of the parameter k, will also have to be determined. In the literature, Carson's rule is often used for this purpose. However, in the present case Carson's rule only gives an approximation, since the exact form of the distortion and of the frequency

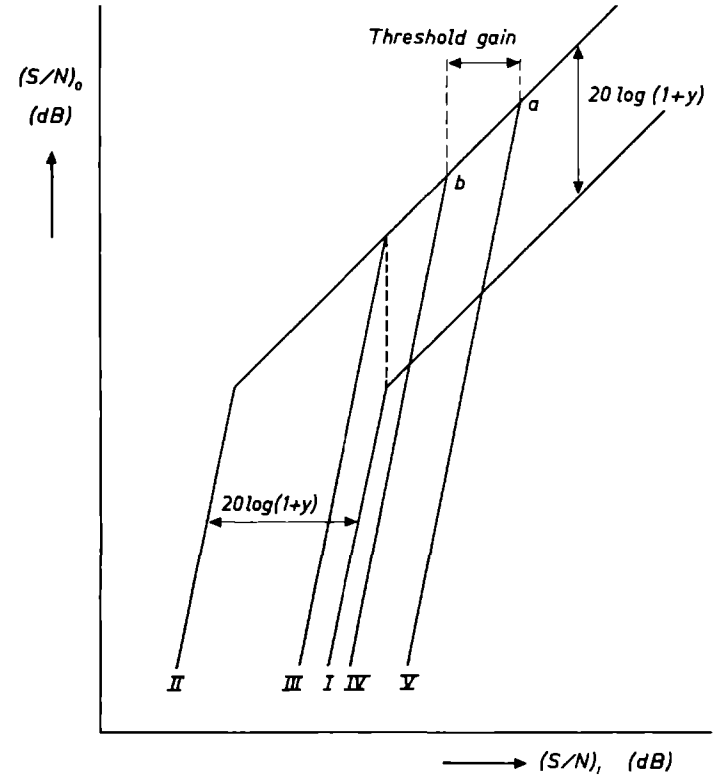

Fig. 4.2. Sketch of a number of closed-loop and open-loop S/N curves.
I : Open-loop curve;
II : curve I, shifted 20 log (1 + y) dB to the left;
III: theoretical limiting curve for the FMFB receiver;
IV: S/N curve found for the FMFB receiver in practice;
V : curve found in practice for a comparable receiver without feedback.

characteristic of the IF filter is not taken into consideration. However, what is even more important, is that in the system with feedback the distortion is also fed back, so that if the distortion requirement is maintained the bandwidth of the IF filter will be influenced. This bandwidth has in its turn a strong influence on the threshold, as will be demonstrated. This means that little can be said in advance about the value of k for the various systems. It will be clear, however, that the value of S_o will be 20 log (1 + y) dB greater than that for the open-loop system between the points A and B of fig. 4.1. However, the detected noise will remain practically constant as long as the system is above the threshold so that only a narrow noise band about the carrier wave is detected (the form of the amplitude characteristic of the IF filters has little influence on this). It follows that the S/N curve for the corresponding open-loop system to the right of the threshold is found by shifting curve I of fig. 4.2 upwards by a distance 20 log (1 + y) dB. This gives curve V. The threshold of curve V

depends on the IF filter used and on the value of k. The threshold gain is the horizontal projection of the line segment ab. To the right of the thresholds, curves IV and V coincide.

In fig. 4.2, curve V is drawn to the right of curve IV. This means that there really is a threshold gain. Depending on the purpose for which the feedback is realized (improved threshold or improved distortion), however, it may also happen that curve V is to the left of curve IV, in which case we have a threshold loss.

So far, we have assumed the feedback to be constant over the whole bandwidth of the baseband filter. In general, however, this will not be the case. The reduction in frequency deviation will then be less than with ideal feedback. In other words, we shall have to reckon with an effective feedback factor which is always less than y.

The steep portions of curves I–V have been drawn parallel to one another. This has only been done for the sake of elegant presentation, and has no practical significance.

It will be clear that there is no point in talking about threshold gain if we do not first of all specify the distortion requirements.

In order to make it possible to use the curves of fig. 4.2 more easily for the purposes of our further argument, we shall give some of them names:
I will be called the open-loop S/N curve;
IV will be called the closed-loop S/N curve;
V will be called the comparative open-loop S/N curve.

The thresholds will be given corresponding names; the concept of the open-loop threshold will be used particularly often. As we have explained, this means the threshold for the part of the receiver between A and B in fig. 4.1, without feedback; or the threshold of curve I of fig. 4.2. Unless special mention is made to the contrary, we shall assume in this connection that the IF carrier wave is unmodulated.

The reader will now have an idea about the comparison of the S/N curves for the open-loop and closed-loop systems, and the determination of the threshold gain. In a concrete situation, the calculations will have to be carried out in full for the system in question; the distortion specifications will play an important part in this connection. We have already shown how the influence of the feedback on the distortion should be calculated. In this chapter, we shall consider the calculation of the threshold.

4.3. Study of the quasi-stationary nature of frequency modulation

4.3.1. *Introduction*

The threshold calculations described in this chapter are based to a great extent on the realization that a frequency-modulated signal can be regarded

as quasi-stationary during its passage through the IF filter. This means that the carrier wave is shifted through the frequency range of the IF filter in accordance with the instantaneous frequency. It will be useful to start by showing that it really is possible to regard FM in this way. We shall do this with reference to measurements and calculations. The measurements show the influence of the modulation frequency on the S/N curves. In the "calculations", a number of open-loop and closed-loop S/N curves will be determined. These calculations are based on the results of measurements, as calculation of these curves on a purely theoretical basis would involve a great deal of work. However, this method will not be used for the final threshold calculations, but only to give an insight into the real nature of the modulation process.

4.3.2. *Measurements on the open-loop FM receiver*

The open-loop S/N curves have been measured for a large number of combinations of maximum frequency deviations and modulation frequencies. IF filter I was used as the IF filter. The baseband filter had a variable bandwidth, which was matched to the modulation frequency. The normalized maximum frequency deviation z and the normalized modulation frequency f_{mn} varied from 0 to 3. Inspection of the results of these measurements has shown that the S/N curves for a given value of z are practically independent of f_{mn} as long as both z and f_{mn} are less than 1. For $z < 1$ and $f_{mn} > 1$, the thresholds are found to shift to the left with increasing f_{mn}, while for $z > 1$ the thresholds shift first to the right with increasing f_{mn} and then to the left again. The shift of the thresholds to the left with increasing modulation frequency can be ascribed to the departure of the frequency-modulation process from its quasi-stationary state, while the shift to the right is connected with the distortion. We shall be returning to the relation between the S/N curves and the distortion in sec. 4.12.

It will be seen from fig. 2.4 that the distortion at $z = 1$ can amount to more than 5%, which is inacceptable for most applications. Summing up, we may state that for combinations of maximum frequency deviations and modulation frequencies for which the distortion is less than 5%, the S/N curves are independent of the modulation frequency both above and below the threshold. This implies that, with this constraint, for the purposes of calculating S/N curves the frequency-modulation process can be regarded as quasi-stationary.

4.3.3. *Calculation of the open-loop S/N curves for a modulated RF carrier wave*

These calculations are based on the experimental results plotted in fig. 4.3, which gives the measured noise (in dB) in baseband filter I as a function of the frequency shift of the carrier wave from the centre frequency of IF filter I. The noise level with the carrier in the middle is taken as 0 dB. The measured curves are plotted with $(S/N)_i$ as a parameter. For example, we see that at $(S/N)_i =$

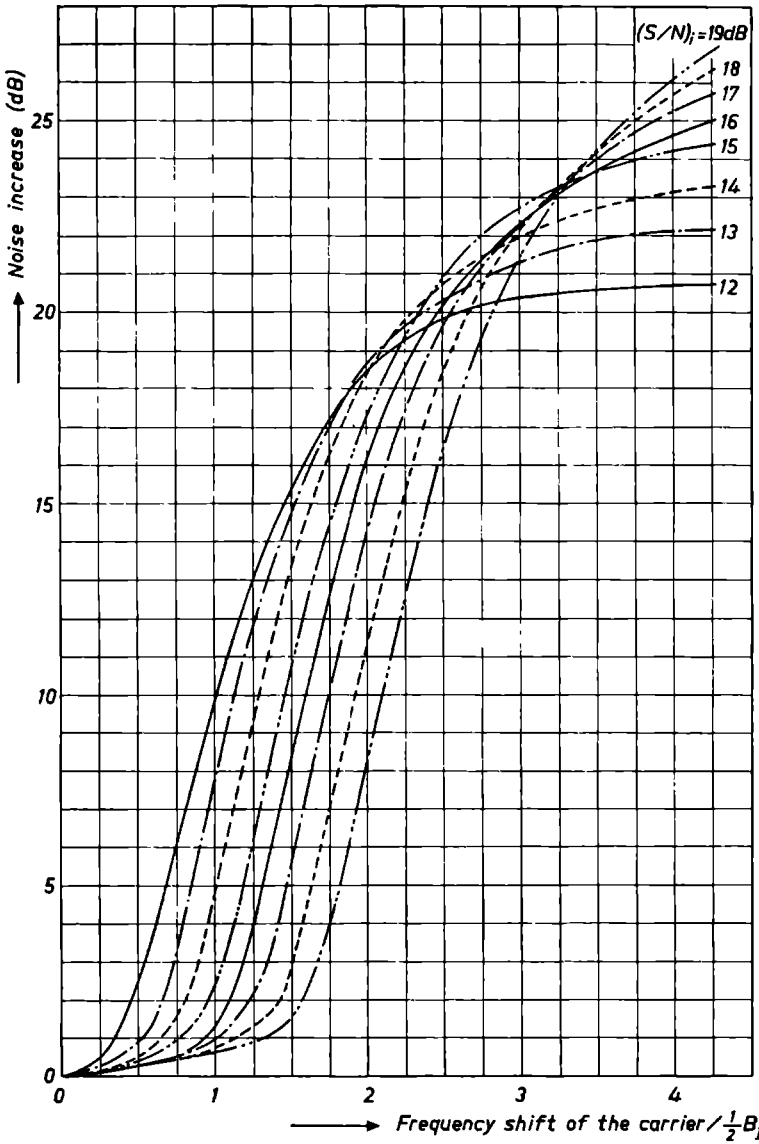

Fig. 4.3. Noise increase in baseband filter I as a function of the normalized frequency shift of the carrier wave from the middle of the frequency range of IF filter I, with $(S/N)_i$ as parameter.

18 dB, shifting the carrier wave away from the middle of the filter's frequency band $2B_{IF}/2$ Hz increases the noise in the baseband filter by 11·5 dB with respect to the situation with the carrier wave in the middle. The value of $(S/N)_i$ remains at 18 dB, but the carrier wave is attenuated as a result of the frequency shift. In this example, the attenuation of the carrier wave is in fact so great

that the system now operates under the threshold. The form of the curves can be explained as follows. For small frequency shifts, the increase in noise is slight, and is only due to the asymmetrical detection of the noise spectrum. When the frequency shift reaches a certain value, the carrier wave will be attenuated so much that the threshold is reached; any further frequency shift will now cause the detected noise to increase sharply. It will be clear that with higher values of $(S/N)_i$, the threshold is only reached with greater frequency shifts of the carrier wave. With very large frequency shifts, the curves tend to flatten off, because the carrier wave is now so strongly attenuated that it has less and less influence on the detected noise. The curves were measured under static conditions (each measured for a fixed frequency shift).

The S/N curves for modulated carrier waves can now be calculated as follows. We assume the carrier wave to be modulated by a sine wave. The frequency of the carrier wave thus varies sinusoidally, so that the carrier wave can be regarded as moving up and down in the frequency band of the IF filter. At a given value of $(S/N)_i$, we can read from fig. 4.3 the increase in noise corresponding to a given shift of the carrier wave. We now divide the sine wave up into a number of time intervals; in each interval, the frequency deviation is taken as constant. This value of the deviation corresponds to a certain frequency shift of the carrier wave and hence, at given $(S/N)_i$, to a certain increase in the noise level. The increase in noise is averaged over all time intervals, to give the mean noise increase for sinusoidal modulation. This process must be

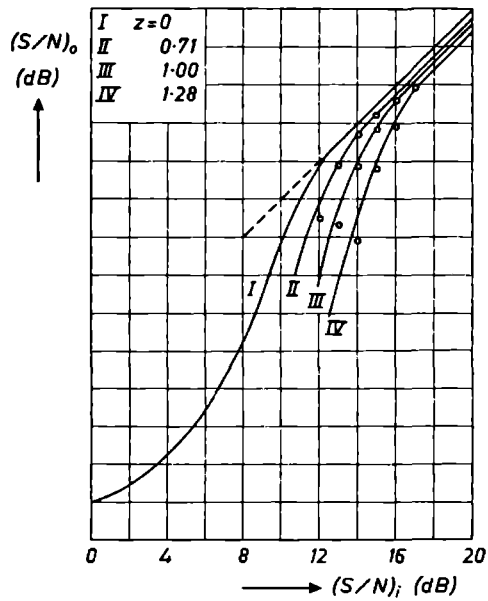

Fig. 4.4. Open-loop S/N curves for modulated carrier wave. The full curves represent the results of the measurements, and the circles the results of the calculations.

repeated for each value of $(S/N)_i$. The results for normalized maximum frequency deviations of $z = 0{\cdot}71$, $1{\cdot}0$ and $1{\cdot}28$ are plotted in fig. 4.4, for a modulation frequency of $f_{mn} = 0{\cdot}43$. The full curves represent measured results, and the circles give the calculations. It will be seen that the agreement between measurement and calculation is good. For example, if the maximum frequency deviation used for the calculation of curve IV had been reduced by 2%, the calculated curve would have coincided with the measured one.

During the writing of this thesis we discovered that for the open-loop system the idea of a variable carrier amplitude, caused by the instantaneous frequency which varies in accordance with the modulation, has also been dealt with by Ryskin [53]). In his publication he states that use must be made of the dynamic and not the static IF response. However, no proof is given of the correctness of his ideas and there is a rather large discrepancy between his theoretical and experimental results.

4.3.4. *Calculation of the closed-loop S/N curves for unmodulated RF carrier waves*

We have seen in chapter 1 that two frequency-modulated signals are applied to the inputs of the mixer stage of an FMFB receiver, viz. the RF signal and the VCO signal. The RF signal consists of the FM signal to be received, plus noise. This noise is also detected and is fed to the VCO together with the detected baseband signal. The VCO signal is only frequency-modulated, not amplitude-modulated. When calculating the effect of the modulation on the detected noise in the open-loop system, we have only taken into account the variation of the instantaneous frequency resulting from the imposed information modulation, not that resulting from the RF noise. We follow the same procedure in the present case and as long as the RF signal is not modulated with information, we assume that all the imposed modulation comes from the noise modulating the VCO carrier wave (the VCO noise). The VCO noise is thus assumed to cause a shift in the frequency of the carrier wave. Of course, there is a correlation between the VCO noise and the RF noise. Yet, we shall assume that, in the first instance, the VCO noise is only responsible for the shift of the carrier, while the RF noise remains responsible for the noise-increase curves as given in fig. 4.3. The theoretical and experimental results will show whether this assumption needs further refinement.

At high values of $(S/N)_i$, the IF filter can be assumed to be linear for the FM noise; the VCO noise will then have a normal distribution (assuming that the RF noise has a normal distribution). Depending on the effective value of the VCO noise, we can determine a number of levels, each of which has a certain probability of being occupied. Each such level corresponds to a certain frequency deviation and a certain frequency shift of the carrier wave. This thus again allows us to calculate the mean noise increase.

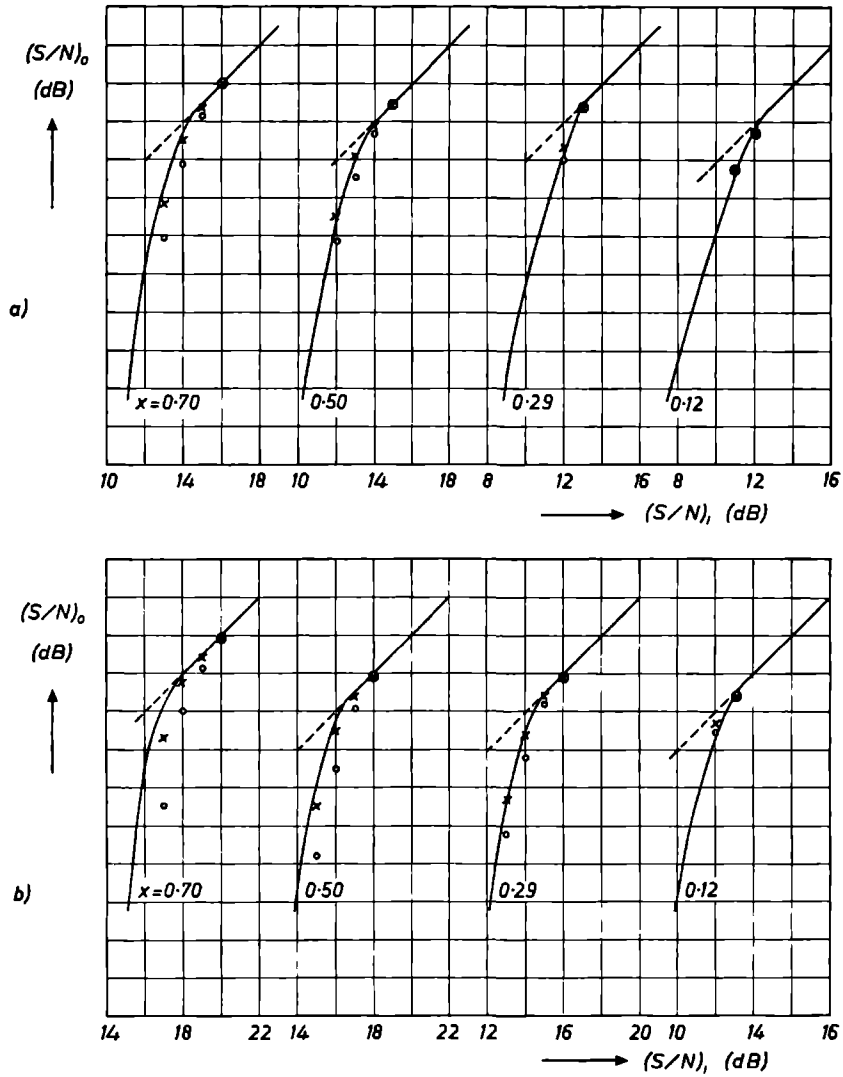

Fig. 4.5. Closed-loop S/N curves for unmodulated carrier waves with (*a*): $y = 4$ and (*b*): $y = 8$. The full curves represent the results of the measurements, the circles the 100% calculation and the crosses the 97% calculation.

The measured S/N curves of fig. 4.5 are plotted for feedback factors of $y = 4$ and $y = 8$, and for four feedback filters (with $x = 0{\cdot}70$, $0{\cdot}50$, $0{\cdot}29$ and $0{\cdot}12$) at each feedback factor. The calculated values are indicated by circles; these values were determined starting from the measured VCO noise. The agreement between the measured and calculated S/N curves is not bad for a first approximation. One of the reasons for the observed differences will lie in

the assumption that there is no correlation between the VCO modulation and the RF noise. However, the difference might also be explained by the dependence of the S/N curves on the modulation frequency (the noise driving the VCO is wide-band with respect to the bandwidth of the IF filter, as a result of the feedback). In order to illustrate the sensitivity of the calculations, we have repeated them for the same effective VCO noise, but neglecting the part of the noise which lies above that level which is only passed 3% of the time. The results of these calculations are denoted by crosses in fig. 4.5. The agreement between calculation and measurement is now striking.

4.3.5. *Calculation of the closed-loop S/N curves for modulated RF carrier waves*

Three points on the S/N curve for $y = 4$, $x = 0{\cdot}70$ and $z = 0{\cdot}71$ have been calculated. For this purpose, the IF frequency deviation due to the sinusoidal modulation is split up into a number of levels, as will be described in greater detail in connection with the calculation of the threshold for modulated carrier waves (sec. 4.8). At each level, the VCO noise deviation is added and the instantaneous frequency deviations corresponding to this total signal are calculated, together with the corresponding probabilities and the associated increases in noise. The average noise increase for each level is determined, and finally the noise increase is averaged over all levels. The full curve in fig. 4.6 represents the measured results, and the crosses the calculated results (again neglecting that part of the noise which lies above the level which is only passed 3% of the time). Here again, the agreement between measurements and calculation is good.

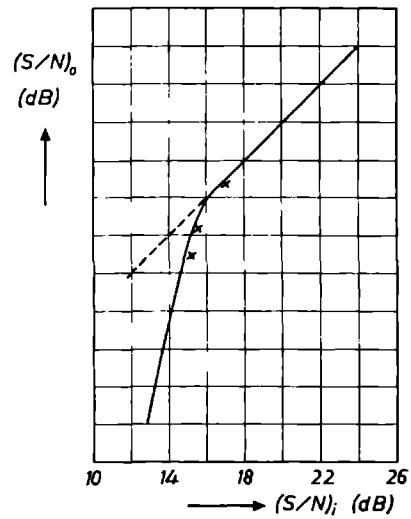

Fig. 4.6. Closed-loop S/N curves for modulated carrier waves with $x = 0{\cdot}70$, $y = 4$ and $z = 0{\cdot}71$. The full curves represent the results of the measurements, and the crosses those of the 97% calculation.

4.3.6. *Conclusion*

The calculations and measurements described in this section have shown that calculation of the open-loop and closed-loop S/N curves is quite a practical proposition. These calculations make use of the measured VCO noise curves. The calculation of the VCO noise is discussed in the next section. Use has also been made of experimentally determined curves for the increase in noise associated with a frequency shift of the carrier wave, as plotted in fig. 4.3. Until these curves have been calculated too, we cannot speak of complete calculation. The calculation of these curves is not difficult in principle, but it does involve a great deal of work. However, a complete calculation of the S/N curves in this way was not the aim of this investigation: what we wanted to do was to show that the FM process can be regarded as quasi-stationary for the purposes of the calculation of the S/N curves. This has now been demonstrated, and in the rest of this chapter we shall make use of this fact for the calculation of the thresholds.

4.4. Calculation of the effective noise deviation of the VCO carrier wave with unmodulated RF carrier waves

As we shall discuss in the next section, in the calculation of the thresholds we shall make use of the frequency and phase deviation of the VCO carrier wave caused by the feedback noise. The effective frequency deviation of the VCO carrier wave will be found to be of particular importance for the threshold calculations. We shall therefore start by investigating how the effective frequency deviation must be calculated. In this section, the calculation is carried out for an unmodulated RF carrier wave, and in sec. 4.7 for a modulated one.

The LF model of the FMFB receiver has already been given in figs 3.1 and 3.2. In chapter 1, we have mentioned that the RF phase noise $\theta(t)$ of the unmodulated carrier wave is equal to $n_s(t)$ at high values of $(S/N)_t$. Now $n_s(t)$ has a power spectrum which is wide compared with the bandwidth of the receiver; and within this range its power density N is constant. The input variable R of fig. 3.2 is thus a flat noise spectrum of power density N. The phase noise ϕ of the VCO carrier wave is now found with the aid of eq. (3.3):

$$\phi(j\omega_m) = R(j\omega_m)\, F(j\omega_m), \tag{4.1}$$

where $F(j\omega_m)$ is the LF closed-loop amplitude characteristic between the two inputs of the mixer stage. It follows that the effective phase deviation ϕ_{eff} can be written:

$$(\phi_{\text{eff}})^2 = \frac{N}{2\pi} \int_{-\infty}^{\infty} |F(j\omega_m)|^2 \, \mathrm{d}\omega. \tag{4.2}$$

Similarly, we find for the effective frequency deviation $(\dot{\phi}_{\text{eff}})^2$:

$$(\dot{\phi}_{\text{eff}})^2 = \frac{N}{2\pi} \int_{-\infty}^{\infty} \omega^2 \, |F(j\omega_m)|^2 \, \mathrm{d}\omega. \tag{4.3}$$

The effective phase and frequency deviations have been calculated as functions of $(S/N)_i$ for a number of system configurations, making use of the measured closed-loop characteristics. The results for the configurations with feedback factor $y = 4$ and the feedback filters with $x = 0{\cdot}70$, $0{\cdot}50$, $0{\cdot}29$ and $0{\cdot}12$ are plotted in fig. 4.7, while those for $y = 8$ and $x = 0{\cdot}70$, $0{\cdot}50$, $0{\cdot}29$ and $0{\cdot}12$ are given in fig. 4.8. These figures also include the corresponding measured curves of the effective frequency deviation (in all cases, the measured curve is the upper of a pair of curves in this figure). The arrow against each curve indicates the value of $(S/N)_i$ at which the threshold is found. It will be seen that the calculations and measurements agree completely with one another at high values of $(S/N)_i$, while the measured values gradually come to exceed the calculated values more and more, from just to the right of the threshold. This difference will be taken into account in our further calculations. The reason for this deviation is that at the lower values of $(S/N)_i$, extra pulse noise must be added

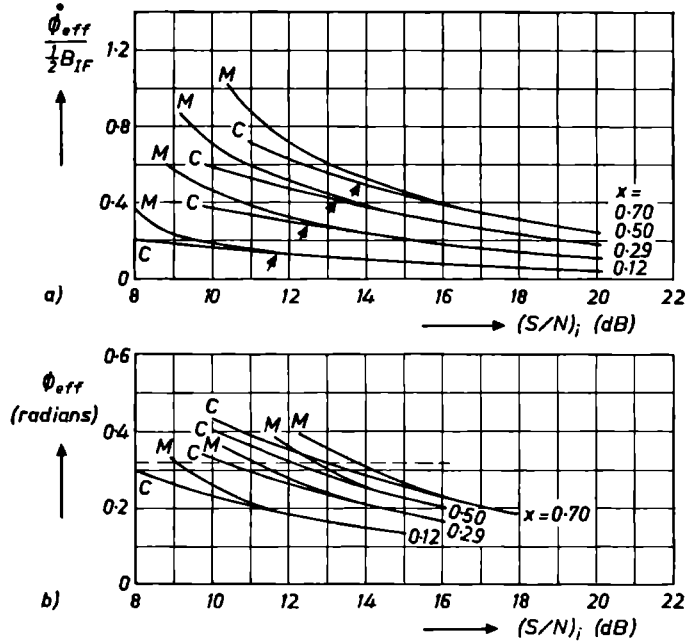

Fig. 4.7. Effective frequency deviation (*a*) and phase deviation (*b*) of the VCO carrier wave as functions of $(S/N)_i$ for $y = 4$, $z = 0$ and variable feedback filter. The calculated curve is marked C, and the measured curve M. The arrows indicate the threshold positions.

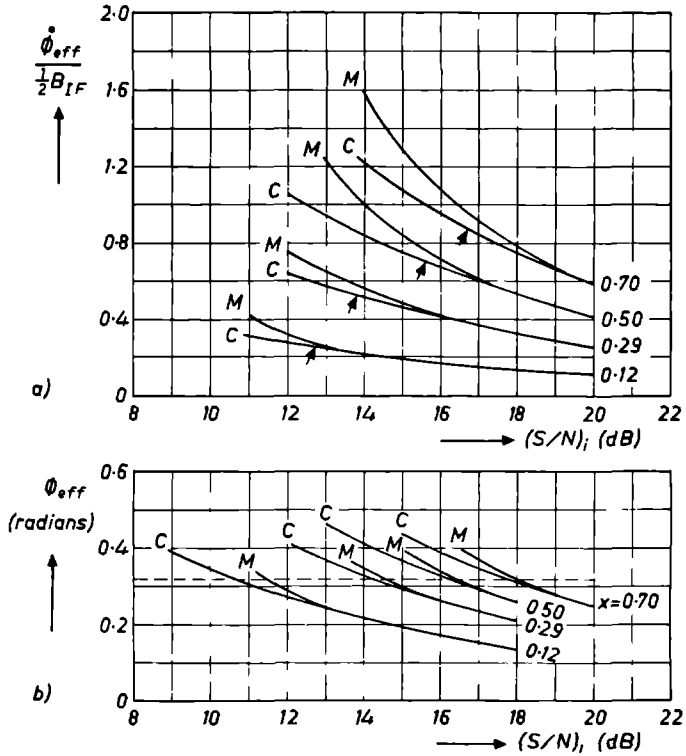

Fig. 4.8. Effective frequency deviation (*a*) and phase deviation (*b*) of the VCO carrier wave as a function of $(S/N)_i$ for $y = 8$, $z = 0$ and variable feedback filter The calculated curve is marked C, and the measured curve M. The arrows indicate the threshold positions.

to the normal detected noise. The calculation, on the other hand, is based on the assumption that the system is completely linear, and thus neglects this pulse noise. The effective phase deviation has not been measured. However, figs 4.7 and 4.8 also include curves drawn to give the same relative deviation as found at the effective frequency deviation. We shall be returning to this point during our discussion of Enloe's [13]) theory in sec. 6.2.

By way of illustration, the measured amplitude characteristics of $F(j\omega_m)$ are plotted as well; for $y = 4$ in fig. 4.9 and for $y = 8$ in fig. 4.10. The measurements were carried out with a low maximum frequency deviation, so that $G_L(j\omega;\Delta\omega)$ remains linear over the whole frequency range. This seems to be a reasonable step to take, in view of the values of the effective frequency deviation given in figs 4.7 and 4.8.

The effective frequency deviation $\dot{\phi}_{eff}$ will also be called the effective VCO noise from now on. Where the phase noise is meant, this will be specially mentioned. The curve giving the relation between the effective VCO noise and $(S/N)_i$ is called the VCO noise curve.

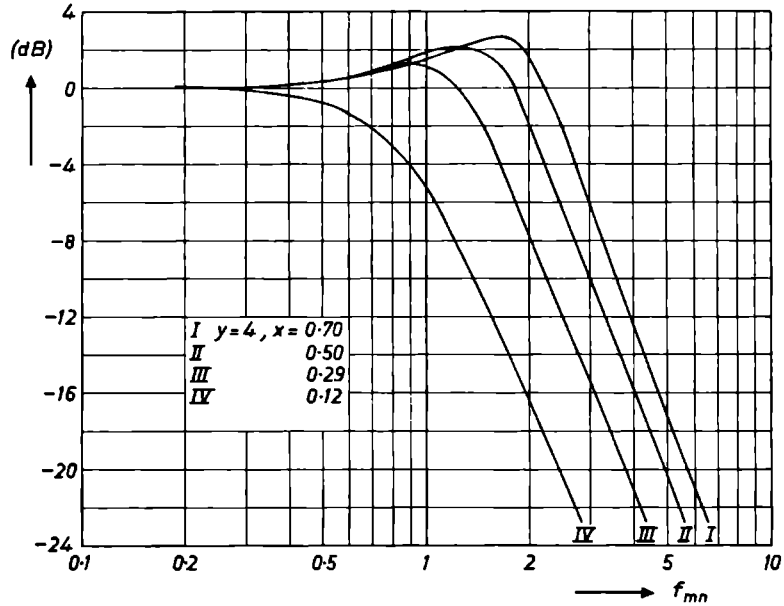

Fig. 4.9. Closed-loop amplitude characteristics measured after the feedback filter for $y = 4$ and various values of x.

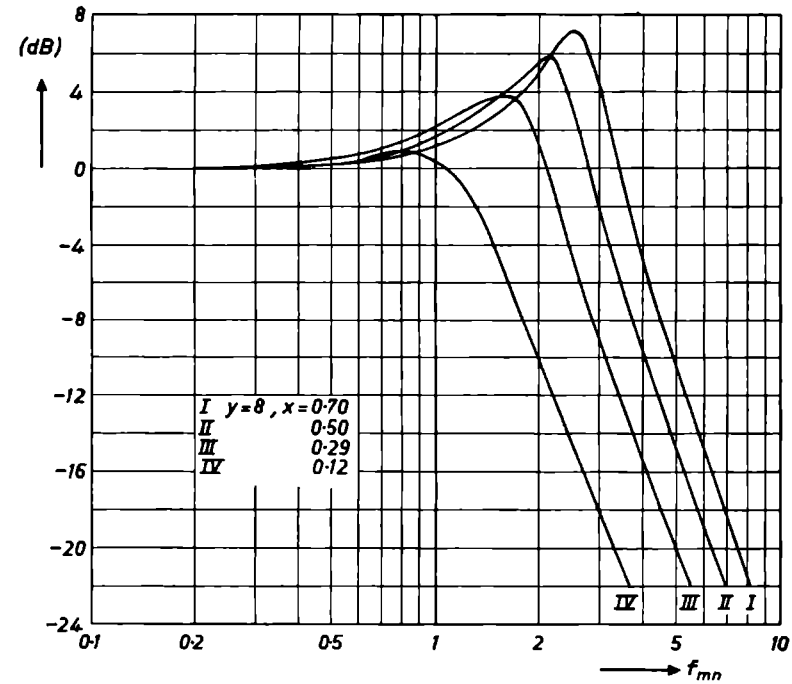

Fig. 4.10. Closed-loop amplitude characteristics measured after the feedback filter for $y = 8$ and various values of x.

4.4.1. *A note on the accuracy of the measurements*

Now that we have discussed the measured and the calculated VCO noise curves, it is appropriate to consider the accuracy of the measurements in general. The maximum deviation between the measured and the calculated VCO noise, for values of $(S/N)_i$ substantially above the threshold, was 4% of the effective value; for most of the points the error was much smaller. This gives a good impression of the accuracy of the measurements, since if the curves are to coincide at high values of $(S/N)_i$ both the VCO noise and $(S/N)_i$ must be measured accurately. The influence of an error in the VCO noise on the threshold calculations will be discussed in sec. 4.7.3. There we shall see that a deviation of 10% in the effective value of the VCO noise gives at most a deviation of 0·3 dB in the calculated thresholds.

The accuracy of the measured S/N curves cannot be determined by direct comparison of the measured S/N curves with calculated S/N curves from other publications. Calculated S/N curves for the open-loop system do exist (Stumpers [3]), but these curves were calculated for other IF filters than those we used. However, comparison of the S/N curves for the same value of k and for filters with a rectangular and a Gaussian amplitude characteristic (see Stumpers [3]) shows that there is only a very slight difference in the threshold values. The difference between the S/N curves for a Gaussian filter and an LRC filter will thus also be small. We find by interpolation from fig. 1.3 that for a Gaussian filter the threshold for $k = \frac{1}{2}\pi\,(1/0{\cdot}57) = 2{\cdot}75$ ($\frac{1}{2}\pi$ is the ratio of the noise bandwidth to the 3-dB bandwidth of a simple LCR filter, and the bandwidth of baseband filter I is 0·57 $B_{IF}/2$) is equal to 11·4 dB, while we have measured 10·9 dB. For $k = 2$ the threshold values for filters with a rectangular and a Gaussian amplitude characteristic are 10·0 and 9·7 dB respectively (N_i is in both cases normalized with respect to $2B_{LF}$). We may conclude from this that the error in the threshold measurement is certainly smaller than 0·5 dB. This can also be seen in another way. N_o was measured relatively in the determination of the S/N curves. This means that the accuracy of the S/N curves is certainly as good as that of the VCO noise curves, because the VCO noise has been measured absolutely. The reproducibility of the S/N curves is also good. Repetition of the measurements never gave differences in threshold values larger than 0·2 dB.

4.5. Calculation of the threshold for the closed-loop FM receiver (unmodulated carrier wave)

4.5.1. *Description of the threshold mechanism*

We have seen in sec. 4.3 that the S/N curve for the FMFB receiver can be calculated to quite a good approximation by regarding the FM process as

quasi-stationary. We also found in that section that the S/N curve is shifted with respect to the open-loop S/N curve, as a result of the feedback. This shift is due to the fact that the carrier wave is frequency-modulated by the VCO noise. As a result, whereas the in-phase noise after the IF filter remains constant, the carrier wave is attenuated in the IF filter so that the threshold shifts to the right. This basically is the threshold mechanism of the FMFB receiver. This basic idea can also be expressed in other words, as follows. If the closed-loop threshold occurs at a certain value of $(S/N)_i$, this is because the carrier wave is attenuated in the IF filter part of the time (as a result of the noise modulation of the VCO) to such an extent that the receiver comes to operate under the open-loop threshold during this time. On the basis of this idea, we have looked for a relation between the open-loop threshold, the closed-loop threshold and the effective VCO noise. It will be shown with reference to a number of experiments that for each system configuration, the same relation exists between the attenuation of the carrier wave on the one hand and the positions of the open-loop and closed-loop thresholds on the other. This makes it possible to calculate the closed-loop thresholds for any system configuration with the aid of a single empirically determined figure.

From a theoretical viewpoint, it is of course more interesting to calculate the complete S/N curves than to calculate only the thresholds. However, the shape of the curve below the threshold is not of practical interest. In sec. 4.3 we have shown how to calculate the S/N curves roughly. However, the amount of computation involved turned out to be so large that we decided to look for a simple method for calculating the thresholds only.

4.5.2. *Measurement and calculation of the threshold*

The closed-loop S/N curves and the VCO noise curves have been measured for six system configurations (IF filter I and baseband filter I with $x = 0{\cdot}70$, $0{\cdot}50$ and $0{\cdot}29$, for both $y = 4$ and $y = 8$). The results for $y = 4$ are plotted in fig. 4.11, and those for $y = 8$ in fig. 4.12. The open-loop S/N curve is also given in both figures, for the sake of comparison. The open-loop threshold is situated at 10·9 dB. A number of data concerning these measurements are collected in table I.

In this table the closed-loop thresholds (curve IV) of fig. 4.2 are compared with the open-loop threshold (curve I of fig. 4.2). Owing to the feedback, the closed-loop threshold is always worse than the open-loop threshold. However, we should not conclude from this that the feedback does not give rise to any threshold gain. To find the threshold gain, we must compare the closed-loop threshold with the threshold of the comparative open-loop system (curve V of fig. 4.2) and in general this threshold will occur at higher values of $(S/N)_i$ than the closed-loop threshold (see sec. 5.1). This has been dealt with in sec. 4.2. An example of the calculation of the threshold gain will be given in sec. 5.1.

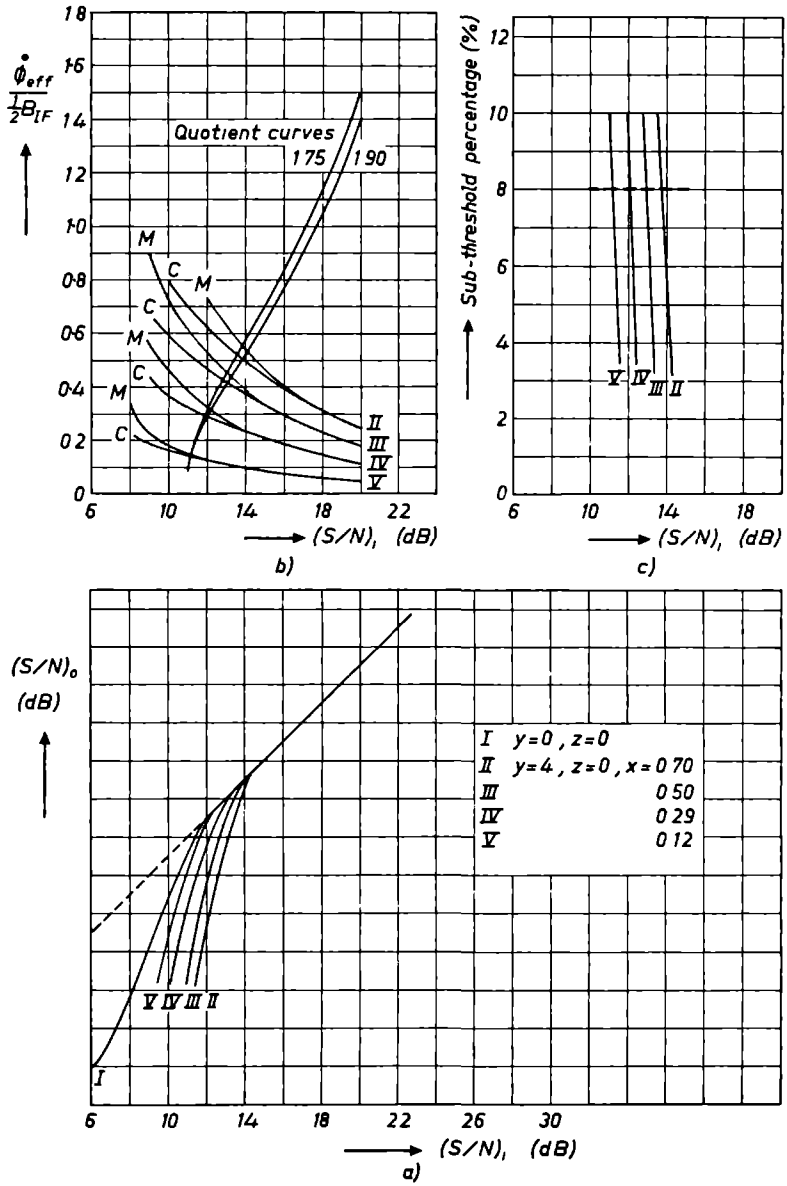

Fig 4.11 Measurements and calculations for the FMFB receiver with $y = 4$, $z = 0$ and various values of x

(*a*) Closed-loop S/N curves for unmodulated carrier waves,

(*b*) effective VCO noise as a function of $(S/N)_i$ (C = calculated, M = measured), with the quotient curves for 1·75 and 1·90,

(*c*) percentage of the time that the receiver operates below the open-loop threshold as a result of the measured VCO noise, as a function of $(S/N)_i$

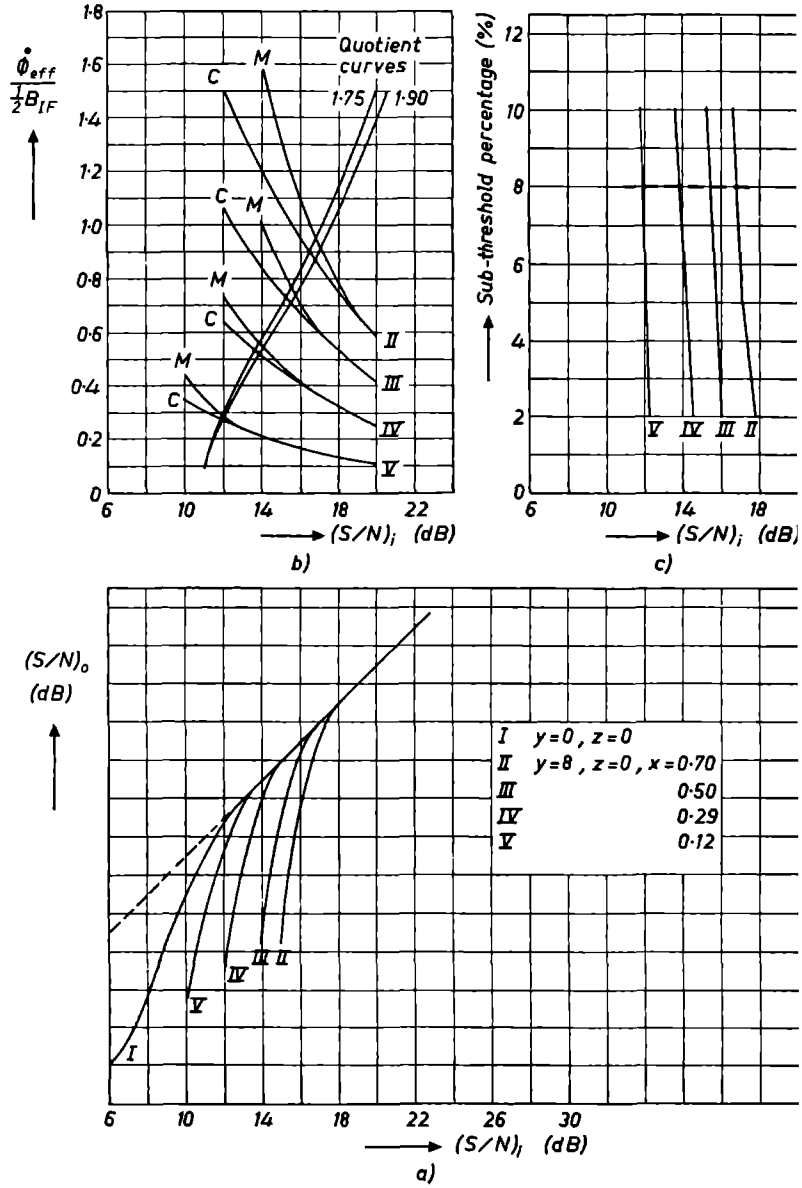

Fig. 4.12. Measurements and calculations for the FMFB receiver with $y = 8$, $z = 0$ various values of x.
(*a*) Closed-loop S/N curves for unmodulated carrier waves;
(*b*) effective VCO noise as a function of $(S/N)_i$ (C = calculated, M = measured), wit quotient curves for 1·75 and 1·90;
(*c*) percentage of the time that the receiver operates below the open-loop threshold result of the measured VCO noise, as a function of $(S/N)_i$.

TABLE I

Relation between the open-loop and the closed-loop thresholds.

y: feedback factor,
x: normalized bandwidth of the feedback filter,
a: measured closed-loop threshold (dB),
b: difference between closed-loop and open-loop threshold ($a - 10{\cdot}9$) (dB),
c: shift from the middle of the frequency band of the IF filter required to give the same damping as under b, divided by $B_{IF}/2$,
d: measured effective VCO noise at the threshold, divided by $B_{IF}/2$,
e: calculated effective VCO noise at the threshold, divided by $B_{IF}/2$ (linear system),
f: c/d,
g: c/e

$y = 4$							
x	a	b	c	d	e	f	g
0·70	13·6	2·5	0·90	0·56	0·52	1·61	1·73
0·50	13·0	2·1	0·78	0·44	0·42	1·77	1·86
0·29	12·2	1·3	0·60	0·32	0·29	1·87	2·06
$y = 8$							
x	a	b	c	d	e	f	g
0·70	16·7	5·8	1·64	0·96	0·88	1·71	1·87
0·50	15·6	4·7	1·39	0·75	0·69	1·85	2·01
0·29	13·8	2·9	0·97	0·56	0·52	1·75	1·86

The quotients in columns f (for the measured effective VCO noise) and g (for the calculated noise) are now found to vary so little within each column that we can regard them as constant. We shall show below how the calculations of the threshold depend on the constant value chosen and the deviations from this. We take the mean quotient for the measured effective VCO noise as 1·75, and that for the calculated effective VCO noise as 1·90. The quotient 1·75 means that the measured effective VCO noise attenuates the carrier wave to such an extent that the system operates below the open-loop threshold 8% of the time (Gaussian noise), while the quotient 1·90 corresponds to 5·7% of the time. The difference in the quotients or percentages is due to the fact that the calculated noise neglects certain components which are present in reality (pulse noise).

The thresholds can be calculated with the aid of the constants 1·75 and 1·90. For this purpose, we calculate the "quotient curves" for 1·75 and 1·90, which give for each value of $(S/N)_i$ the effective VCO noise level needed to bring the system to its closed-loop threshold at this value of $(S/N)_i$. The threshold is

found where these quotient curves cut the VCO noise curve. The quotient curves are calculated in much the same way as the quotients themselves, as described above.

4.5.3. *Results*

Figures 4.11 and 4.12 include not only the measured S/N curves (part *a*) but also the VCO noise curves (part *b*), for measured and calculated (linear model) VCO noise. The quotient curves for 1·75 and 1·90 are included in the same graphs as the VCO noise curves. The thresholds should now be found where the quotient curve for 1·75 cuts the measured VCO noise curve, and where the quotient curve for 1·90 cuts the calculated VCO noise curve.

In order to give an idea of the magnitude of the errors involved, table II gives some calculated thresholds for each measured threshold. The values in columns *b* and *c* give the thresholds according to the theory described in this chapter.

TABLE II

Determination of closed-loop thresholds for different quotient curves.

y: feedback factor,
x: normalized bandwidth of the feedback filter,
a: measured closed-loop threshold (dB),
b: value of $(S/N)_i$ in dB at which the measured VCO noise curve cuts the quotient curve for 1·75,
c: value of $(S/N)_i$ in dB at which the calculated VCO noise curve cuts the quotient curve for 1·90

$y = 4$				$y = 8$			
x	a	b	c	x	a	b	c
0·70	13·6	13·7	13·8	0·70	16·7	16·8	16·8
0·50	13·0	13·0	13·0	0·50	15·6	15·5	15·6
0·29	12·2	12·1	12·0	0·29	13·8	13·8	13·8

It may be seen from this table that the quotient 1·75 does very well for the measured VCO noise curve, while the quotient 1·90 gives excellent results for the calculated curve. The maximum difference between corresponding measurements and calculations is 0·2 dB.

Now that we have found a clear relation between the open-loop and closed-loop thresholds for a number of system configurations, it remains to check whether the same good agreement between measurement and calculation is

found when the same method of calculation is used for other system configurations. For this purpose, the closed-loop thresholds for a large number of systems have been calculated and measured. The results are summarized in table III, where y represents the feedback factor and x the feedback filter. The calculated values are found in column C, and the measured values in column M (in dB). The measured VCO noise curves have been used for these calculations.

TABLE III

Closed-loop thresholds for unmodulated RF carrier waves (dB)

	$x = \infty$		2·57		1·05		0·70		0·50		0·29		0·12	
y	M	C	M	C	M	C	M	C	M	C	M	C	M	C
2	15·0	16·7	14·5	14·6										
3	17·0	18·4												
4	19·0	19·4	16·9	17·3	14·6	14·7	13·6	13·8	13·0	13·0	12·2	12·0	11·4	11·4
5			18·7	18·7										
6			20·6	19·9	16·1	16·3	15·0	15·2	14·2	14·2	13·1	13·0	11·9	11·4
8					18·3	18·4	16·7	16·8	15·6	15·6	13·8	13·8	12·3	12·0
10					20·2	19·7	18·3	18·0	16·4	16·3	14·3	14·6	12·5	12·4
15											16·0	15·7		
20													14·0	14·0

The agreement is found to be quite good for a large number of random samples. Only for $x = \infty$ (no feedback filter at all) are the deviations quite large. This may be because the feedback noise spectrum is very wide-band and, as we have seen, the S/N curves can shift to the left at high modulation frequencies (sec. 4.3.2). Further, it is evident that the system with $x = \infty$ has very bad noise properties. On the other hand, the distortion properties of this system are good because there is no extra filter in the loop. In this way we get a better feedback of the baseband frequencies.

At high feedback factors, only filters with low values of x come into consideration. This is because the smaller the value of x, the larger y may be without making the system unstable. Further, care should be taken to ensure that with a given feedback filter, the value of y is appreciably less than that at which the system becomes unstable. We shall be returning to this point in sec. 4.12.

When the difference between the closed-loop and open-loop threshold exceeds 9 dB, the measured and calculated values may diverge. This is also discussed in sec. 4.12.

4.5.4. *Alternative method of calculation*

Instead of using the quotients 1·75 and 1·90 for our calculations, we can work directly with the corresponding percentages 8% and 5·7%. We shall see that this latter method has certain advantages, especially for the calculation of the threshold for modulated RF carrier waves. Owing to the extra sine function present in this case, there is no longer a simple relation between the effective frequency deviation and the "sub-threshold percentage" (the percentage of the time the receiver operates under the threshold). In this section, we shall show how the calculation using the percentages is carried out for unmodulated RF carrier waves. This has the further advantage of giving an impression of the influence of the sub-threshold percentage on the threshold calculation.

The calculation is carried out as follows. For a number of values of $(S/N)_i$ we calculate (on the basis of the corresponding VCO noise) the percentage of the time that the receiver will be working below the open-loop threshold. In this way, we get for each system configuration with its corresponding VCO noise curve a percentage curve giving the relation between the percentage of the time that the receiver is working below the open-loop threshold and the value of $(S/N)_i$. This calculation is similar to that used for the determination of the quotient curve. The percentage curves determined in this way are given separately in fig. 4.11*c* and 4.12*c*. These calculations make use of the measured effective VCO noise. The threshold is now found at that value of $(S/N)_i$ at which the probability that the receiver will work below the open-loop threshold is 8%. We can also make use of the calculated effective VCO noise. The percentage line obtained in this way is shifted somewhat with respect to the first, and the threshold is found at a percentage of 5·7%.

The percentage curve is found to have a very steep slope. This means that the position of the threshold can be determined accurately.

4.5.5. *Conclusion*

We have shown that the closed-loop threshold can be calculated, on the basis of the theory that the closed-loop threshold is found when the receiver works below the open-loop threshold a certain percentage of the time. This is due to the VCO noise which shifts the carrier wave in the frequency band of the IF filter, thus attenuating it. It has been found that the percentage of the time involved is the same for all system configurations. This fact can thus be used as the basis of a method for the calculation of the closed-loop threshold. We have also shown that the difference between the measured and calculated VCO noise curves can be taken into account in the calculation. In other sections of this chapter, this calculation will be carried out for other configurations. The theory will also be used for the calculation of the threshold for modulated

RF carrier waves. The agreement between theory and experiment is found to be good in this case too.

Our theory thus implies that there is only one mechanism determining the threshold in an FMFB receiver. This is not in agreement with current theories (Enloe [13]), which assume two different mechanisms.

The IF filter is found to have a great influence on the occurrence of the threshold. This is because it determines not only the position of the open-loop threshold but also the attenuation of the carrier wave. Further, together with the feedback factor and the feedback filter it also determines the VCO noise which is responsible for the frequency shift of the carrier wave. Since the IF filter also plays an important role in determining the stability of the control loop and the distortion, it will be clear that the characteristic of the IF filter is a very important design factor for the closed-loop FM receiver.

4.6. Calculation of the open-loop threshold for modulated RF carrier waves

During our investigation of the threshold of closed-loop S/N curves for unmodulated RF carrier waves we found that this threshold occurs when, as a result of the VCO noise, the FM receiver operates under the open-loop threshold more than 8 % of the time. We may expect to find a similar effect with the open-loop S/N curves for a carrier wave modulated by a sine function. Here too, the IF frequency deviation will cause the carrier wave to be attenuated to such

TABLE IV

Open-loop thresholds for modulated RF carrier waves (dB)

z	M	C	M — C
0	10·9	—	—
0·29	11·5	11·3	+0·2
0·43	11·8	11·7	+0·1
0·57	12·0	12·1	—0·1
0·71	12·4	12·6	—0·2
0·86	13·3	13·3	0·0
1·00	14·1	14·0	+0·1
1·14	14·8	14·6	+0·2
1·28	15·6	15·2	+0·4
1·43	16·3	15·8	+0·5
1·72	17·8	17·0	+0·8
2·00	19·6	18·0	+1·6
2·28	21·2	18·9	+2·3

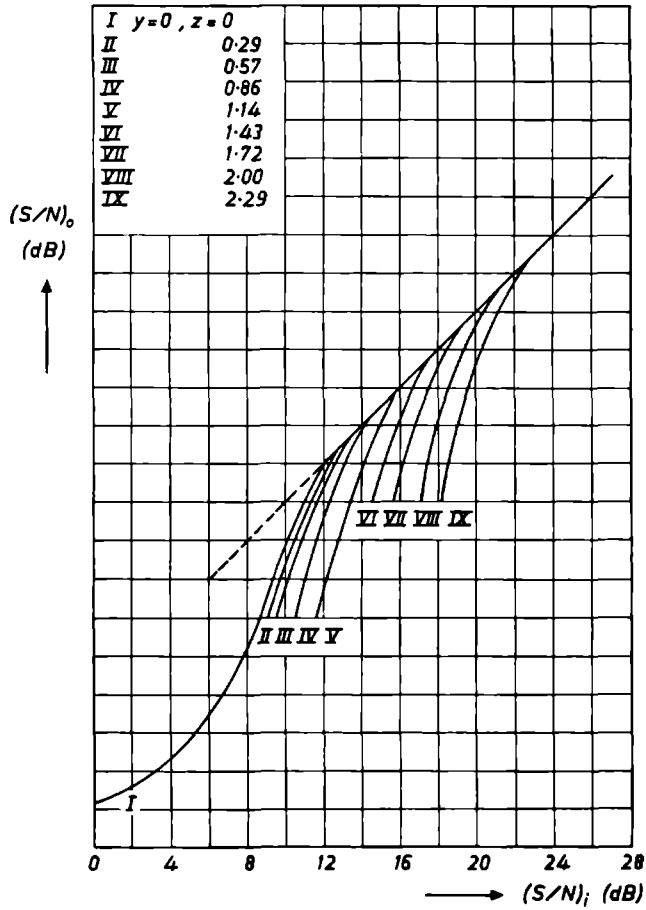

Fig. 4.13. Open-loop S/N curves for modulated carrier waves.

an extent that the receiver operates under the open-loop threshold for a certain part of the time. However, the percentage at which the threshold occurs may differ from that in the above case. With noise, if a certain level is exceeded 8% of the time, we may expect that an appreciably higher amplitude level will also be exceeded for a certain proportion of the time, but that in this case the percentage will be smaller. With a sine wave the situation is different. Here, if a certain level is exceeded 8% of the time, this must be practically the highest level found. On the other hand, even a slight lowering of the level may be expected to give rise to a sharp increase in the percentage. We have concluded from this that in the case of sinusoidal modulation, we can to a good approximation work with the 8% sub-threshold percentage too; and because the difference between 8% and 0% is negligible for modulation with a sine function, we can also work with the 0% sub-threshold percentage, or the maximum frequency

deviation. The calculation is now carried out as follows. For a given value of Δf_{IF}, we calculate the maximum attenuation (in dB) of the carrier wave by the IF filter. The open-loop threshold will now be shifted by the modulation by the same number of dB, with respect to the open-loop threshold for unmodulated carrier waves. The results of a number of measurements and calculations are summarized in table IV. It may be seen from this table that the agreement between theory and measurement is good for values of z up to and even slightly greater than 1. For larger values of z, the discrepancy increases with increasing z. This is due to the distortion; we shall be returning to this point in sec. 4.12. At $z = 1{\cdot}14$, the distortion is already about 5%, which means that the calculated threshold is still accurate at those maximum frequency deviations which are of interest as regards the distortion.

Figure 4.13 shows a number of measured S/N curves for values of z from 0 to 2·28. The modulation frequency f_{mn} is 0·43.

4.7. Calculation of the effective VCO noise for modulated carrier waves

4.7.1. *Introduction*

The method used to calculate the threshold of an FMFB receiver for modulated RF carrier waves is basically the same as that used for unmodulated carrier waves. However, measurements show that the effective VCO noise is influenced by the modulation; it may be increased by up to 30%, depending on the maximum frequency deviation. This means that we will also have to calculate the effective VCO noise for a modulated carrier wave.

First of all, however, we shall give the ratio Q of the measured effective VCO noise with and without modulation (at the same values of $(S/N)_i$) for a large number of system configurations, and extract a general trend from these values. We shall then give a method for calculating Q, and shall finally estimate the magnitude of the error caused by a difference between the measured and calculated values of the effective VCO noise.

4.7.2. *Measurements*

The VCO noise curves were measured for values of the feedback factor of $y = 4$, 6, 8 and 10, and with feedback filters with $x = 0{\cdot}70$, 0·50 and 0·29 at each value of y. For each configuration, z was taken equal to 0, 0·29, 0·57 and 0·86. All the measurements for $y = 8$ are plotted in fig. 4.14. The curves for $z = 0$ and $z = 0{\cdot}29$ coincide. The calculated VCO noise curve for $z = 0$ is also given for each feedback filter (sec. 4.4). The arrows indicate the positions of the measured thresholds. It follows from these measurement that the measured VCO noise curves for modulated and unmodulated carrier waves are parallel to the right of the threshold for modulated carrier waves, and to a certain extent also to the left of this threshold. By parallel, we mean here that

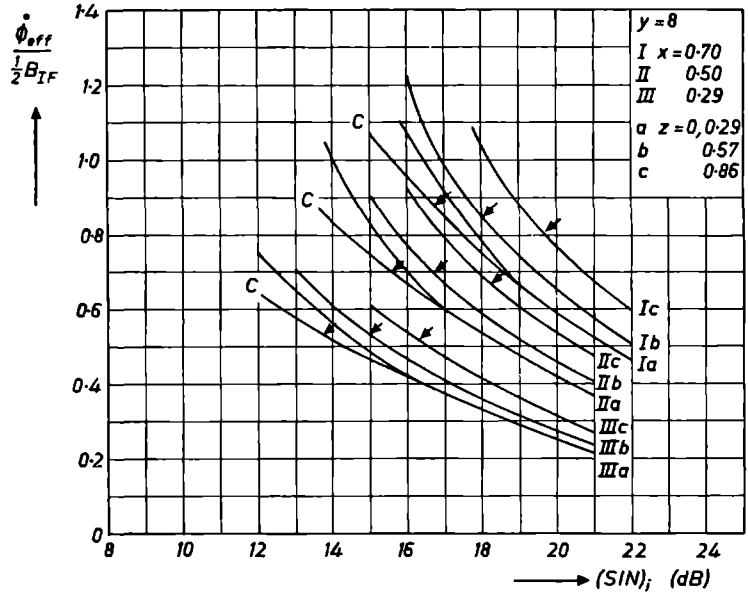

Fig. 4.14. Effective VCO noise as a function of $(S/N)_i$ for $y = 8$ and various values of x and z. The curves marked C were calculated, the others measured. The arrows indicate the threshold positions.

the quotient of the values of the effective VCO noise as a function of $(S/N)_i$ is constant. Since the threshold for modulated carrier waves lies to the right of that for unmodulated carrier waves, the divergence between the measured and calculated VCO noise curves for $z = 0$ is still not very noticeable at this point. We may thus state that to the right of the threshold for modulated carrier waves, the curves for the calculated effective VCO noise for $z = 0$ and for the measured effective VCO noise with modulated carrier waves will be practically

TABLE V

Q (from measurements)

	$y = 4$			$y = 6$			$y = 8$			$y = 10$		
z	$x = 0{\cdot}70$	$0{\cdot}50$	$0{\cdot}29$	$0{\cdot}70$	$0{\cdot}50$	$0{\cdot}29$	$0{\cdot}70$	$0{\cdot}50$	$0{\cdot}29$	$0{\cdot}70$	$0{\cdot}50$	$0{\cdot}29$
$0{\cdot}29$	$1{\cdot}01$	$1{\cdot}01$	$1{\cdot}01$	$1{\cdot}01$	$1{\cdot}01$	$1{\cdot}01$	$1{\cdot}02$	$1{\cdot}02$	$1{\cdot}01$	$1{\cdot}02$	$1{\cdot}02$	$1{\cdot}01$
$0{\cdot}57$	$1{\cdot}08$	$1{\cdot}08$	$1{\cdot}07$	$1{\cdot}10$	$1{\cdot}09$	$1{\cdot}08$	$1{\cdot}11$	$1{\cdot}09$	$1{\cdot}09$	$1{\cdot}12$	$1{\cdot}10$	$1{\cdot}09$
$0{\cdot}86$	$1{\cdot}19$	$1{\cdot}18$	$1{\cdot}16$	$1{\cdot}20$	$1{\cdot}19$	$1{\cdot}17$	$1{\cdot}24$	$1{\cdot}21$	$1{\cdot}20$	$1{\cdot}28$	$1{\cdot}26$	$1{\cdot}22$

parallel. The higher the value of z, and thus the higher the value of the threshold, the better the agreement, because the threshold then lies more to the right. Thus, if we can calculate the constant ratio between these two curves, then we can calculate the VCO noise curve for modulated carrier waves to a good approximation up to the threshold. In order to be able to test the calculations given below, we have worked out the value of the quotient Q for all measurements. The results are collected in table V.

It may be seen from this table that the quotient Q is reasonably constant for a given value of z, but that there is a tendency for Q to be slightly lower for lower values of x, and slightly higher for higher values of y.

4.7.3. *Calculations*

We assume that modulation with a sine function can be regarded as quasi-stationary. At a given moment, there will be an instantaneous deviation and hence an instantaneous shift of the carrier wave with respect to the middle of

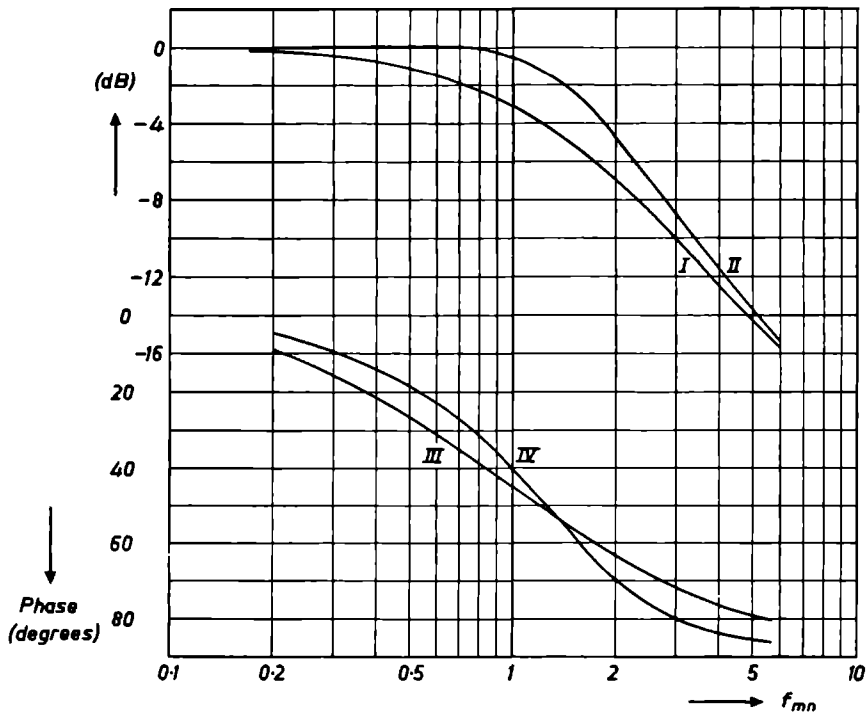

Fig. 4.15. LF transfer functions for IF filter I.
I : Amplitude characteristic with carrier-wave shift of 0 Hz,
II : idem, 0·86 $B_{IF}/2$ Hz,
III: phase characteristic with carrier-wave shift of 0 Hz,
IV: idem, 0·86 $B_{IF}/2$ Hz.

the frequency range of the IF filter. Both the carrier wave and the noise about the carrier wave are attenuated by this shift. Further, the noise spectrum of the detector is no longer symmetrical about the carrier wave. This makes it difficult to take the influence of the feedback into account. This problem can be solved by working with an instantaneous LF model of the IF filter. The LF transfer functions are then dependent on the position of the carrier wave. We have seen in chapter 2 how the LF transfer functions of the IF filter can be calculated for the case where the carrier wave is situated in the middle of the frequency range of the IF filter. The model for the displaced carrier wave can be calculated in the same way. It is found that the amplitude and phase characteristics are changed by the frequency shift of the carrier wave; this may be seen from fig. 4.15, which shows the calculated amplitude and phase characteristics of the LF model of IF filter I for shifts of the carrier wave of 0 and 0·86 $B_{IF}/2$ Hz. The characteristics have been calculated for a small maximum frequency deviation ($z \ll 1$). It will be clear that the changes in question will have a great effect on the closed-loop characteristic. This is demonstrated in fig. 4.16, which gives the calculated and measured closed-loop amplitude characteristics for the configuration with $y = 8$ and $x = 0{\cdot}7$, for carrier-wave shifts of 0 and 0·86 $B_{IF}/2$ Hz. The agreement between measurements and calculations is good.

The calculation of the effective VCO noise for sinusoidally modulated carrier waves is now a simple matter, and can be carried out in just the same way as for unmodulated carrier waves as follows. A quarter-period of the sine wave is divided up into a number of intervals. For each interval, we determine the instantaneous carrier-wave shift in the frequency range of the IF filter for a given maximum frequency deviation. The LF transfer function of the IF filter is then calculated for each carrier-wave shift. The closed-loop amplitude characteristic is now calculated with the aid of these transfer functions. The squared closed-loop characteristics are integrated and finally these integrals are averaged over all intervals. The quotient of this mean value for a given z and that for $z = 0$ (unmodulated carrier wave) gives the value of Q for this z. Table VI gives the values of Q calculated for $z = 0{\cdot}86$, for the system configurations dealt with in sec. 4.7.2. The calculated values are given in the columns marked C, and the measured values (taken from table V) in the columns marked M. The values given in this table show the same trend as that already noticed in table V: higher values of Q at higher values of y, and lower values of Q at lower values of x. The agreement between measurement and calculation is good. The maximum error is 5%, and in most cases the error is much less than this.

In order to know what the effect is of an error in the VCO noise calculation we have carried out a large number of threshold calculations with this end in view. First of all, we calculated the treshholds corresponding to the measured VCO noise; then we raised and lowered the VCO noise curves by 10%, and

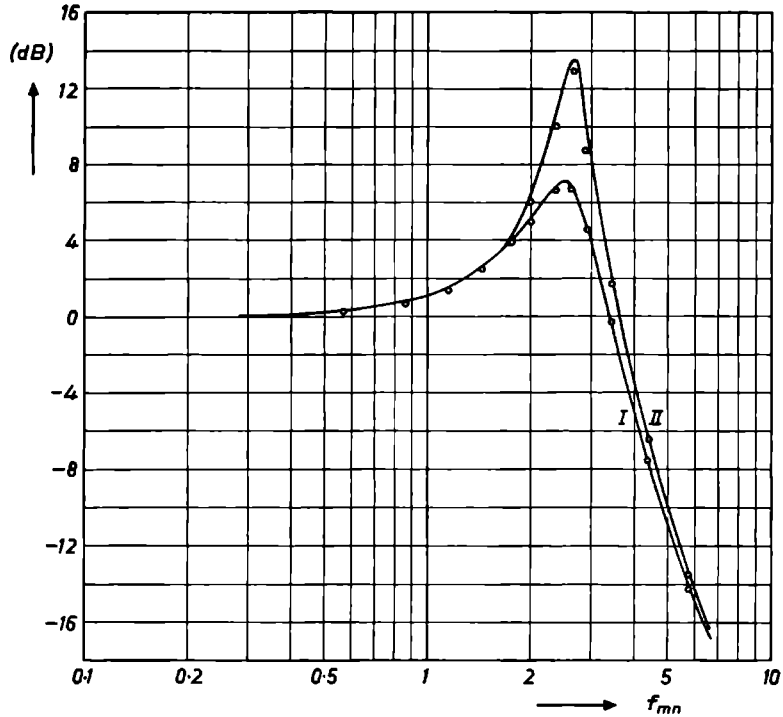

Fig. 4.16. Closed-loop amplitude characteristics after the feedback filter for IF filter I, $x = 0{\cdot}70$ and $y = 8$. The full curves represent the results of the calculations, and the circles the results of the measurements.
I : Carrier-wave shift = 0 Hz,
II: idem, $0{\cdot}86\ B_{IF}/2$ Hz.

TABLE VI

Q (calculated)

	$x = 0{\cdot}70$		$x = 0{\cdot}50$		$x = 0{\cdot}29$	
y	M	C	M	C	M	C
4	1·19	1·16	1·18	1·16	1·16	1·14
6	1·20	1·19	1·19	1·18	1·17	1·17
8	1·24	1·25	1·21	1·21	1·20	1·19
10	1·28	1·34	1·26	1·27	1·22	1·21

calculated the thresholds again for these new curves (the method of calculation is described in sec. 4.8). The maximum error caused by a change of 10% in the effective VCO noise was found to be 0·3 dB, while the change of 20% gave a

maximum error of 0·6 dB. Since the largest discrepancy in the calculated value of Q was 5%, this will give a maximum error of 0·15 dB.

The calculation of the effective VCO noise for modulated RF carrier waves is again based on the assumption that the FM process is quasi-stationary in nature. As in the cases dealt with above, we must show that this assumption is a reasonable one. This can be done e.g. by showing that the measured quotient Q of the values of the effective VCO noise with and without modulation is independent of the modulation frequency used. The measurements of table V were all carried out for a modulation frequency of $f_{mn} = 0{\cdot}43$. We have also measured Q as a function of the modulation frequency for the configuration with $y = 8$, $x = 0{\cdot}7$ and $z = 0{\cdot}86$. The results are plotted in fig. 4.17. The calculated quotient is 1·25. Inspection of this figure shows clearly that in this case the frequency modulation can be regarded as quasi-stationary for values of f_{mn} below 0·57 (LF filter I). Even for values of f_{mn} up to 0·86 (LF filter III), the error involved (7%) is not such as to have serious effects. In practice, the error will be even less, since the carrier wave is not modulated with a sine wave but with a function that covers the whole baseband. The average discrepancy will thus be much lower.

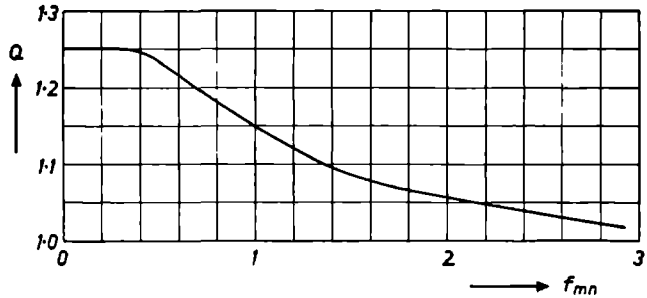

Fig. 4.17. Quotient of the values of the effective VCO noise for modulated and unmodulated RF carrier waves as a function of the modulation frequency, for $x = 0{\cdot}70$, $y = 8$ and $z = 0{\cdot}86$.

4.7.4. *Conclusion*

In this section, we have explained why the effective VCO noise increases when the RF carrier wave is modulated. It has been shown that the effective VCO noise can be calculated to a good approximation on this basis, and that the discrepancies between the measured and calculated values are so slight that the error in the calculated threshold is negligible.

4.8. Calculation of the closed-loop threshold for modulated RF carrier waves

The threshold for the closed-loop system with modulated carrier waves can be calculated along the same lines as that for unmodulated carrier waves.

However, now we have two frequency modulations in the IF filter, namely the desired modulation, within a relatively narrow frequency band, and the modulation by the VCO noise, which covers a relatively wide band. In this case, we start by calculating the reduced Δf_{IF} due to the sinusoidally modulated carrier wave. The sine wave is again divided into a number of intervals, each with its corresponding frequency deviation. At each frequency deviation, we sum the frequency deviations of the VCO carrier wave caused by the noise at a given value of $(S/N)_i$. We now calculate the percentage of the time during which the system is operating below the open-loop threshold with this total signal. This calculation is carried out for all intervals, and finally the percentages are averaged over all intervals. When this is done for a number of values of $(S/N)_i$, each with its corresponding effective VCO noise, we get a percentage curve in the same way as in the threshold calculation for the closed-loop system with unmodulated carrier waves (sec. 4.5.4). The threshold to be calculated is now found at the value of $(S/N)_i$ corresponding to 6%.

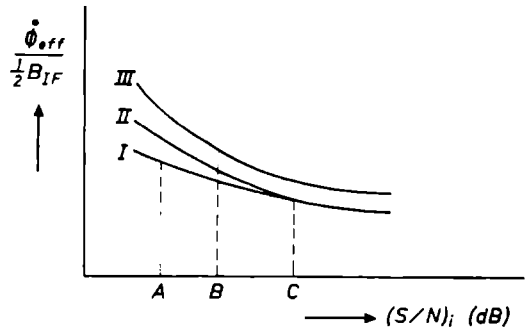

Fig. 4.18. General form of various effective VCO noise curves.
I : Calculated curve for unmodulated carrier waves,
II : measured curve for unmodulated carrier waves,
III: measured curve for modulated carrier waves.

The choice of the percentage can be explained as follows. When we plot the effective VCO noise as a function of $(S/N)_i$, we get the curves of fig. 4.18. Curves I and II are for unmodulated carrier waves, curve I being calculated and curve II measured. Curve III is the measured VCO noise curve for a modulated carrier wave. The points A and B indicate the thresholds for unmodulated and modulated carrier waves. Curves I and II start diverging at point C, (thus to the right of A), while curves II and III have a constant Q up to a point to the left of B. We have already shown in sec. 4.5 that in order to calculate point A with the aid of curve I, we should reckon with a time percentage of 5·7%, while the corresponding percentage for curve II is 8%. Curve III can be calculated from I down to point C. The discrepancy is already noticeable at the threshold (point B) and there the calculation of III is no longer quite

correct. The percentage to be used must thus lie between 5·7 and 8%. To be on the safe side, we take 6% because this gives the highest threshold values. This percentage will now be used for all values of z, including $z = 0$ (no modulation). The error caused by using the same percentage throughout is very

TABLE VII

Closed-loop thresholds (dB)

	$x = 1{\cdot}05$		$x = 0{\cdot}70$		$x = 0{\cdot}50$		$x = 0{\cdot}29$		$x = 0{\cdot}12$	
z	M	C	M	C	M	C	M	C	M	C
	$y = 4$									
0	14·6	14·7	13·8	13·8	13·2	13·1	12·5	12·1	11·4	11·2
0·29	15·0	15·1	14·1	14·4	13·5	13·7	12·8	12·8	12·0	11·7
0·57	15·8	15·8	14·9	15·0	14·3	14·4	13·5	13·6	12·6	12·6
0·86	16·8	16·5	16·2	16·0	15·5	15·3	14·8	14·8	13·8	13·8
	$y = 6$									
0	16·1	16·3	15·0	15·2	14·2	14·2	13·1	13·0	11·9	11·5
0·29	16·5	16·7	15·6	15·6	14·6	14·6	13·6	13·4	12·3	11·9
0·57	17·0	17·2	16·1	16·2	15·3	15·3	14·0	14·2	12·9	13·0
0·86	18·3	18·0	17·2	17·0	16·3	16·2	15·1	15·1	13·8	14·0
	$y = 8$									
0	18·3	18·4	16·7	16·8	15·6	15·5	13·8	13·8	12·3	11·9
0·29	18·8	18·8	16·8	16·9	15·8	15·6	14·4	14·2	12·6	12·4
0·57	20·0	19·2	18·0	17·6	16·7	16·4	15·0	15·0	13·4	12·9
0·86	21·3	20·0	19·7	18·5	18·3	17·4	16·3	16·0	14·5	14·5
	$y = 10$									
0	20·0	19·7	18·3	18·0	16·4	16·3	14·3	14·6	12·4	12·3
0·29	20·6	20·1	18·4	18·3	17·0	16·7	15·0	15·0	12·9	12·9
0·57	21·5	20·6	19·8	18·8	17·8	17·4	15·6	15·6	13·9	13·7
0·86	23·6	21·4	21·6	19·6	19·7	18·0	17·3	16·6	14·9	14·7

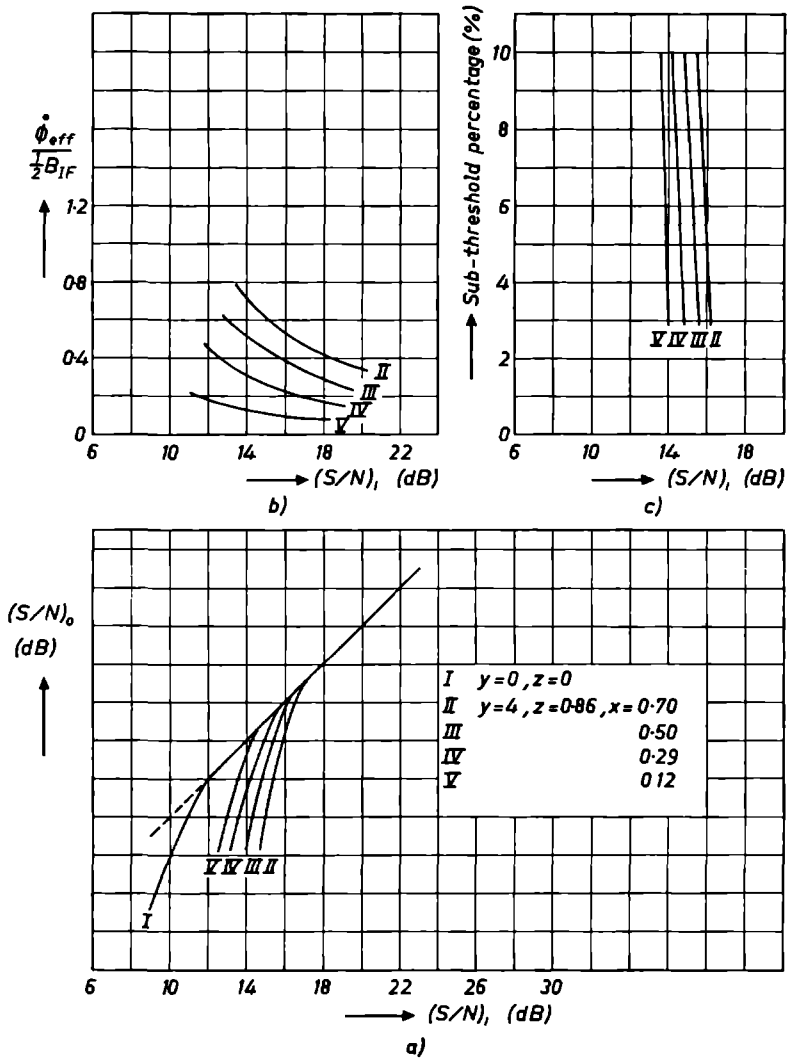

Fig 4 19. Measurements and calculations for the FMFB receiver with $y = 4$, $z = 0{\cdot}86$ and various values of x
(*a*) Closed-loop S/N curves for modulated carrier waves;
(*b*) measured effective VCO noise as a function of $(S/N)_i$;
(*c*) percentage of the time that the receiver operates under the open-loop threshold as a result of the sinusoidal modulation and the VCO noise, as a function of $(S/N)_i$.

slight: examination of a large number of percentages curves has shown that even when the 6% is replaced by 4% or 8%, the maximum error is only about 0·3 dB.

In order to test the agreement between measurement and calculation, we have measured and calculated the thresholds for a large number of system

configurations, namely those with $y = 4$, 6, 8 and 10 and $x = 1{\cdot}05, 0{\cdot}70, 0{\cdot}50, 0{\cdot}29$ and $0{\cdot}12$ at each value of y, and $z = 0$, $0{\cdot}29$, $0{\cdot}57$ and $0{\cdot}86$ for each combination of x and y. The results are collected in table VII. The measured threshold for each combination is given in the column marked M, and the calculated threshold under C. By way of illustration, we have plotted a number

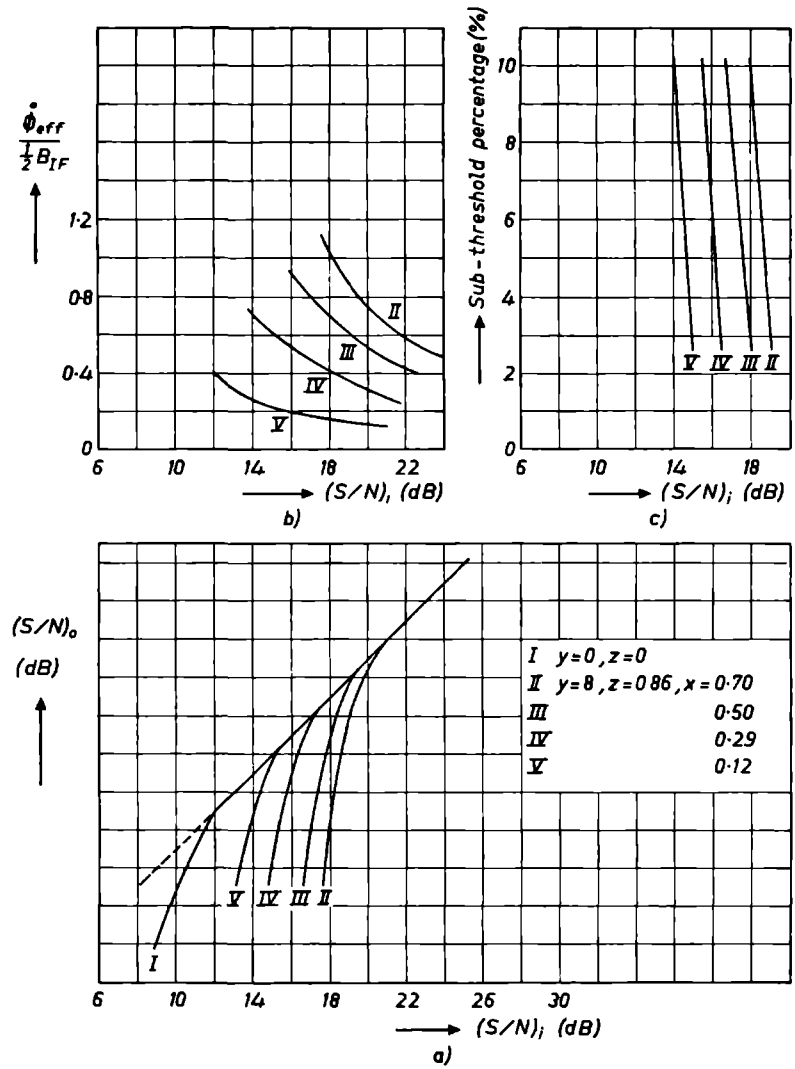

Fig. 4.20. Measurements and calculations for the FMFB receiver with $y = 8$, $z = 0{\cdot}86$ and various values of x.
(*a*) Closed-loop S/N curves for modulated carrier waves;
(*b*) measured effective VCO noise as a function of $(S/N)_i$;
(*c*) percentage of the time that the receiver operates under the open-loop threshold as a result of the sinusoidal modulation and the VCO noise, as a function of $(S/N)_i$.

of S/N curves for $y = 4$ in fig. 4.19, and for $y = 8$ in fig. 4.20 (part *a*). The feedback filters used for both values of y correspond to $x = 0{\cdot}70$, $0{\cdot}50$ and $0{\cdot}29$. The value of z was $0{\cdot}86$ throughout. The corresponding VCO noise curves (part *b*) and belonging percentage curves (part *c*) are also included in these figures.

The measurements and calculations for $y = 4$ and $y = 6$ agree completely. For $y = 8$ and $z = 0{\cdot}86$, we see clear discrepancies at higher values of x. This trend is seen to an even greater extent at $y = 10$; here, the divergence starts at $z = 0{\cdot}57$. These discrepancies occur at a higher value of the threshold. We shall be returning to these discrepancies in sec. 4.12.

We have seen that a shift of the carrier wave in the frequency range of the IF filter gives rise to a change in the LF transfer functions of the IF filter, as a result of which the effective VCO noise increases. For the threshold calculations, the average value of this increase in the effective VCO noise has been used. However, it is of course more correct to say that each instantaneous shift of the carrier wave corresponds to a different instantaneous increase in the effective VCO noise. Strictly speaking, therefore, we should use this instantaneous increase in the noise when calculating the percentage of the time that the system works under the open-loop threshold. The threshold has been calculated in this way for a number of system configurations. Comparison of these results with those obtained by calculation using the average noise increase has shown that no difference at all is found with $z = 0{\cdot}29$ and $z = 0{\cdot}57$, while a shift of at most $0{\cdot}2$ dB to the right occurs with $z = 0{\cdot}86$. This correction is not taken into account in table VII.

4.9. Variations in the bandwidth of the baseband filter

So far, the feedback factor, the feedback filter and Δf_{IF} have been the only variables we have considered in our study of the FMFB receiver. The IF filter and the baseband filter have always been left alone. In this section, we shall consider the effect of the bandwidth of the baseband filter on the threshold. IF filter I was again used for all measurements, and x, y and z were again varied for each baseband filter. The point in varying the bandwidth of the baseband filter with respect to that of the IF filter is that we want to study the threshold calculations for different values of the parameter k. So far, baseband filter I with $B_{LF} = 0{\cdot}57\ B_{IF}/2$ ($k = \frac{1}{2}\pi/0{\cdot}57 = 2{\cdot}75$) has been used for all measurements. Measurements and calculations will now be performed for baseband filters II and III, with bandwidths of $0{\cdot}43$ ($k = 3{\cdot}65$) and $0{\cdot}86$ ($k = 1{\cdot}82$) times $B_{IF}/2$, respectively. The bandwidth of the input noise N_i is again normalized at $1{\cdot}14\ B_{IF}/2$ Hz, in the interests of the comparability of the curves.

The results are again given in tabular form. Tables VIII and IX give the thresholds for unmodulated RF carrier waves (table VIII for baseband filter II

TABLE VIII

Closed-loop threshold (dB) for unmodulated RF carrier waves with baseband filter II

	$x = 0{\cdot}70$		$x = 0{\cdot}50$		$x = 0{\cdot}29$	
y	M	C	M	C	M	C
2	12·2	12·6	12·0	12·1	11·5	11·7
4	14·0	14·2	13·1	13·4	12·4	12·5
6	15·4	15·7	14·5	14·7	13·3	13·4
8	16·9	16·9	15·4	15·5	13·8	14·0
10	18·3	18·3	16·7	16·8	14·6	14·9

TABLE IX

Closed-loop threshold (dB) for unmodulated RF carrier waves with baseband filter III

	$x = 0{\cdot}70$		$x = 0{\cdot}50$		$x = 0{\cdot}29$	
y	M	C	M	C	M	C
2	11·7	11·4	11·2	10·8	10·9	10·3
4	13·2	13·2	12·4	12·3	11·6	11·4
6	15·0	15·0	13·8	13·8	12·6	12·4
8	16·2	16·2	14·9	14·5	13·4	13·0
10	17·7	17·6	15·9	16·1	14·0	14·0

and table IX for baseband filter III), while tables X and XI give the results for modulated RF carrier waves. In both the latter cases, baseband filter III was used, and f_{mn} was equal to 0·64. Table X is for the open-loop system, and table XI for a number of closed-loop systems. The open-loop thresholds for baseband filters I, II and III are 10·9, 11·4 and 9·8 dB, respectively.

Agreement between the measurements and the calculations is about as good as when baseband filter I was used.

It may be remarked that use of the time percentage 6%, as in the previous calculations, still gives good results. This is by no means required by our theory of the threshold mechanism: the percentage of the time during which the system

TABLE X

Open-loop threshold (dB) for modulated RF carrier waves with baseband filter III

z	M	C
0	9·8	—
0·29	10·2	10·2
0·43	11·2	11·0
0·86	12·2	12·2
1·14	13·4	13·4
1·43	14·5	14·6
1·72	16·8	15·9
2·00	18·7	16·9

TABLE XI

Closed-loop threshold (dB) for modulated RF carrier waves with baseband filter III

y	x	z	M	C
2	0·70	0·86	13·3	13·5
4	2·57	0·43	17·0	17·2
6	0·50	0·86	15·4	15·5
8	0·70	0·43	17·0	16·9
8	0·70	0·86	19·1	17·9
10	0·29	0·29	14·2	14·2

must operate below the open-loop threshold to give rise to the closed-loop threshold could theoretically be a function of the parameter k of the filters used. In fig. 4.21, idealized S/N curves have been plotted for three different values of k. In order to facilitate comparison of the form of the S/N curves, they have been shifted so that their thresholds coincide. We have chosen $k_1 > k_2 > k_3$. It will be seen that the curve for k_3 is not so steep below the threshold as the curve for k_2. We might therefore expect that the system would have to work under the threshold for a longer percentage of the time with the filter configuration with parameter k_3 than with k_2. However, this effect is counteracted by the fact that the value of $(S/N)_i$ at which the curve for k_3 starts to fall off is further from the threshold than that for the k_2 curve. As a result, the time

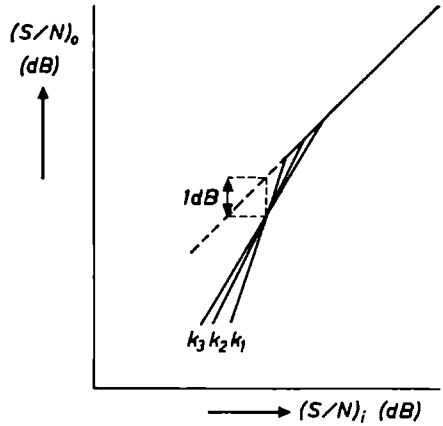

Fig. 4.21. S/N curves for various values of k, shifted so that the thresholds coincide; $k_1 > k_2 > k_3$.

percentage would tend to be smaller. These two effects thus cancel one another out, at least to a certain extent; and the results of the measurements show that they in fact almost completely balance one another. This means that the percentage of 6% used is independent not only of the feedback factor, the feedback filter and Δf_{IF}, but also of the parameter k of the IF filter and the baseband filter.

We have already seen that each configuration gives a certain shift from the open-loop threshold to the closed-loop threshold, and that this shift can be calculated. It might now be thought that this shift is constant for a given system configuration (x, y, z), i.e. independent of the value of k. It may be seen from table XII that this is not the case. This table gives measured values of the threshold shift (in dB) for a number of combinations of x and y ($z = 0$ in all cases), for various baseband filters. Inspection of this table shows clearly that the threshold shift depends on the value of k: the lower the open-loop threshold (which decreases with decreasing k), the higher the threshold shift. The threshold shift varies by up to 1 dB in this way. This effect can be explained as follows. For a given combination of x and y and a given value of $(S/N)_i$, the effective VCO noise is the same for all three baseband filters. However, it should be remembered that the effective VCO noise for $(S/N)_i$ a dB above 9·8 dB is greater than that a dB above 11·4 dB. This means that, for values of $(S/N)_i$ with the same distance to the open-loop threshold, the different baseband filters will give different sub-threshold percentages. This leads to the observed difference in threshold shift. The method of calculating the threshold given in this chapter automatically takes this into account.

TABLE XII

Comparison of the threshold shift with various baseband filters.

x: normalized bandwidth of the feedback filter,
y: feedback factor,
a: baseband filter,
b: value of k for the combination of IF filter and baseband filter (the IF filter remains unchanged),
c: open-loop threshold (dB),
d: measured closed-loop threshold (dB),
e: $d - c$ = the threshold shift due to the feedback (dB)

			$x = 0{\cdot}70$		$x = 0{\cdot}50$		$x = 0{\cdot}29$	
	$y = 4$							
a	b	c	d	e	d	e	d	e
III	1·82	9·8	13·2	3·4	12·4	2·6	11·6	1·8
I	2·75	10·9	13·8	2·7	13·2	2·3	12·5	1·6
II	3·65	11·4	14·0	2·6	13·1	1·7	12·4	1·0
	$y = 6$							
III	1·82	9·8	15·0	5·2	13·8	4·0	12·6	2·8
I	2·75	10·9	15·6	4·7	14·6	3·7	13·6	2·7
II	3·65	11·4	15·4	4·0	14·5	3·1	13·3	1·7
	$y = 8$							
III	1·82	9·8	16·2	6·4	14·9	5·1	13·4	3·6
I	2·75	10·9	16·7	5·8	15·6	4·7	13·9	3·0
II	3·65	11·4	16·9	5·5	15·4	4·0	13·8	2·4
	$y = 10$							
III	1·82	9·8	17·7	7·9	15·9	6·1	14	4·2
I	2·75	10·9	18·3	7·4	16·4	5·5	14·3	3·4
II	3·65	11·4	18·3	6·9	16·7	5·3	14·6	3·2

4.10. Variations in the form of the amplitude characteristic of the IF filter

All the system configurations we have considered so far have had the same IF filter. The parameters of the IF filter which can be changed are the bandwidth and the form of the amplitude characteristic. The influence of variation of the bandwidth has already been covered indirectly in our discussion of the variation of the bandwidth of the baseband filter and of Δf_{IF}. This leaves us with changes in the form of the amplitude characteristic, which will be discussed in this section. However, there is very little play in the choice of this parameter, since it has to represent a compromise between such requirements as the maximum possible feedback factor, a low open-loop threshold and a threshold shift which depends as little as possible on the modulation. If we

TABLE XIII

	y_{max}		
x	IF filter I	IF filter II	IF filter III
∞	10	11	10
2·57	12	6	6
1·05	16	6	7
0·70	19	7	8
0·50	23	8	10
0·29	30	10	13
0·12	50	13	20

TABLE XIV

Open-loop threshold (dB) for modulated RF carrier waves

	IF filter II		IF filter III	
z	M	C	M	C
0	9·1	—	8·2	—
0·29	9·5	9·3	8·5	8·5
0·57	10·2	10·2	9·6	9·4
0·86	11·4	11·4	10·8	11·0
1·43	14·8	14·1	14·7	14·2

make the amplitude characteristic of the IF filter steeper while retaining the same 3-dB bandwidth, we obtain a lower open-loop threshold; but at the same time the threshold shift due to the modulation will increase. The maximum feedback factor will also be lower, in general. In nearly all the publications in this field, the authors intuitively choose a simple LCR circuit for the IF filter. The measurements described in this section confirm that this is indeed a good choice. In order to test the theory of the threshold calculation, however, we have also investigated two other IF filters with a steeper amplitude characteristic. Apart from IF filter I, IF filters II and III, described in sec. 1.3, were thus also tested in the FMFB receiver. Baseband filter I was used for all these measurements. The open-loop thresholds for IF filters I, II and III are 10·9, 9·1 and 8·2 dB, respectively.

The results of the measurements and calculations are again given in tabular form. Table XIII represents the influence of the IF filter on the stability; the quantity given in this table is y_{max}, the measured maximum feedback factor at which the system is still just stable. The open-loop thresholds for IF filters II and III with modulated carrier waves are given in table XIV. Table XV gives a number of closed-loop thresholds for IF filter II, and table XVI for IF filter III.

TABLE XV

Closed-loop threshold (dB) for FMFB receiver with IF filter II

y	x	z	M	C
0	—	0	9·1	—
3	∞	0	15·6	15·8
3	∞	0·86	18·0	17·7
3	0·70	0	12·0	11·8
3	0·70	0·86	14·6	14·3
3	0·29	0	10·3	10·2
3	0·29	0·86	12·7	12·5
5	1·05	0	18·1	16·5
5	0·70	0	15·2	14·4
5	0·50	0	13·0	12·8
5	0·29	0	11·3	11·3
5	0·29	0·86	14·0	13·6
7	0·29	0	13·2	12·6
9	0·29	0	15·9	14·7

TABLE XVI

Closed-loop threshold (dB) for FMFB receiver with IF filter III

y	x	z	M	C
0	—	0	8·2	—
2	∞	0	12·9	12·9
2	∞	0·86	15·8	15·6
2	2·57	0	12·3	12·2
2	2·57	0·86	15·6	15·0
2	1·05	0	11·0	11·0
3	1·05	0	13·3	12·7
3	1·05	0·86	16·8	15·7
3	0·70	0	12·0	11·7
4	0·70	0	13·9	13·2
5	0·50	0	13·9	13·2
6	∞	0	18·8	18·7
6	0·29	0	12·4	11·8
8	0·29	0·86	14·0	12·8
8	0·12	0·86	10·7	10·1

The agreement between calculation and measurement is good over a wide range. The measurements show that despite the steeper amplitude characteristics of the IF filters, a feedback filter is still needed to give a low closed-loop threshold. It appears that IF filters II and III have a very limited applicability (low values of y_{max}), and that the designer of FMFB receivers will be well advised to base his designs in the first instance on use of a simple LCR circuit as IF filter. Just as we found with IF filter I, discrepancies are found between the calculated and measured thresholds at large feedback factors and at large threshold shifts. We shall be returning to this point in sec. 4.12.

4.11. Modulation with noise

In all the measurements discussed so far, the RF carrier wave was either unmodulated or modulated by a sine wave. In practice, however, the baseband signal will be derived from speech, music, TV or telephony channels. A noise signal covering the whole baseband is therefore a more representative signal than a sine wave. Especially when the baseband signal comes from a large number of telephony channels, it is usual practice to replace this signal by Gaussian noise for the purpose of measurement. It is thus desirable to calculate the thresholds for RF carrier waves modulated with noise as well. From now

on, we shall only consider Gaussian noise. The measurement of the S/N curve for RF carrier waves modulated with noise is a difficult matter, because it involves the measurement of small differences in the ratio of two noise powers (of the information noise and the detected interference noise) which differ in level by something like 30 dB. The best way of measuring the interference noise is to compensate completely for the baseband signal in the detected signal. When a sine function is used as the baseband signal, this can be done quite easily because the compensation only has to work for one frequency. The situation is much more difficult when noise is used for the modulation, as the amplitude and phase compensation now has to be correct over a whole frequency band. Even when this is done with the greatest care, it still gives a decrease in the accuracy of the measurement. However, we have measured a number of S/N curves, in order to verify the agreement between calculation and measurement in this case too. For this purpose, we modulated the RF carrier wave with noise with a flat spectrum ("white" noise), with a bandwidth equal to that of baseband filter I. The results for $y = 0$ are given in table XVII, and for $y = 4$ in table XVIII. The effective frequency deviation of the RF carrier wave used, due to the information noise, is given in column D (divided by $B_{IF}/2$). In the calculation, we again determined the value of $(S/N)_t$ at which the receiver works under the open-loop threshold 6% of the time. This value of 6% has been experimentally determined for the FMFB receiver. (The closed-loop threshold is found when, as a result of the VCO noise, the receiver operates under the open-loop threshold more than 6% of the time.) As mentioned in sec. 4.3.3, there is a relation between the VCO noise and the RF noise. This

TABLE XVII

Open-loop threshold (dB) for modulation with noise

D	M	C
0	10.9	—
0·36	12·1	12·3
0·42	12·4	12·7
0·56	13·6	13·8
0·68	15·0	14·7
0·77	16·0	15·4
0·80	16·4	15·6
0·87	17·0	16·2
0·99	18·0	17·0
1·07	19·0	17·5
1·17	20·0	18·2

TABLE XVIII

Closed-loop threshold (dB) for modulation with noise

$x = 0{\cdot}70$, $y = 4$ (instrumental measurement)		
D (RF)	M	C
0	13·8	13·8
1·04	14·1	14·3
1·50	14·6	14·6
$x = 0{\cdot}70$, $y = 4$ (measurement by ear)		
D (RF)	M	C
1·05	14·0	14·3
1·68	15·0	14·9
2·02	16·0	15·4
2·40	17·0	16·0
2·86	18·0	16·6
3·15	19·0	17·0
3·46	20·0	17·4
$x = 0{\cdot}50$, $y = 4$ (measurement by ear)		
D (RF)	M	C
1·35	14·0	14·0
1·88	15·0	15·0
2·18	16·0	15·5
2·63	17·0	16·1
2·94	18·0	16·8
3·23	19·0	17·4
3·54	20·0	17·8

relation is accounted for in this 6%. However, this does not mean that we can automatically assume that the same value of 6% can be used for an open-loop receiver and a carrier wave modulated by noise. On the other hand, we have seen in sec. 4.3.4 that threshold values calculated on the assumption that the VCO noise and the RF noise are independent of one another agree quite well with the measured values; this implies that the value of 6% may well be

practically independent of the relation existing between the RF noise and the VCO noise. Since, moreover, the precise value of the percentage used is not too critical as regards the threshold calculation (secs 4.5 and 4.8), we decided to start by trying the 6% method for the open-loop receiver too. The results show that this approach is justified.

The measurements for thresholds of 14, 15, 16, 17, 18, 19 and 20 dB were done by ear. The system was first set to a certain value of $(S/N)_i$. The effective frequency deviation of the RF carrier wave was now increased until the pulse noise produced in this way sounded the same as the output pulse noise at an instrumentally measured threshold. It goes without saying that the information noise was compensated for as well as possible in this case too. A well-trained ear is required if reproducible results ($< 0{\cdot}5$ dB) are to be obtained in this way. One of the difficulties is that the thresholds at different values of $(S/N)_i$ sound somewhat different. This limits the accuracy of the measurement. The agreement, and discrepancies, between the measured and calculated values for $y = 0$ show the same pattern as found for modulation with a sine wave (table IV). When the threshold shift is not too large, the agreement between measurement and calculation is good. As the threshold shift increases, however, the discrepancies increase with it. These differences can once again all be attributed to the effect of distortion (intermodulation). The calculations give the impression that the noise can be regarded as equivalent (as far as its effect on the threshold shift is concerned) to a single sine wave of amplitude about 1·9 times the effective value of the noise.

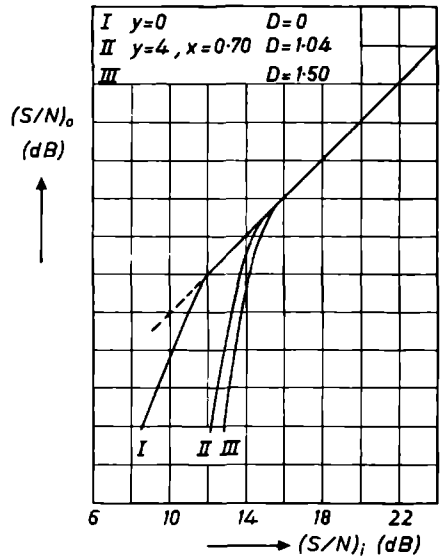

Fig. 4.22. S/N curves for RF carrier waves modulated with noise.

Measurements on feedback systems with noise-modulated RF carrier waves are even more difficult than those for open-loop systems. This is because the baseband spectrum of the information noise to be compensated for now depends on the parameters x and y as well. This measurement has therefore only been carried out instrumentally for one combination of x and y ($x = 0{\cdot}70$, $y = 4$) and two values of the effective RF frequency deviation. The results are plotted in fig. 4.22. In order to get a few more measured results, we also did some measurements by ear. The threshold for the feedback system was calculated as follows. Given the effective frequency deviation of the RF carrier wave, we calculate that of the IF carrier wave. The feedback factor and the non-ideal feedback across the frequency band of the baseband signal are taken into account in this calculation. The effective VCO interference noise is calculated for an unmodulated RF carrier wave. To get the result for modulated RF carrier waves, we have to multiply by the factor Q. We have seen how to calculate this factor in our discussion of the modulation by a sine wave (sec. 4.7.3). The same method may be followed for the calculation of the threshold for modulation with noise. Starting from the effective IF frequency deviation due to the information noise, we again select a number of levels, each of which is occupied a certain percentage of the time. Each level corresponds to a certain instantaneous frequency deviation, which gives rise to a certain instantaneous increase in the VCO interference noise. Averaging over all levels, we find the factor Q. The calculated effective VCO noise and the effective IF information noise are added by taking the square root of the sum of these squares. The closed-loop threshold is now calculated from the resultant effective frequency deviation, by the 6% method.

The instrumentally measured thresholds agree well with the calculated values. The thresholds measured by ear also agree with the calculated values for not too large threshold shifts (with respect to 10·9 dB). As the threshold shift rises, discrepancies are found. These can be partly attributed to experimental error, but are partly to be expected; similar discrepancies are found in the case of sinusoidal modulation, as we have seen.

4.12. The limits of the theory

4.12.1. *Introduction*

Inspection of the tabulated values of the measured and calculated thresholds shows that there are a number of configurations for which the agreement between measurement and calculation is not good. These discrepancies occur for large feedback factors, for large frequency deviations of the IF carrier wave due to the information signal, and in particular when these two factors are combined. In all cases where such a discrepancy is found, the measured threshold is higher than the calculated one; this suggests that some additional effect

is involved, which causes a shift in the threshold. It may be suggested that a system in which this effect occurs has been incorrectly designed, in view of the extra threshold shift encountered. However, it is still worth while studying the effect in question, so as to learn more about the limits within which the theory developed in this thesis is applicable, and about the mechanism giving rise to this effect. This investigation will be split into two parts: we shall start by discussing the open-loop receiver, and continue with the closed-loop receiver.

4.12.2. *Extra threshold shift in the open-loop FM receiver*

The calculated and measured open-loop thresholds have been given in table IV for a number of values of z. We have seen that a discrepancy is found between the measurements and the calculations for $z > 1$, and that this discrepancy increases with increasing z. Figure 2.4 shows that the distortion is also appreciable at these values of z. The detected signal then has the form shown in fig. 4.23, with sharp spikes near the maxima and minima of the sine wave. This creates the impression that the frequency deviations in the IF filter are larger than those before the IF filter; this "extra" frequency deviation might be responsible for the extra threshold shift (for the calculation of the instantaneous amplitude, see Stumpers [7,8]). We have tested this hypothesis as follows. We started with a certain maximum frequency deviation and modulation frequency before the IF filter and the corresponding distorted signal after the IF filter. For this combination, we now calculated as a function of time the frequency deviation needed in front of the IF filter to give the same distorted signal after the filter (now assumed to be free of distortion). We then calculated for these deviations the probabilities that the signal should exceed a number of different levels, and used these data to calculate the threshold. It proved possible to calculate the threshold to quite a good approximation in this way, even for quite large frequency deviations (and correspondingly large distortion). We shall not go into further details, as this would be of little practical significance. The above line of reasoning was however only intended to give an idea of the relationship between the threshold shift and the distortion; the insight gained in this way can be used to explain the extra threshold shift found with the

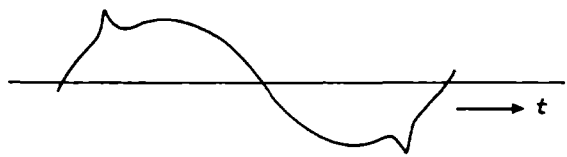

Fig. 4.23. Output signal as a function of time, for large values of z.

FMFB receiver. It can also help us to explain why, when f_{mn} increases for $z > 1$, the S/N curves shift first to the right and then to the left, as described in sec. 4.2. This effect is connected with the distortion, which first increases with increasing f_{mn} (thus giving rise to an increase in the extra threshold shift) and then decreases again (see fig. 2.4 for the third-harmonic distortion). For $z < 1$, the distortion is so slight that it has no appreciable effect on the threshold.

4.12.3 *Extra threshold shift in the closed-loop FM receiver*

In the closed-loop receiver, we have to deal with two signals, namely the desired FM signal and the VCO noise. The frequency deviations of these two signals will generally be such that individually they are hardly distorted by the IF filter. Their sum may however have such a value as to give rise to intermodulation in the IF filter. This intermodulation gives rise to an extra threshold shift, just as the distortion in the open-loop system does. In order to test whether intermodulation really occurs in this situation, we proceeded as follows. The RF carrier wave of the open-loop system was modulated with a sine wave and a noise signal. The spectrum and effective value of this noise signal were made equal to those of the noise at the input of the VCO of a closed-loop system operating at its threshold. No RF interference noise was present. The detected noise was studied as a function of increasing Δf_{IF} (sine modulation). It was found under these circumstances that when Δf_{IF} reached a certain value, larger peaks appeared in the detected noise. The value of Δf_{IF} at which this occurred depended on the noise-modulation setting. It was also found that the combination of Δf_{IF} and the effective frequency deviation due to the noise at which these larger peaks occurred practically coincided with the corresponding combinations for the closed-loop system at which differences between the measured and calculated thresholds started to be found. We concluded from this that the extra threshold shifts are indeed caused by the intermodulation of the sine function and the VCO noise in the IF filter.

It is hardly useful to calculate this intermodulation, and to determine the exact value of the resulting threshold shift. We have therefore restricted ourselves to determining the limit at which intermodulation starts to play a role. For this purpose, we had to supplement the results of the measurements tabulated above with a large number of measurements on system configurations adjusted so as to give a marked difference between measurements and calculations. By a marked difference, we understand here a difference of 0·5 dB or more between the measured and calculated thresholds. On the basis of these measurements, the following conclusions may be drawn.

The higher the value of z, the lower the threshold at which a discrepancy appears between measurement and calculation. At $z = 0{\cdot}86$, the system is found to be able to deal with a threshold shift of 7 dB with respect to the

open-loop threshold. At $z = 0{\cdot}57$, the corresponding threshold shift is 7·5 dB, and at $z = 0$ it is 8·5 dB. The values found with the feedback filters with $x = 0{\cdot}12$ and $0{\cdot}29$ were somewhat lower, and those for $x = 1{\cdot}05$ and $2{\cdot}57$ were somewhat higher.

The lower the frequency of the 3-dB point of the feedback filter (and thus the lower the value of x), the lower was the threshold at which discrepancies started to make themselves evident. This is what we would expect from the intermodulation theory, for the lower the 3-dB frequency of the feedback filter, the lower the maximum in the closed-loop characteristic (see figs 4.9 and 4.10), and the greater the intermodulation under otherwise equal deviation conditions. For the analogy with the distortion, see fig. 2.4.

For threshold values where the difference between measurement and calculation was 0·5 dB, the combined effective frequency deviation

$$\{z^2/2 + (\dot{\phi}_{\text{eff}}/\tfrac{1}{2}B_{\text{IF}})^2\}^{1/2}$$

was found to be more or less the same for the different system configurations, and to be only slightly dependent on the value of z. For $z = 0{\cdot}57$, this combined effective frequency deviation is approximately equal to 1; for $z = 0{\cdot}86$ it is about 10% greater, and for $z = 0$ about 10% less. Slight deviations from the above pattern are found for the feedback filters with very high and very low cut-off frequencies (3-dB points).

Care should be taken to ensure that the feedback factor chosen is not too close to the maximum feedback factor permitted in connection with the stability. We have already shown in sec. 4.7 that the maximum value of y decreases in the presence of modulation. When the feedback factor is too large, oscillations occur at the maxima of the frequency deviations. Further, it will be clear that the larger the value of y, the larger the effective VCO noise. This thus also imposes limitations on the maximum value of y; and this restriction is in fact more severe than that connected with the stability requirements.

In view of the restrictions which are imposed on the feedback filter, it is probably a good idea to consider now what are the most suitable values for the feedback filter. For this purpose, we have calculated the actual reduction in the maximum frequency deviation for a number of systems. With ideal feedback, this reduction should be by a factor of $(1 + y)$. However, the use of filters makes the feedback non-ideal; in fact, the feedback is highly frequency-dependent under these conditions. The factor is then reduced by a further factor T. It has been found that the value of T depends mainly on the feedback filter used, and only very slightly on the value of y. The value of T has been calculated for all feedback filters, for the modulation frequency $f_{mn} = 0{\cdot}57$ (maximum frequency passed by baseband filter I). The effective reduction factor T_{eff} has also been calculated over the whole bandwidth of baseband filter I, on the assumption that the RF carrier wave is modulated with flat-spectrum

TABLE XIX

Reduction of the feedback factor

x	$T(f_{mn} = 0{\cdot}57)$	T_{eff} (for base-band filter I)
∞	1·12	1·03
2·57	1·16	1·04
1·05	1·32	1·11
0·70	1·51	1·16
0·50	1·78	1·25
0·29	2·70	1·79
0·12	5·90	3·51

noise. The values of T are given in table XIX.

It will be clear that a given effective feedback factor can be obtained with different combinations of x and y. Comparison of the measured thresholds and the effective feedback factors has shown us that for a given effective feedback factor the threshold shift with respect to the open-loop threshold is practically independent of the feedback filter used. Only the filters with $x = \infty$ and $x = 2{\cdot}57$ give a slightly greater threshold shift. However, all this tells us little about the quality of the system. For a given effective feedback factor, if the feedback filter has the lowest value of x, the value of y will have to be the highest; for these filters, the lowest modulation frequencies will be fed back most strongly. However, a feedback filter with a high value of x is to be preferred in the interests of good feedback at higher modulation frequencies (which is of importance in connection with the intermodulation). Since moreover the filters with a high value of x also give more uniform feedback of the intermodulation products and the distortion, it will be clear that feedback filters with a low value of x do not come into consideration for this application in practice.

4.13. Signal fall-off

We mentioned in chapter 1 that if the instantaneous noise amplitude after the IF filter exceeds the amplitude of the carrier wave, there is the risk of an extra phase shift in the total signal, which results in a noise pulse after detection. The noise pulses produced in this way give an increase in the over-all noise level which is responsible for the increased steepness of the lower part of the S/N curves. When determining the measured S/N curves, we only measured the increase in noise and assumed the detected signal power to be constant for all values of $(S/N)_i$. However, it will be clear that each time a phase shift of 2π radians occurs, the signal information will be lost for a short time, so that the

detected signal power will fall off. In order to obtain the real S/N curves, therefore, we must determine not only the increase in noise (which is what has been done so far) but also the signal fall-off as a function of $(S/N)_i$. The signal fall-off is measured in dB. The detected signal in the absence of noise is taken as 0 dB. The sum of the curves for noise increase and for signal fall-off gives the real S/N curve. The signal fall-off has been measured for a number of configurations. The results are plotted in fig. 4.24; in part *a* for $y = 0$ and $z =$ 0·29, 0·57, 0·86 and 1·43, in part *b* for $y = 4$ and $z = 0{\cdot}86$, with $x = 0{\cdot}70$, 0·50, 0·29 and 0·12, and in part *c* for $y = 8$ (the other variables being as in part *b*). The noise-increase curves for the configuration of part *a* agree with those of fig. 4.13, those of part *b* with those of fig. 4.19 and those of part *c* with those of fig. 4.20. It can be seen clearly from these figures that the increase in noise

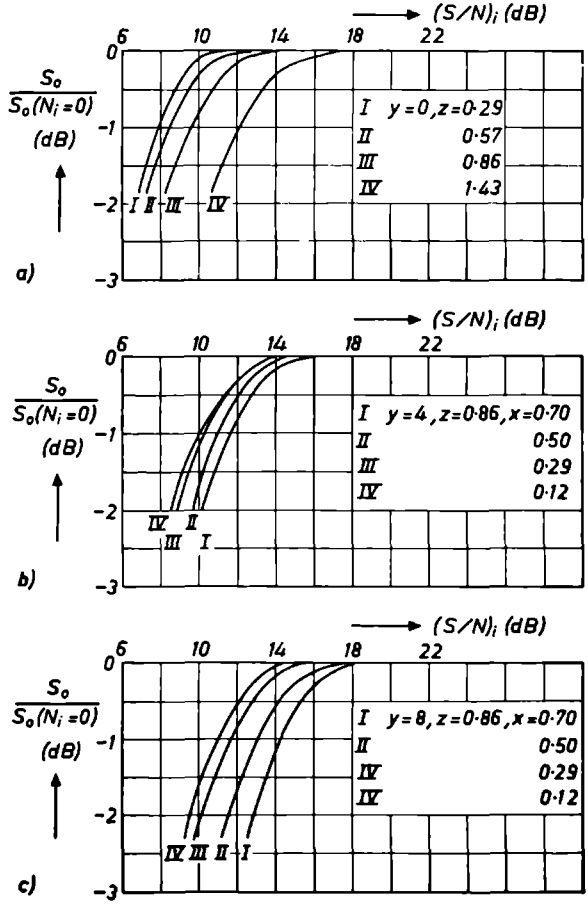

Fig. 4.24. Signal fall-off as a function of $(S/N)_i$.
(*a*) $y = 0$ and various values of x;
(*b*) $y = 4$, $z = 0{\cdot}86$ and various values of x;
(*c*) $y = 8$, $z = 0{\cdot}86$ and various values of x.

always begins at a higher value of $(S/N)_i$ than the signal fall-off, and that the signal fall-off has hardly any influence on the 1 dB extra deviation for which the threshold is defined. Since we are only interested in calculating the threshold of the S/N curves, we need thus pay no further attention to the signal fall-off.

5. DISCUSSION ON THE DESIGN OF THE FMFB RECEIVER

5.1. Specimen calculation of the threshold gain

Before we discuss the design of the FMFB receiver we shall show first, with the aid of an example, how we can calculate the closed-loop threshold, the open-loop threshold and the threshold gain for a given situation (see also sec. 4.2). The calculation that will be given only serves as an example, and does not pretend to give optimal results. The signal parameters and the system parameters will be chosen in such a way that the largest possible use can be made of calculations and measurements of the preceding chapters. For this reason we start with the calculation of the closed-loop receiver and then consider the open-loop receiver.

In practice, the carrier will be modulated with an information signal covering the whole baseband. The closed-loop and open-loop systems can then be compared on the basis of the intermodulation requirements. However, to keep the calculations simple we shall here use as a measure of the intermodulation the third-harmonic distortion of that sine wave which gives the largest distortion. For the closed-loop system, we must take the feedback of the intermodulation into account. Because we consider the distortion as a measure of the intermodulation the distortion must be divided by the factor $(1 + y)/T_{\text{eff}}$ (see sec. 4.12).

In the closed-loop system, IF filter I (simple LCR circuit with bandwidth B_{IF}) and baseband filter I (bandwidth 0·57 $B_{\text{IF}}/2$) are used. For the comparative open-loop system we naturally use baseband filter I again. However, the bandwidth of the IF filter will be larger and the amplitude characteristic can be steeper than that of IF filter I. Two simple LCR circuits in cascade (tuned to the same frequency) are used for the IF filter. The bandwidth of this filter must be calculated in accordance with the distortion specifications. This bandwidth will again be normalized with respect to the bandwidth of IF filter I (B_{IF}).

In the following calculation a closed-loop system has been chosen with a feedback filter with $x = 0{\cdot}70$, a feedback factor $y = 6$ and a normalized maximum IF frequency deviation $z = 0{\cdot}86$. We see from table XIX that the reduction factor T_{eff}, by which the factor $(1 + y)$ is reduced, is equal to 1·16. Figure 2.4 shows that for the open-loop receiver with IF filter I and $z = 0{\cdot}86$ the maximum distortion for modulation frequencies in the baseband, is equal to 3·4%. We thus find a distortion of $\{3{\cdot}4/(6 + 1)\} \times 1{\cdot}16 = 0{\cdot}55\%$ for the closed-loop receiver.

From table VII we see that the closed-loop threshold for the given configuration is 17·2 dB.

The maximum RF frequency deviation is

$$\frac{6+1}{1{\cdot}16} \times 0{\cdot}86 \times B_{IF}/2 = 2{\cdot}6\, B_{IF}\,.$$

The bandwidth of the IF filter in the open-loop receiver must be such that the distortion for $\Delta f_{RF} = 2{\cdot}6\ B_{IF}$ and $f_{mn} = 0{\cdot}57$ is equal to 0·55%. The calculated 3-dB bandwidth is $6{\cdot}86\ B_{IF}$. The noise bandwidth of the above-mentioned IF filter is 1·22 times the 3-dB bandwidth. We thus find for the value of the parameter k (see sec. 1.1):

$$k = \frac{1{\cdot}22 \times 6{\cdot}86 \times B_{IF}}{2 \times 0{\cdot}57 \times B_{IF}/2} = 14{\cdot}7\,.$$

Because there is only a slight difference between the S/N curves (for the same value of k) for filters with a rectangular and a Gaussian amplitude characteristic (see Stumpers [3]), the difference between the S/N curves for a Gaussian filter and a filter with two LCR filters in cascade will also be very small.

TABLE XX

Calculation of the threshold gain

y: feedback factor,
x: normalized 3-dB bandwidth of the feedback filter,
z: normalized maximum IF frequency deviation,
a: baseband filter,
b: percentage distortion,
c: threshold gain (dB),
d: RF modulation index,
e: closed-loop threshold (dB)

y	x	z	a	b	c	d	e
6	1·05	0 86	I	0·47	5·5	9·5	18·3
6	0·70	0·86	I	0·55	6·3	9·1	17·2
6	0·50	0·86	I	0·59	6·9	8·4	16·3
6	0·29	0·86	I	0·87	6·4	5·8	15·1
6	0·29	0·66	I	0·55	6·3	4·4	14·2
6	0·70	0·86	II	0·50	6·7	13·1	17·2
6	0·70	0·57	I	0·25	6·5	6·1	16·1
4	0·70	0·86	I	0·76	6·0	6·5	16·2
8	0·70	0·86	I	0·42	6·0	11·1	18·5

The threshold of the open-loop system can thus be found to a good approximation with the aid of fig. 1.3. Extrapolation gives a value of 21·7 dB for the comparative open-loop threshold.

In the comparative open-loop receiver the modulation will also have some influence on the threshold. The maximum carrier attenuation for $\Delta f_{RF} = 2{\cdot}6\ B_{IF}$ is equal to 1·8 dB. The comparative open-loop threshold for modulated carrier is thus: 21·7 + 1·8 = 23·5 dB (see sec. 4.10). The threshold gain is therefore: 23·5 — 17·2 = 6·3 dB.

These calculations have also been performed for a number of other configurations. The results are given in table XX.

5.2. Design of the FMFB receiver

Frequency feedback can be used in FM receivers for a variety of reasons. For example, we may want a receiver with the lowest possible threshold at the maximum permissible distortion, or one with the minimum distortion at the highest permissible threshold.

The design procedure will of course be completely different for these different receivers. The present study of the closed-loop FM receiver has mainly been carried out in the interests of satellite communication (lowest possible threshold); we shall therefore go into somewhat greater detail about the design considerations for this particular case.

We have seen that in the open-loop FM receiver, when the baseband filter is given, the threshold is primarily determined by the bandwidth of the IF filter: the narrower the bandwidth, the lower will this threshold be. However, this frequency band cannot be made narrower without limit, because of the associated increase in the distortion. It would thus seem to be reasonable to base the design on the search for the lowest possible threshold at a specified maximum permissible distortion. Similar considerations will naturally hold for the closed-loop FM receiver, except that here the IF filter is not the only factor determining the distortion and the threshold.

The signals to be detected by the closed-loop FM receiver may be modulated by different baseband signals. The distortion specifications will depend on the type of baseband signal involved, and on the reason why feedback has been used. In certain cases, the baseband signal can be replaced by a single sine function, the distortion of which after detection must satisfy certain requirements. In other cases, the whole baseband signal will have to be taken into consideration, and the distortion specifications will take the form of requirements concerning the intermodulation.

In the case of satellite communication, the baseband signal consists of a large number of telephony channels. It is normal to replace the baseband signal by Gaussian noise for measurement purposes in this case. The distortion specifications can then be given in terms of the maximum permissible intermodula-

tion power with respect to a relative zero level. The calculation of this intermodulation power is not difficult, but it does involve a great deal of computation. This calculation can be carried out as follows. The noise signal together with the baseband signal is replaced by a number of sine functions at equal frequency intervals, with random phases. The carrier wave frequency-modulated by these sine functions is resolved into its frequency components. After passage through the IF filter, these components are combined again, and the detected signal is calculated and resolved into harmonics. The course of the calculation resembles that used in chapter 2 for a baseband signal consisting of a single sine function. The intermodulation spectrum is obtained by repeating these calculations a large number of times for different combinations of random phases, and averaging the results. The way this spectrum is modified by the feedback has been described in chapter 3.

The design calculations will involve the calculation of the open-loop threshold for a large number of combinations of IF filters and baseband filters. For IF filters with rectangular and Gaussian characteristics, these calculations have been carried out by Stumpers [3]). It would be possible in principle to repeat these calculations for other IF filters. However, it will probably be simpler to perform the calculations as described for the intermodulation. The difference is that now the RF noise is represented by a number of sine waves. The S/N curves for an IF filter with a rectangular amplitude characteristic have already been calculated by this method. The agreement with Stumpers' calculated results is good. The open-loop S/N curves for a sinusoidally modulated carrier wave can also be conveniently calculated in this way. During the writing of this thesis, we became aware of similar calculations for open-loop FM receivers, published by Medhurst and Roberts [51]) and Ruthroff [52]). The calculation of the closed-loop curves by this method is a much more complicated matter, however.

The design calculations for FMFB receivers come down to optimization of the threshold (i.e. making the threshold as low as possible), with the IF filter, the feedback filter and the feedback factor as variables in the calculation. Further, there are a number of boundary conditions which must be fulfilled. The most important of these is the maximum permissible distortion or intermodulation of the information signal. Secondary boundary conditions include the maximum permissible feedback factors and frequency deviations due to the intermodulation between the interference noise and the information signal. The relation between the variables is very complex, and can be illustrated as follows. The open-loop threshold is determined by the IF filter while the closed-loop threshold is determined by the reduced IF frequency deviation (due to the information signal) and the VCO noise. The reduction in the FM frequency deviation is mainly determined by the feedback factor, but also by the feedback filter and the IF filter. The VCO noise is determined by the IF filter, the

feedback filter, the feedback factor and the IF frequency deviation. The open-loop distortion is determined by the reduced IF frequency deviation and the IF filter, while the closed-loop distortion is determined by the IF filter again, and further by the feedback filter and the feedback factor. We thus see that in the closed-loop system too, the IF filter plays the dominant role, but that the feedback filter and the feedback factor also have important roles to play.

Owing to the complexity of the system, we have not yet been able to carry out the design calculations by one of the standard optimalization methods. This would probably be possible with the aid of some simplifying assumptions. The simplifications most commonly found in the literature are the assumptions that the IF filter is a simple LCR filter whose bandwidth can be determined with the aid of Carson's rule, and that the modulation has no effect on the threshold. As we have shown above (sec. 4.10), a simple LCR filter is indeed a good choice for the IF filter. The use of Carson's rule appears more questionable to us. According to this rule, the bandwidth of the IF filter is taken to be independent of the exact distortion specifications, which can themselves differ from application to application. Further, Carson's rule is also used for the open-loop FM receiver. The influence of the feedback on the distortion is thus completely neglected. The influence of the modulation on the threshold has already been discussed in detail in chapter 4. As we saw there, this factor is by no means negligible.

Since classical optimalization methods are not applicable to our particular problem, we must have recourse to some kind of trial-and-error method. When making use of such a trial-and-error method, we assume the parameters of the signal to be detected to be known, including the effect of such operations as pre-emphasis on the signal. The IF filter, the feedback filter and the feedback factor of the receiver can be varied. In principle, both the bandwidth and the form of the amplitude characteristic of the filters can be changed. In order to keep the trial-and-error procedure relatively simple, however, we assume in the first instance that the IF filter is a simple LCR filter, and that the feedback filter is a simple integrating RC filter. Consequently, only the bandwidths of the filters are variable. The frequency characteristics of the non-variable parts of the receiver must also be known. It is tacitly assumed that these parts are optimally designed, which means mainly that the phase shift and the distortion they cause are minimum.

The trial-and-error procedure can now be carried out in the following stages.

We start from a configuration with certain bandwidths for the IF filter and the feedback filter, and a certain feedback factor. We now determine the intermodulation noise for this configuration. The bandwidth of the feedback filter is varied until the maximum permissible intermodulation is obtained. The closed-loop threshold for this configuration is now determined. This threshold is called sub-optimum A.

We now take another value of the feedback factor, and vary the feedback filter again until the maximum permissible intermodulation is obtained. In this way, we can calculate sub-optimum *A* for each value of the feedback factor. The best sub-optimum *A* is called sub-optimum *B*.

The next step is to change the bandwidth of the IF filter. A certain value of sub-optimum *B* is found for each bandwidth; the best sub-optimum *B* is called sub-optimum *C*.

Sub-optimum *C* will probably be quite close to the real optimum. Nevertheless, the influence of other forms of the amplitude characteristics of the IF filter and the feedback filter still has to be investigated. In principle, this should be done by carrying out the whole procedure for other IF filters. However, this can never be done in practice, because of the mass of calculations involved. What can be done is to repeat the calculations for a number of variations, so as to get an idea of the influence of these variations.

In principle, a trial-and-error method of this type can be carried out completely by computer. However, the programming work and the computing time involved are large so that this is not always a practical solution. Another solution is to design the FMFB receiver not by means of calculations alone, but by a mixture of measurement and calculation. This can be done as follows. We build a closed-loop FM receiver in which all non-variable parts have been given the optimum design (as regards distortion and phase shift). The IF filter, the feedback filter and the feedback factor of the receiver are made variable. The RF signal for which the receiver has to be optimalized is now applied to the input; a noise source can also be connected here. Equipment can be connected to the output of the receiver for the measurement of the noise and the intermodulation. In principle, the optimalization process described above can now be carried out again, except that we now have the choice between measurement and calculation for any given step.

6. DISCUSSION OF PREVIOUS PUBLICATIONS

6.1. Introduction

A great deal has already been published in the literature about the FMFB receiver [10–43]). These various publications represent a great many different views concerning the operating mechanism of this receiver. Since the different views have not so far been seriously compared and criticized in relation to one another, they can all still be regarded as more or less provisional, and hence somewhat lacking in significance. We consider therefore that it would be wrong to introduce a new view in this field without providing an opportunity for discussion. This discussion can be initiated by means of a thorough criticism of a number of the most important previous publications; the criticism may refer to certain points in the individual publications themselves, but can also consist in a comparison of the different theories expressed in various publications. We hope that the latter approach will also help to give the reader a better insight into the present work, which might lead to fruitful criticism of our views too.

It would go far beyond the scope of this thesis to discuss all the publications in this field. We have therefore restricted ourselves to the most important ones. This criterion of "importance" which we adopted is naturally rather vague, but entailed at least that the publication in question introduced a new view of the problem, and discussed the consequences of this new view for the theoretical treatment and practical design of the receiver. On this basis, we selected the publications of Enloe [13,14]), Frutiger [31]) and Kühne [35,36]) for discussion.

Any reference to a numbered equation in the discussion below will follow the numbering of the original publication. The symbols used will likewise follow the original publications.

6.2. Enloe's theory

The best-known and most important work on the FMFB receiver is that of Enloe [13,14]). He gives a theory, based on experiments, which allows the threshold of a closed-loop FM receiver to be calculated. This theory has been used as the basis for further discussion in a large number of later publications. It would thus seem useful to compare Enloe's theory with ours in some considerable detail.

The threshold calculation proposed by Enloe is based on a single empirical figure: he states that the threshold occurs when the effective phase modulation of the VCO carrier wave due to the feedback noise becomes equal to 1/3·11 radian. The explanation given for this effect is that at this point the VCO noise becomes so strong that it gives rise to extra noise when it is mixed with the RF noise. This implies the existence of an independent closed-loop threshold mechanism in the FMFB receiver, in addition to the open-loop threshold

mechanism. However, it is not very clear how this is supposed to happen. According to Enloe, the phase noise $N_s(t)$ at one input of the mixer stage gives rise to the phase noise $\phi_s(t)$ at the other input. The mixing in the mixer stage also gives rise to the extra phase noise $N_c(t)\,\phi_s(t)$. If this extra phase noise exceeds a certain limit, this produces still more phase noise in the mixer stage, leading to a cumulative process which produces the threshold. Enloe states that this process starts when the ratio of the spectral densities of $N_c(t)\,\phi_s(t)$ and $N_s(t)$ exceeds 1/10. However, it is not clear to us how a small change in the value of $N_s(t)$ at this point can lead to such a large increase in the extra phase noise: an increase of $N_s(t)$ by 1 dB is supposed to change the role of the extra phase noise from a subsidiary one to a dominant one.

Another point of discussion lies in the difference made between the two threshold mechanisms. The open-loop threshold is caused by the pulse noise, while the closed-loop threshold is due to the extra increase in the phase noise. The extra phase noise, being the product of two Gaussian noise signals, is no longer Gaussian itself, but neither can it be described as pulse noise. It might thus be expected that no pulse noise would be observed after detection in those situations where the closed-loop threshold mechanism is predominant. However, our measurements have shown that, no matter at what value the threshold is found, pulse noise is always present. Enloe himself actually made use of the counting of noise pulses when determining the position of the threshold by ear.

While there thus seems to be some doubt about the explanation given for the empirical relation found between ϕ_{rms} and the threshold, this does not mean that this empirical relation is of no practical value. In order to test the value of this empirical relation, we have used it to calculate the threshold for a number of the system configurations investigated by us. The method of calculation will now be explained and commented on.

The method of calculating the effective frequency deviation of the VCO noise has been described in sec. 4.4. We saw there that the agreement between measurement and calculation is good. In a similar way, the effective phase deviation has been calculated as a function of $(S/N)_i$; these results were plotted in fig. 4.7 and 4.8. The threshold occurs at that value of $(S/N)_i$ at which $\phi_{rms} = 1/3{\cdot}11 = 0{\cdot}32$. The results obtained in this way are given in table XXI. Column C I gives the thresholds calculated according to Enloe's theory, while C II gives the calculated thresholds according to the same theory with slight modifications by us (see below). Columns M I, M II and M III give the measured thresholds for systems with baseband filter I, II and III, respectively.

Comparison of the calculated (C I) and measured thresholds gives rather a confused picture; for most configurations, the difference between measurement and calculation is 2 dB or less, while for quite a large number of configurations the difference is less than 1 dB. The following comments may be made in this connection.

TABLE XXI

Threshold calculations in accordance with Enloe's theory

y : feedback filter,
x : normalized bandwidth of feedback filter,
C I : calculated threshold according to Enloe's theory (dB),
C II : calculated threshold according to a modified version of Enloe's theory (dB),
M I : measured threshold for systems with baseband filter I (dB),
M II : measured threshold for systems with baseband filter II (dB),
M III: measured threshold for systems with baseband filter III (dB)

C I	C II	M I	M II	M III	C I	C II	M I	M II	M III
$y = 4$									
$x = 0{\cdot}70$					$x = 0{\cdot}50$				
12·9	13·6	13·8	14·0	13·2	12·1	12·7	13·1	13·2	12·4
$x = 0{\cdot}29$					$x = 0{\cdot}12$				
10·6	11·0	12·5	12·4	11·6	7·2	9·0	—	12·5	—
$y = 8$									
$x = 0{\cdot}70$					$x = 0{\cdot}50$				
17·6	18·1	16·7	16·9	16·2	16·2	16·4	15·4	15·6	14·9
$x = 0{\cdot}29$					$x = 0{\cdot}12$				
14·2	14·6	13·9	13·8	13·4	10·6	11·2	—	12·7	—

Enloe made his measurements by ear. We also did this for the modulation with baseband noise (see sec. 4.11). In our experience, the reproducibility of these measurements only began to be good after long training of the ear, combined with instrumental measurements.

Enloe's threshold is defined as that value of $(S/N)_i$ at which one noise pulse per second occurs. Our threshold is defined as that value of $(S/N)_i$ at which

$(S/N)_o$ differs by 1 dB from the extrapolated S/N curve for high values of $(S/N)_i$. According to our experiments, Enloe's thresholds should lie up to 0·3 dB to the right of our threshold. For $y = 4$, this effect is found to be disadvantageous, while for $y = 8$ it is advantageous.

Enloe made direct use of curves giving the effective phase deviation of the VCO carrier wave as a function of $(S/N)_i$. These curves are quite flat. This means that a slight error in the empirical value found will lead to a large error in the calculated threshold. The estimated error of 7% quoted by Enloe results in an error of 0·6 dB in the threshold.

The sign of the error for $y = 4$ is opposite to that for $y = 8$. This would seem to imply that the discrepancies are not due to a systematic error.

Enloe assumes that the curves for the effective phase deviation can be exactly calculated above the threshold. However, we have found that divergences occur between the calculated and measured curves for the effective frequency deviation, even to the right of the threshold. We have now applied the divergence found for the effective frequency deviation to the curves for the effective phase deviation (see figs 4.7 and 4.8). The curves obtained in this way were again used to calculate the thresholds, using the constant 0·32. The results are given in column C II of table XXI. The results for $y = 4$ are found to be better, while those for $y = 8$ are worse. While the divergence need not have exactly the same form for the phase noise and the frequency noise, the difference between the corresponding values in columns C I and C II may be expected to give a reasonable impression of the error produced by neglecting the divergence. This is found to be about 0·6 dB.

Enloe assumes that the bandwidth of the baseband filter has no influence on the threshold shift. As may be seen from table XII and the discussion of sec. 4.9, this can lead to an error of up to 1 dB. Enloe used an IF filter with a bandwidth of 6 to 7 kHz, and a baseband filter with a bandwidth of 3 kHz. As far as these filters are concerned, his measurements are best comparable with our measurements given in column M III.

Enloe realized that modulation of the carrier wave can lead to attenuation of the latter. However, he thought that this need have no effect on the threshold in a well-designed system. Our experiments have shown clearly, however, that the modulation does have an effect on the threshold, and that the magnitude of this effect depends on the frequency deviation.

6.3. Frutiger's theory

Frutiger [31]) was the first after Enloe to give a completely new theoretical treatment of the FMFB receiver. All the quantities of interest in the system were determined by a combination of theory and experiment. It is of interest to analyse his results in some detail.

The main conclusion of the work is embodied in eq. (36), which gives the relation between $(S/N)_i$ and $(S/N)_o$ for an FMFB receiver. The derivation of this equation is based on the assumptions of a Gaussian IF filter and ideal feedback for all baseband frequencies. It is further assumed that it makes little difference to the results whether the IF filter is Gaussian or is a simple LCR filter. In other words, according to these assumptions eq. (36) should be applicable to most of the system configurations. We would like to make the following comments about Frutiger's eq. (36).

Two noise components $P_1(f)$ and $P_2(f)$ (for $n(t)$ respectively larger and smaller than the carrier amplitude) are taken into account in eq. (36). $P_1(f)$ is calculated for the open-loop receiver and then divided by $(1 + h)^2$ (where $h \equiv y$); $P_2(f)$ is also calculated for the open-loop receiver, but is not divided by $(1 + h)^2$. The argument on which this approach is based, as given after eq. (33), is incorrect. Our experiments have shown that the noise pulses really are fed back: the pulse noise, like the distortion, is to be regarded as an extra interference factor. On the other hand, it is quite possible that the feedback of the noise pulses is non-linear, because of the large frequency deviations involved. To settle this issue we performed the following experiment. An extra open-loop receiver was placed behind the mixer of the FMFB receiver. The IF filter and the baseband filter of the extra open-loop receiver were the same as those of the closed-loop receiver. For a feedback factor $y = 0$ (no feedback) the two receivers had the same threshold. For higher values of y the closed-loop threshold shifted to the right, as expected, but at the same time the threshold of the extra open-loop receiver shifted to the right too, and in such a way that the two thresholds coincided all the time. This can only be explained by assuming that the noise pulses are fed back and hence appear in the extra open-loop receiver.

Frutiger also concluded from his measurements that the noise pulses are not fed back. He based this conclusion on the determination of $P_1(f) + P_2(f)$ as a function of f for given p (where $p \equiv (S/N)_i$); see fig. 8 in part II of his article. For $f = 0$ (only pulse noise), $P_1(f) + P_2(f)$ is independent of h. However, we cannot conclude from this that $P_2(f)$ is not reduced by the feedback, since for a given system configuration the threshold shifts to higher values with increasing h. It follows that for a given value of p, $P_2(f)$ will increase with increasing h; this larger value of $P_2(f)$ is then reduced again by the feedback, (probably non-linearly); $P_2(f)$ is thus subject to two opposed influences. That these two influences cancel out completely in the case of fig. 8 seems to be a coincidence, since the balance between the two effects will depend of the value of p at which the measurements are made, and on the system configuration.

Equation (36) gives expression to the assumption that the threshold shift due to the change from the open-loop to the closed-loop FM receiver is caused by

the fact that $P_1(f)$ is reduced by the feedback, while $P_2(f)$ is not. As a result, $P_2(f)$ gives a significant contribution for higher values of p. Since $P_2(f)$ is an exponential function of p, we might thus expect that the S/N curves would become less and less steep below the threshold with increasing y. However, our measurements show that the curves actually become steeper and steeper under these conditions.

During our measurements we have also observed that pulse noise is no longer found 2 dB above the open-loop threshold in the open-loop system. According to Frutiger's theory, this should imply that no pulse noise at all will be found with a closed-loop threshold situated 2 dB or more above the open-loop threshold. This is however in contradiction with our observations.

Equation (36) does not take the feedback filter into account. However, our measurements have shown that the feedback filter has an important influence on the S/N curves. Neglecting the effect of this filter is just about the same as neglecting the effect of the VCO noise.

Use was made in the derivation of eq. (36) of the auxiliary functions $\eta(n)$, which define $P_2(0)$ as a function of n. These functions were found by measurement. One criticism which may be made of these measurements is that the carrier wave was not mixed with plain Gaussian noise, but with clipped Gaussian noise. The sum signal obtained after mixing was limited and detected. The aim of the experiment was to determine how noise with a given instantaneous value is detected. However, the noise occurring in practice is quite different in nature from that used in these measurements. Another drawback is that $P_2(f)$ can only be measured for $f = 0$. It is assumed that the function $\eta(n)$ found at $f = 0$ also holds at other frequencies. However, no proof is given of this frequency independence.

In the derivation of eq. (36), the functions $P_1(f)$ and $P_2(f)$ are treated separately. It is assumed that $P_2(f)$ starts to play a part as soon as $n > 1$. This is not correct, however. It is true that n must be greater than 1 before $P_2(f)$ can play a part, but it is also necessary that the position of the noise vector with respect to the carrier-wave vector should fulfil certain conditions (Rice [2])).

In his design calculations, Frutiger calculates the minimum bandwidth of the IF filter. The following remarks may be made about this calculation.

No justification is given for the value of 10% used in eq. (28).

The value of p is taken as 4·8 in eq. (29). However, for a real optimum a sliding value of p should be used.

Carson's formula is used in eq. (31). The arguments against this formula have already been discussed in chapter 5.

6.4. Kühne's theory

Kühne [35,36]) gives a very interesting theoretical treatment of the FMFB receiver. He applies Rice's theory [2]) to the closed-loop FM receiver. Rice's

theory is based on the assumption that the threshold in the open-loop FM receiver is caused by the extra phase shift which can be produced when the instantaneous value of the noise exceeds the amplitude of the carrier wave. These phase shifts give noise pulses and the threshold can be calculated by counting these pulses. In the mathematical development of his theory, Kühne finds it necessary to introduce a number of approximations. However, in our opinion, insufficient justification is given for a number of these and we have no idea about the consequences of these assumptions on the final results. We would like to make the following remarks here in this connection. All these remarks apply to ref. 36.

In eq. (88), Kühne introduces an attenuation of the carrier wave by the VCO noise. However, he neglects the attenuation of the carrier in the IF filter. Besides, he then works with the effective attenuation of the carrier wave, while we consider that we have proved that the instantaneous attenuation of the carrier wave must be taken into consideration. Of course, this point also affects the validity of Kühne's equivalent circuits.

Equation (103) gives the frequency of the zero crossings of the in-quadrature components. This equation was derived for a rectangular noise spectrum. However, the spectrum in the FMFB receiver is strongly coloured. Nothing is said about the effect of this approximation on the final result. The same is true of eq. (107).

Kühne uses Frutiger's assumption that the noise pulses are not fed back. As we have mentioned, our experiments showed that there definitely is feedback of the noise pulses (sec. 6.3).

It seems to us that insufficient justification is given for the hypothesis that the threshold at high feedback is due to the fact that the feedback of the noise becomes non-linear under these conditions, while the feedback of the information signal remains linear. This statement really needs experimental justification.

In eq. (109), the quantities (exp σ^2) N_{b0} and N_{b2} were derived for small values of ϱ, and N_{b1} for small values of σ. Consequently, it will not do to add these three calculated noise contributions directly in an arbitrary situation (eq. (109)).

Kühne completely neglects the influence of the modulation on the threshold.

Design problems are considered in sec. 3.5. Here again, Carson's formula is used (though, as we have mentioned, it is not really applicable here). No proof is given of the statement that B_{sn} and hence the VCO noise should be minimum for optimum design.

List of symbols

$f_i(t)$	FM signal at input of receiver
$f_o(t)$	FM signal after passage through filter and limiter
$f_0 = \omega_0/2\pi$	carrier-wave frequency
$f_m = \omega_m/2\pi$	modulation frequency
$f_{mn} = \omega_{mn}/2\pi = f_m/\frac{1}{2}B_{IF}$	normalized modulation frequency
$\Delta f = \Delta\omega/2\pi$	maximum frequency deviation (for modulation with a sine function)
$\Delta f_{IF} = \Delta\omega_{IF}/2\pi$	ditto, after mixer stage
$\Delta f_{RF} = \Delta\omega_{RF}/2\pi$	ditto, at RF input of mixer stage
$\Delta f_{VCO} = \Delta\omega_{VCO}/2\pi$	ditto, at VCO input of mixer stage
k	noise bandwidth of the IF filter divided by $2B_{LF}$
$m = \Delta f/f_m$	modulation index
$n(t)$	Gaussian RF noise in a band of the carrier wave
$n_c(t)$	in-phase component of noise with respect to the carrier wave
$n_s(t)$	in-quadrature component of noise with respect to the carrier wave
$r(t)$	baseband signal
t	time
x	3-dB bandwidth of feedback filter, divided by $B_{IF}/2$
y	feedback factor = open-loop amplification for those frequencies at which feedback is ideal
$z = \Delta f_{IF}/\frac{1}{2}B_{IF}$	
z_t	value of z for those frequencies at which feedback is ideal
B_{IF}	bandwidth (3-dB) of IF filter
B_{LF}	bandwidth of baseband filter
$G_L(j\omega_m;\Delta\omega)$	LF transfer function of filter with limiter for FM signal
$J_n(m)$	Bessel function of the first kind of order n and argument m
N_i	noise power at input of FM receiver
N_o	detected noise power after baseband filter
Q	quotient of effective VCO noise with and without modulation
$R(j\omega_m)$	Fourier transform of $r(t)$
S_i	power of the input FM signal
S_o	detected signal power
T	factor by which the real reduction in feedback differs from $(1 + y)$

$\theta(t)$	phase noise of unmodulated RF carrier wave, due to the RF noise
$\phi(j\omega_m)$	Fourier transform of the phase of the VCO carrier wave due to the RF noise
$\psi_i(t)$	information-carrying phase angle of input FM signal
$\psi_o(t)$	information-carrying phase angle of FM signal after passage through filter and limiter

REFERENCES

[1]) S. O. Rice, Statistical properties of a sine wave plus random noise Bell Sys. tech. J. **27**, 109-157, 1948

[2]) S O. Rice, Noise in FM receivers In. M Rosenblatt, Time series analysis. Wiley and Sons, 1963, pp 395-422

[3]) F. L. H. M. Stumpers, Theory of frequency-modulation noise. Proc. IRE **36**, 1081-1092 1948.

[4]) P. F. Panter, Modulation, noise and spectral analysis. McGraw-Hill, 1965

[5]) J R Carson and T. C Fry, Variable-frequency electric circuit theory Bell Sys tech J **16**, 513-540, 1937

[6]) B. van der Pol, The fundamental principles of frequency modulation. J IEE (London) **93**, part 3, 153-158, 1946

[7]) F. L H. M Stumpers, Eenige onderzoekingen over trillingen met frekwentiemodulatie. Thesis Delft, 1946

[8]) F. L. H M Stumpers, Distortion of frequency modulated signals in electrical networks, Commun. News **9**, 82-93, 1948.

[9]) D Middleton, An introduction to statistical communication theory. McGraw-Hill, 1960.

[10]) J. G. Chaffee, The application of negative feedback to FM systems. Bell Sys. tech. J. **18**, 403-437, 1939

[11]) M. O. Felix and A. J. Buxton, The performance of FM scatter systems using frequency compression. Proc. Natl Electronics Conf. **1958**, 1029-1043.

[12]) C L. Ruthroff, FM demodulators with negative feedback. Bell Sys tech J **40**, 1149-1156, 1961.

[13]) L. H. Enloe, Decreasing the threshold in FM by frequency feedback Proc. IRE **50**, 18-30, 1962

[14]) L. H Enloe, The synthesis of frequency feedback demodulators. Proc Natl. Electronics Conf **1962**, 477-497.

[15]) E. Baghdady, The theory of FM demodulation with frequency-compressive feedback. IRE Trans. Comm. Syst. **10**, 226-246, 1962

[16]) R E Heitzman, Minimum power FM reception using frequency feedback. Proc. IRE **50**, 2503, 1962 (correspondence).

[17]) R. E. Heitzman, A study of the threshold power requirements of FMFB receivers. IRE Trans Space El and Tel. **8**, 249-256, 1962.

[18]) C L Ruthroff and W. F Bodtman, Broadband FM demodulator with frequency compression Proc. IRE **50**, 2436-2445, 1962

[19]) J J Spilker Jr, Analysis of the FM discriminator with frequency feedback. Proc. IRE **51**, 233-234, 1963 (correspondence)

[20]) J. J Downing, Threshold suppression by FM feedback Proc IEEE **51**, 387-388, 1963 (correspondence)

[21]) R. M Gagliardi, Transmitter power reduction with frequency tracking FM receivers Proc. IRE **51**, 18-26, 1963

[22]) A J Giger and J G. Chaffee, The FM demodulator with negative feedback. Bell Sys. tech J **42**, 1109-1135, 1963

[23]) E. J Baghdady, Theoretical comparison of exponent demodulation by phase-locks and frequency-compressive feedback techniques Conv Record of the IRE **12**, Part 6, 402-422, 1964

[24]) V L. Bykov, Threshold in frequency modulation and methods of reducing it. Telecommunications and Radio Engineering **18**, Part 1, 17-26, 1964

[25]) D L Schilling and J Billig, On the threshold extension capability of the PLL and FDMFB Proc IEEE **52**, 621-622, 1964 (correspondence)

[26]) E J. Baghdady and L H Enloe, Decreasing the threshold in FM by frequency feedback. Proc IEEE **52**, 1039-1045, 1964 (correspondence).

[27]) B. R. Davis, Factors effecting the threshold of feedback FM receivers. IEEE Trans. Space El and Tel **10**, 90-94, 1964

[28]) V L Bykov, The limit to the improvement of PM and FM receiver threshold properties. Telecommunications and Radio Engineering **19**, Part 1, 41-46, 1965

[29]) F. Kuhne, Optimaldimensionierung von Frequenzkopplungsempfangern Nachrichtentechnische Zeitschrift **19**, 347-351, 1966

[30]) S Kobayashi and S Saito, Optimal design for frequency-compression demodulator. Electronics and Telecommunications in Japan **49**, No 2, 59-70, 1966

[31]) P Frutiger, Noise in FM receivers with frequency feedback Proc IEEE **54**, 1506-1521, 1966
[32]) J Frankle, Threshold performance of analog FM-demodulators RCA Rev **27**, 520-563, 1966
[33]) F Lefrak, H Moore, A Newton and L Ozolins, The frequency-modulation feedback system for the lunar-orbiter demodulator RCA Rev **27**, 563-577, 1966
[34]) A Wojnar, Noise and threshold in FM systems Proc IEEE **55**, 1639-1640, 1967 (correspondence)
[35]) F Kuhne, Gegenkopplungsdemodulation von frequenzmodulierten Signalen I Archiv el Übertr **21**, 383-391, 1967
[36]) F Kuhne, Gegenkopplungsdemodulation von frequenzmodulierten Signalen II Archiv el Übertr **21**, 507-519, 1967
[37]) J W Bayless, Concerning noise in FM receivers with negative frequency feedback. Proc IEEE **56**, 341, 1968 (correspondence)
[38]) J Heineman, A Newton and J Frankle, Multiple-loop frequency-compressive feedback for angle modulation detection RCA Rev **29**, 252-270, 1968
[39]) O Shimbo and C Loo, A simple formula for the threshold characteristics of FM-signals Proc IEEE **56**, 1241-1242, 1968 (correspondence)
[40]) O Shimbo and C Loo, Noise in FM receivers with negative feedback Proc IEEE **56**, 1372, 1968 (correspondence)
[41]) J H Roberts, Frequency feedback receiver as a low threshold demodulator in FMFDM satellite systems Proc IEE **115**, 1607-1619, 1968
[42]) M G Umkauf and R J Schulman, Experimental signal/noise-ratio comparison of the second order phase-locked loop and the second order frequency-locked loop Electronics Letters **4**, No 26, 585-586, 1968
[43]) J W Bayless and S C Gupta, Comments on "Noise in FM receivers with negative frequency feedback" Proc IEEE **57**, 247-248, 1969 (correspondence)
[44]) L Y Kantor, The effect on fluctuation noise on a tracking FM receiver Telecommunications and Radio Engineering **19**, Part 1, 19-26, 1965
[45]) T Osatake and A Fujii, A study of FM reception by tracking filters Electronics and Communications in Japan **50**, No 6, 100-109, 1967
[46]) J H Roberts, Dynamic tracking filter as a low-threshold demodulator in FMFDM satellite systems Proc IEE **115**, 1597-1607, 1968
[47]) M Morita and S Iko, High sensitivity receiver system for frequency modulated waves IRE Conv Record **8**, part V, 228-238, 1960
[48]) J Iltis and C Michaud, Compression de fréquence et regénération de fréquence porteuse Rev Tech Thom-Houst **34**, 1961
[49]) V E Benes, Index reduction of FM waves by feedback and powerlaw nonlinearities Bell Sys tech J **44**, 589-601, 1965
[50]) V L Bykov, Improving threshold properties of the FM receiver by means of a frequency divider Telecommunications and Radio Engineering **19**, Part 1, 14-20, 1965
[51]) A J Viterbi, Principles of coherent communication McGraw-Hill, 1966
[52]) F M Gardner, Phaselock techniques Wiley, 1966
[53]) E V Ryskin, Threshold level of an FM receiver Telecommunications and Radio Engineering, **18**, Part 1, 1-7, 1964
[54]) R G Medhurst and J H Roberts, Evaluation of distortion in f m trunk radio systems by a Monte Carlo method J IEE (London) **113**, 570-581, 1966
[55]) C L Ruthroff, Computation of FM distortion in linear networks for band limited periodic signals Bell Sys tech J **47**, 1043-1064, 1968

Summary

Frequency modulation is used e.g. when high demands are made on the signal-to-noise ratio. If good results are to be obtained in this way, the signal-to-noise ratio at the input of the receiver must remain above a certain level, known as the threshold. The threshold mechanism becomes operative when the instantaneous value of the noise at the input of the detector exceeds the amplitude of the carrier wave: this results in extra phase shifts, which lead to noise pulses after detection. The better the noise properties required, the more bandwidth is needed for the information transfer. However, if the receiver is to continue to operate above the threshold, the signal power at the input of the receiver must now increase because the noise power at the input of the detector is raised with increasing bandwidth. Frequency feedback can be obtained by replacing the local oscillator in the receiver by a voltage-controlled oscillator (VCO) and modulating the latter with the detected signal. This reduces the IF bandwidth and lowers the threshold. In this way, we can e.g. obtain equally good noise properties with a lower signal power. This has proved extremely useful in satellite communication, where (particularly in the early stages) the available transmitter power was very limited.

Although the principle of frequency feedback in the FM receiver has been known for a long time, no adequate theoretical analysis of its operation has hitherto been given. However, it has been demonstrated that the threshold gain due to the feedback is considerably less than would be expected from simple approximations. In this thesis, we have shown that the mechanism which determines the closed-loop threshold is basically the same as that for the open-loop threshold. The partial reduction in the threshold gain is due to the fact that the modulation of the VCO carrier wave by the feedback noise causes the IF carrier wave to shift up and down in the frequency range of the IF filter, as a result of which it is attenuated. This has an unfavourable effect on the signal-to-noise ratio at the input of the detector. This way of looking at things implies that FM can be regarded as quasi-stationary, at least as regards noise calculations. We have found by empirical methods that the closed-loop threshold occurs when the receiver operates below the open-loop threshold (obtained by "cutting open" the closed-loop receiver) 6 % of the time, as a result of the modulation and the resultant attenuation of the carrier wave. We have also shown that when the RF carrier wave is modulated with a sine wave or with Gaussian noise, the threshold can be appreciably higher than for the unmodulated carrier wave. The method of calculating the new thresholds has been given for both the open-loop and the closed-loop FM receiver.

It has been found in practice that the distortion is an important design criterion for FM receivers with frequency feedback. The system often has to give the lowest possible threshold at the maximum permissible distortion. It was

thus necessary to calculate the distortion in the closed-loop FM receiver. This calculation was preceded by that of the distortion in the open-loop FM receiver.

The LF closed-loop amplitude characteristics are also required for the calculation of the closed-loop distortion and the feedback noise at the input of the VCO. The calculation of these characteristics, and of the LF open-loop characteristics, has therefore been discussed in detail.

The design of the FM receiver has only been dealt with briefly. These calculations represent an optimalization process with a large number of boundary conditions. It has been shown that classical optimalization methods are not likely to lead to a solution here, and details are given of a trial-and-error method which should give results.

A great deal has already been published in the literature on the FM receiver with feedback. Our theory differs from all previously published theories. Our discussion of the literature is restricted to those publications we consider to be the most important.

Samenvatting

Frekwentiemodulatie wordt onder andere dan toegepast als er hoge eisen aan de signaal/ruis-verhouding gesteld worden. Om dit te bereiken moet de signaal/ruis-verhouding aan de ingang van de ontvanger boven een bepaalde waarde, de drempelwaarde, blijven. Het drempelmechanisme treedt in werking als aan de ingang van de detector de momentele waarde van de ruis groter wordt dan de amplitude van de draaggolf. Hierdoor kunnen namelijk extra fazedraaiingen ontstaan, die na detectie resulteren in ruisimpulsen. Hoe betere ruiseigenschappen men wenst te verkrijgen des te meer bandbreedte is er voor de informatie-overdracht nodig. Tegelijkertijd moet dan echter, om boven de drempel te blijven, het signaalvermogen aan de ingang van de ontvanger groter worden omdat, met de grotere bandbreedte, het ruisvermogen aan de ingang van de detector ook toeneemt. Door in de ontvanger de lokale oscillator te vervangen door een VCO en deze te moduleren met het gedetecteerde signaal kan een frekwentieterugkoppeling worden verkregen. Hierdoor wordt de MF-bandbreedte verkleind en wordt de waarde van de drempel verlaagd. Dit betekent b.v. dat dezelfde goede ruiseigenschappen nu met minder signaalvermogen verkregen kunnen worden. Dit is van groot belang geweest bij de satellietcommunicatie, waarbij vooral in de beginfaze het beschikbare zendervermogen zeer beperkt was.

Hoewel het principe van de frekwentieterugkoppeling in de FM-ontvanger al lang bekend is, is er tot nu toe geen sluitende analyse gegeven van de werking van deze ontvanger. Wel is aangetoond dat de drempelwinst ten gevolge van de terugkoppeling beduidend minder is dan volgens de meest eenvoudige benadering te verwachten zou zijn. In dit werk is aangetoond dat het mechanisme dat de gesloten-lus drempel beperkt wezenlijk hetzelfde is als dat van de open-lus drempel. Het gedeeltelijke verlies van de drempelwinst wordt veroorzaakt, doordat, door de modulatie van de VCO-draaggolf tengevolge van de teruggekoppelde ruis, de MF-draaggolf in het MF-filter heen en weer schuift en daardoor verzwakt wordt. Hierdoor wordt de signaal/ruis-verhouding aan de ingang van de detector ongunstig beïnvloed. Met deze zienswijze hangt samen dat FM, althans wat betreft de ruisberekeningen, kwasi-stationair beschouwd mag worden. Op empirische wijze is door ons gevonden dat de gesloten-lus drempel optreedt als, vanwege de modulatie en daarmee samenhangende draaggolfverzwakking, de open-lus drempel (van de opengeknipte gesloten-lus ontvanger) 6% van de tijd overschreden wordt. Tevens hebben we laten zien dat als de RF-draaggolf gemoduleerd wordt met een sinusfunctie of met Gaussische ruis, dat dan de waarde van de drempel beduidend hoger kan zijn dan vergeleken met de waarde voor ongemoduleerde draaggolf. Zowel voor de open-lus als voor de gesloten-lus FM-ontvanger is aangegeven hoe de nieuwe drempelwaarden berekend kunnen worden.

Bij het ontwerpen van FM-ontvangers met frekwentietegenkoppeling is gebleken dat de vervorming een belangrijk ontwerpcriterium is. Er wordt vaak gezocht naar een zo laag mogelijke waarde van de drempel bij de maximaal toelaatbare vervorming. Daarom was het nodig de vervorming in de gesloten-lus FM-ontvanger te kunnen berekenen. Hieraan vooraf ging de berekening van de vervorming in de open-lus FM-ontvanger.

Voor het berekenen van de gesloten-lus vervorming en de teruggekoppelde ruis op de ingang van de VCO zijn de LF gesloten-lus amplitudekarakteristieken nodig. Aan het berekenen hiervan en aan die van de LF open-lus karakteristieken is ruime aandacht besteed.

De synthese van de teruggekoppelde FM-ontvanger is slechts kort besproken. Het is een optimaliseringsproces met vele randvoorwaarden en er is aannemelijk gemaakt dat er met de klassieke optimaliseringsmethoden niet tot een oplossing te komen is. Wel is aangegeven hoe m.b.v. zoekmethodes een oplossing gevonden worden kan.

Over de teruggekoppelde FM-ontvanger is reeds veel literatuur verschenen. Bij geen van de daarin beschreven theoriën hebben we onze theorie aan kunnen laten sluiten. In de bespreking van de literatuur hebben we ons beperkt tot de, in onze ogen, voornaamste publicaties.

STELLINGEN

bij het proefschrift van F. G. M. BAX

23 oktober 1970

I

Het drempelmechanisme bij de open-lus en de gesloten-lus FM-ontvanger is wezenlijk hetzelfde.

Dit proefschrift.

II

De door de modulatie veroorzaakte drempelverschuiving wordt voornamelijk bepaald door de draaggolfverzwakking in het MF-filter.

Dit proefschrift.

III

Een deel van de door frekwentietegenkoppeling verkregen drempelwinst kan worden toegeschreven aan de vervormingstegenkoppeling.

Dit proefschrift.

IV

Voor de bepaling van de bandbreedte van het MF-filter in de FMFB-ontvanger is de regel van Carson niet bruikbaar.

Dit proefschrift.

V

De methode ter verkrijging van drempelverbetering waarbij aan het FM-signaal draaggolf toegevoegd wordt, is uit vervormingsoverwegingen alleen dan bruikbaar als de toegevoegde draaggolf in amplitude gelijk is aan de amplitude van het FM-signaal en de fase ervan gelijk is aan de fase van de draaggolfcomponent.

M. Morita en S. Iko, High sensitivity receiver system for frequency modulated waves, IRE Conv. Record **8**, part V, 228-238, 1960.
J. Iltis en C. Michaud, Compression de fréquence et régénération de fréquence porteuse, Rev. Tech. Thom.-Houst. **34**, 1961.

VI

De door het MF-filter veroorzaakte vervorming van het gedetecteerde FM-signaal wordt evenzeer door de amplitude- als door de fasekarakteristiek van dat filter bepaald.

VII

Het bewijs dat de optimale signaal-ruis karakteristieken van Akima werkelijk optimaal zijn, wordt door Akima niet geleverd.

H. Akima, Theoretical studies on signal-to-noise characteristics of an FM-system, IEEE Trans. on Space El. and Tel., **SET-9**, 101-109, Dec. 1963.

VIII

Interferentieberekeningen en metingen voor amplitude-gemoduleerde signalen waarbij de draaggolf- en zijbandstoring zonder meer in vermogen worden opgeteld, geven niet voldoende inzicht wat betreft de hinderlijkheid; de extra hinderlijkheid van de draaggolfstoring vereist de invoering van een weegfaktor.

E. Belger en F. von Rautenfeld, The objective measurement of the RF wanted-to-interfering signal ratio in amplitude modulation sound broadcasting, EBU Review **90A**, 57-73, April 1965.
C.C.I.R., Documents de la XI^{e} assemblée plénière, Oslo 1966, Rapport 399, Radiodiffusion sonore à modulation d'amplitude. Méthode de mesure objective à deux signaux pour la détermination des rapports signal/brouilleur HF.

IX

Om tot een sanering van de radio-omroep op de midden- en kortegolf te kunnen komen, is het gewenst van dubbelzijband-amplitudemodulatie over te gaan op enkelzijband modulatie.

X

Het volledig onderdrukken van de draaggolf bij amplitude-gemoduleerde signalen is voor omroepdoeleinden onpraktisch, zelfs indien er gebruik gemaakt wordt van een vaste frekwentieafstand tussen de nabuurzenders.

R. Netzband, A novel arrangement for the reception of single-sideband and double-sideband transmissions in AM sound broadcasting, EBU Review **114A**, 60-64, April 1969.

XI

Daar bij een rangschikking van n symbolen, bestaande uit een keuze van m verschillende symbolen waarbij het i^{de} symbool k_i maal voorkomt, het aantal mogelijke combinaties gelijk is aan

$$\frac{n!}{k_1!\, k_2! \ldots k_m!}$$

en dit overeenkomstig de asymptotische Sterlingontwikkeling praktisch gelijk is aan 2^{nH}, waarbij

$$H = \sum_{i=1}^{m} -\frac{k_i}{n} \log_2 \frac{k_i}{n}$$

de maat voor de hoeveelheid informatie voorstelt, kan deze H veel inzichtelijker met bovenstaand verband gedefiniëerd worden dan volgens de tot nu toe algemeen gebruikte methode waarbij de optelbaarheid van hoeveelheden informatie voorop staat.

XII

Het is onbillijk op duurzame goederen tijdelijke belastingen te heffen die van kortere duur zijn dan de gemiddelde levensduur van het desbetreffende goed.

XIII

De opbrengst van de reclameprogramma's via radio en televisie kan het best worden besteed aan het verbeteren van die programma's.